Mesonic
Final State Interactions

Dissertation

zur Erlangung der naturwissenschaftlichen

Doktorwürde (Dr. sc. nat.)

vorgelegt der

Mathematisch-naturwissenschaftlichen Fakultät

der Universität Zürich

von

Frederik Orellana

aus Dänemark

Begutachtet von

Prof. Dr. Daniel Wyler

Dr. Gilberto Colangelo

Zürich 2002

Die vorliegende Arbeit wurde von der Mathematisch-naturwissenschaftlichen Fakultät der Universität Zürich auf Antrag von Prof. Dr. Daniel Wyler und Prof. Dr. Ben Moore als Dissertation angenommen.

A mi abuela : Christina Orellana

A mi tía : Consuelo Orellana

Zusammenfassung

Die vorliegende Arbeit beschäftigt sich mit zwei unterschiedlichen aber verwandten Problemen: 1) Die Grössenordnung der Korrekturen infolge von Endzustandswechselwirkungen in mesonischen Prozessen. 2) Die Frage, wie weit es möglich ist, die Berechnung solcher Korrekturen zu automatisieren.

Insbesondere wird untersucht, ob die Diskrepanz zwischen theoretischen und experimentellen Werten von ε'/ε durch die Berüchsichtigung mesonischer Endzustandswechselwirkungen im Zerfall $K \to \pi\pi$ erklärt werden kann. Für die präzise Auswertung solcher Korrekturen wurde ein konsistenter Rahmen entwickelt. Das Ergebnis ist ein System von Integralgleichungen, das mit zwei Konstanten als Eingabe iterativ gelöst werden kann. Von diesen zwei Konstanten kann die eine bestimmt werden durch das Soft-Pion Theorem, die andere ist nicht bekannt. Es folgt, dass im Moment die Unsicherheit bei der Auswertung von Endzustandswechselwirkungen zu gross ist, um eine definitive Aussage zu machen, *aber* dass das sich ändern wird, sobald die zweite Konstante bekannt ist. Eine Ward-Identität wurde hergeleitet, welche die Berechnung der Konstante in der Gittertheorie erleichtern sollte. Die vollständige Berechnung des Zerfalls $K \to \pi\pi$ in chiraler Störungstheorie ist durchgeführt worden. Sie ist von begrenztem direkten Nutzen wegen der vielen unbekannten Konstanten, hat aber während der Berechnung der Endzustandwechselwirkungen als Leitfaden gedient.

Für das durchgeführte Studium von $K \to \pi\pi$ sind die niederenergetischen Phasen der $\pi\pi$-Streuung wichtig. Ein Kapitel ist der Berechnung elektromagnetischer Korrekturen zu diesen Phasen in chiraler Störungstheorie gewidmet. Die Ergebnisse werden für das DIRAC Experiment wichtig sein, sobald die angekündigte Messung der 2P-2S Energiedifferenz in Pionium Ergebnisse liefert. Die Berechnung dient auch als Test der entwickelten Computerberechnungsprogramme.

Diese Programme werden im letzten Kapitel beschrieben und sind in der ganzen Arbeit verwendet worden. In diesen Kapiteln werden auch viele analytische Berechnungen der chiraler Störungstheorie beschrieben und mit der Literatur verglichen.

Das Studium der Verletzung der CP-Symmetrie und der Parameter ε' und ε sowie das Studium des Vakuums und des Mechanismus spontaner chiraler Symmetrieverletzung, die sich in der Streuung von Pionen aneinander manifestiert, sind Teil der laufenden Verifikation/Falsifikation und Erforschung des elektroschwachen Standardmodels und der Quantenchromodynamik.

Summary

In the present work, two distinct but interrelated subjects are investigated: 1) The importance of corrections due to final state interactions in mesonic processes. 2) The question of how far it is possible to automatize the calculation of such corrections.

In particular it is explored whether or not the discrepancy of theoretical predictions with experimental values of ε'/ε can be explained by the inclusion of mesonic final state interactions in the amplitude of the decay $K \to \pi\pi$. A framework has been developed for the precision evaluation of these corrections in a consistent way. The outcome is a set of integral equations that can be solved iteratively, requiring as input two constants of which one is known from the soft pion theorem and the other largely unknown. This is at present all that can be done. The conclusion is that the uncertainties involved in the evaluation of final state interactions are too large for the method to be of any use at present *but* that this will change as soon as the second constant becomes known. A Ward identity is given which should facilitate the lattice evaluation of the constant. The full calculation of $K \to \pi\pi$ in Chiral Perturbation Theory (although of limited direct use, due to the abundance of unknown constants) served as a guideline when calculating the final state interactions.

For the study of $K \to \pi\pi$ presented, the low energy $\pi^+\pi^- \to \pi^+\pi^-$ phases are crucial, and a chapter has been devoted to the study of the inclusion of electromagnetic corrections to these using Chiral Perturbation Theory. The results will be relevant for the DIRAC experiment due to the planned measuring of the energy difference between the 2P-2S levels of pionium. The calculation also provides checks of the calculational software developed.

The computational tools developed, are presented in the last chapter and are used throughout. Many calculations in Chiral Perturbation Theory, that have been worked out and checked with the literature, are described.

The study of the violation of CP-symmetry and the parameters ε' and ε as well as the study of the structure of the vacuum and the mechanism of spontaneous chiral symmetry breaking as revealed by the scattering of pions, are part of the ongoing verification/falsification and exploration of the electro-weak Standard Model and Quantum Chromo-Dynamics.

Contents

Chapter 1

Introduction

The dynamics of quarks, which are regarded as the bulk constituents of matter on earth, becomes untractable or irrelevant in the low energy world which is dominated by the strong interaction. This world is described in terms of particles called hadrons, which are thought to be bound states of quarks, and, in contrast to quarks, directly observable. The most abundant hadrons in nature are the ground states of the possible two- and three-quark ensembles of the lightest two quark flavors: The proton, the neutron and the positive, negative and neutral pion. With more quark flavors, other particles can be formed. In the low energy regime one restricts to the lightest two or three flavors, and thus to the light pseudoscalar triplet or octet (pions, kaons and the eta-meson) and their interactions, that is, the strong, electromagnetic (EM) and weak interactions. The low energy description and interplay of these forces is subtle: They are all governed by the symmetries underlying the electro-weak Standard Model [Gla61, Wei67a, Sal68] (SM) and Quantum Chromo-Dynamics [GW73a, GW74, GW73b, Pol73] (QCD), but for instance, whereas the weak and strong interactions of mesons are described solely in terms of the contact interactions of the mesons allowed by the symmetries, the EM interaction is additionally described by including the exchange of photons. The reason for the feasibility of this is that the weak gauge bosons are heavy, the strong interaction is a short-range force, but the photon is light and electromagnetism is a long-range force. The tool for the description of these particles and forces is effective field theory and in particular the effective field theory known as Chiral Perturbation Theory [GL84, GL85] (CHPT). When comparing with experimental data, other supplementary tools become useful, namely dispersion relations exploiting the analytic properties of the amplitudes.

Symmetries of the Standard Model

The symmetries governing low energy phenomena are the fundamental symmetries of nature as well as the symmetries imposed by the SM. That is: The amplitudes have to satisfy Lorentz invariance, analyticity, unitarity and crossing symmetry, as well as approximate chiral SU(N) $\times$ SU(N) flavor symmetry spontaneously broken down to vectorial symmetry and explicitly broken by small mass terms. Moreover the strong and electromagnetic lagrangians satisfy charge-parity (CP) invariance, whereas the weak lagrangian has CP violating terms. What will be explored is whether these unbroken and broken symmetries and their effective lagrangians give a realistic description of the material world as seen by experiment. The symmetry issues under consideration here are:

- Verification of the mechanism of approximate chiral symmetry - size of the quark condensate.
- Determination of the size of the direct CP symmetry breaking parameter ε'/ε.
- Determination of the size of isospin symmetry breaking.

Low energy data

The amplitudes calculated in the present work are for the following processes: $K_S \to \pi^0\pi^0$, $\pi^\pm\pi^\pm \to \pi^\pm\pi^\pm$, $\gamma\gamma \to \pi\pi$ ($\gamma\pi \to \gamma\pi$). The two last amplitudes are not directly accessible to experiment, but can be extracted from other processes as indicated in the listing below of the most recent relevant experiments:

$K_S \to \pi^0\pi^0$

- CERN NA-31 [NA3, B$^+$88, B$^+$93], K$\to \pi^0\pi^0$.
- CERN NA-48 [NA4, F$^+$99], K$\to \pi^0\pi^0$.
- Fermilab E-731 [E73, G$^+$93], K$\to \pi^0\pi^0$.
- KTEV E-832 [E83, AH$^+$99], K$\to \pi^0\pi^0$.

$\pi^\pm\pi^\pm \to \pi^\pm\pi^\pm$

- Brookhaven E-865[E86, P$^+$01], K_{l4} decays.

Notice that the CERN DIRAC [DIR, Sch00, Lan] experiment could in principle also give high precision data for the last amplitude if they would in a next generation measure transition energies.

Calculational ingredients

The primary theoretical ingredient is the perturbative expansion of amplitudes using the chiral lagrangians and straight-forward Feynman diagram analysis. The working out of Feynman diagrams and amplitudes is a tedious and error prone undertaking. Therefore, as much as possible has been done in an automatized fashion. Indeed, one major motivation for the present work was to see how far one can push the envelope w.r.t. computerizing CHPT. The author has developed a computer program christened "*PHI* " for this purpose. The program draws on previous work of others [MBD91a, KEM92, Mera, WMSBa, Hah01]; the new part being the addition of the capability of dealing with effective theories. The programming language used is *Mathematica* [Wol00]. Also, a general feature of this whole thesis is that non-trivial calculations are provided explicitly in form of *Mathematica* notebooks [Ore]. As mentioned above, the amplitudes calculated will be unitarized or improved by means of dispersion relations. Other ways of saying this are that final state interactions shall be included or that pion (or meson) rescattering shall be accounted for. Two technical ways of doing this are common: The Omnès method and the inverse amplitude method. Here, the first of these shall be used.

Structure of the thesis

The chapters fall in two main categories:

1) The first three chapters and the last appendix, which deal with low energy formalism, that is, CHPT and dispersion relations: In chapter, 2 the strong CHPT formalism is briefly described. In chapter 3, this is extended to include electromagnetism. Chapter 4 contains a discussion of mesonic final state interactions in $K_s \to 2\pi^0$. The amplitude is worked out using CHPT to one loop and dispersion relations to sum the final-state (unitarity) diagrams to all orders. Appendix C contains formulae too large to be displayed in the main text.

2) Chapter 5 and appendices A and B, which deal with computerization of CHPT and field theory in general as implemented in the calculational package *FeynCalc* and extended by the author with the package *PHI*: In chapter 5, basic concepts of quantum field theory are introduced in a computerized fashion, that is, a *Mathematica* syntax for these is defined, some of the computational tools developed are described and some examples are worked out. Appendix A is a reference manual to *PHI*. Appendix B contains short descriptions of calculations carried out with *PHI*. These include the calculations used in chapter 3 and chapter 4, as well as calculations of results already avaliable in the literature. These last calculations serve as tests of the program. They all agree with results available in the literature. The actual calculations are available in form of *Mathematica* notebooks that can be downloaded from the *FeynCalc*

web-site.

Typography

For abbreviations SMALL CAPS are used. **`Bold typewriter tekst`** is used for *MATHEMATICA* code. *ITALIC SMALL CAPS* are used for names of *MATHEMATICA* packages. Filenames are quoted. Excerpts from *MATHEMATICA* notebooks are indicated with a beginning and an ending horizontal line.

Chapter 2

Chiral Perturbation Theory

In this chapter the framework is set up in which the calculations of the subsequent chapters will be made. This includes a brief introduction to effective lagrangians and CHPT as well as a discussion of some of the main features of CHPT. Towards the end of the chapter a few examples of using computer algebra techniques in calculations are given; the reader is encouraged to consult the notebooks of appendix B containing the full calculations.

2.1 Introduction

According to Weinberg [Wei96], in the early sixties, among quantum field theorists there was a prevailing sense of crisis. Things seemed to be going nowhere in attempting to describe the newly found weak and strong interactions beyond leading order perturbations. One consequence of this was the development of dispersion relation methods (see section 4.4) into an attempt at describing amplitudes completely disregarding the underlying fields using instead postulated properties of amplitudes like analyticity, crossing and unitarity. Another consequence was the development of current algebra which was also an attempt at calculating amplitudes without dealing with fields, but instead dealing with currents and postulating an algebra for these. Ironically the basic postulates of these two directions, although claimed to be "fundamental", were both inspired by leading order perturbative quantum field theory.

At this time, low energy $\pi\pi$ scattering was important as a simple process to test the predictions for the strong interaction. One unique feature of this process is that it displays complete crossing symmetry. Dispersion theorists tried hard [CM60] to use this to device a self consistent system of integral equations, which, assuming the existence of the rho resonance should be able to reproduce the full low energy amplitude - the so-called bootstrap method. Unfortunately this method failed - the rho resonance did not even reappear in the crossed channels

(see section 4.4). This should not be seen as a falsification of dispersion relation theory, rather of one or more of the assumptions involved in the bootstrap method, which all seem plausible but which are not exact and the errors of which it is difficult to estimate. These assumptions involve neglecting high energy inelasticity, inclusion of only the rho exchange singularities, and that the rho is predominantly a $\pi\pi$ resonance. Current algebra was able to provide a reasonable description, but it was equivalent to using a phenomenological lagrangian to leading order and there was no way of calculating higher order corrections. This phenomenological lagrangian was derived in 1967 by Weinberg [Wei67b] by requiring that it be the most general lagrangian respecting Lorentz and CP invariance and chiral symmetry.

As is well known, for the weak interactions 't Hooft, Weinberg and others came to the rescue, introducing the Standard Model and reviving quantum field theory and perturbation theory. For the strong interactions, QCD was then developed. Low energy $\pi\pi$ scattering and other hadronic processes however, were orphaned by these models: In the low energy regime, the blowing up of the strong coupling and confinement makes it impossible to describe experiment using perturbation in the coupling constant and quark degrees of freedom.

Instead, the method already endeavoured by Weinberg in 1967 was expanded by Gasser and Leutwyler into a phenomenological framework fully consistent with QCD, or, in fact, derivable from QCD (and Lorentz and CP invariance) via the external field method and the equivalence theorem. The result was CHPT, which is a low energy theory applying a dual expansion in the quark masses and the external momenta. At each order a new phenomenological lagrangian comes into play.

The shortcoming of CHPT is that the 0,1 and 2-loop calculations available are only valid at very low energies ($\lesssim$ 1GeV) and higher order calculations are senseless because of the huge number of phenomenological parameters in the higher order lagrangians. Examination of a method for extending the domain of validity by other means is the subject of chapter 4. This method involves using dispersion relations in combination with CHPT. The success of this reflects the fact mentioned that although dispersion theory failed miserably with the rho-bootstrap, what was to blame was not the method itself nor the underlying symmetries, but rather the additional assumptions made. Thus, crossing and analyticity remain (by general consensus) perfectly good, exact assumptions and can be applied as additional pieces of information to supplement or test the CHPT predictions. Elastic unitarity is only approximate, but the application of it has more predictive potential. The remainder of this chapter is an introduction to effective lagrangians and CHPT.

2.2 Effective lagrangians

Nowadays effective lagrangians are widely used in particle physics phenomenology when a more fundamental theory is either unknown or unsuited for calculating the quantity one is interested in. Typically, heavy degrees of freedom are integrated out in order to achieve lagrangians containing only the light particles, taking advantage of the fact that large-scale dynamics is largely unaffected by very short distance structures and interactions. The effects from heavy particles are then parameterized by coupling constants which have to be determined from experiment or using some model. Amplitudes are renormalized "order by order" in the energy expansion, each order having a lagrangian with contact interactions to absorb loop infinities from lower order lagrangians. That is, effective theories are not necessarily renormalizable in the traditional sense. Examples include the Euler-Heisenberg theory of photons for $E \ll m_e$ [HE36], the Fermi theory of the weak interactions [Fer34] and indeed, the Standard Model itself can also be considered an effective (renormalizable) theory of an unknown fundamental theory. The general procedure is

- Settle for a set of expansion parameters and a scale.
- At each order in the expansion write down the most general lagrangian consistent with the symmetries of the problem using the physical fields of the problem.
- Calculate the loop divergent parts of the generating functional (that is, the beta functions) up to a given order.
- Calculate the amplitude up to the given order, either using functional differentiation of the generating functional or Feynman rules and diagrams.

In the following, a few examples will be considered.

2.3 The Euler-Heisenberg lagrangian for photon-photon scattering

As a simple example, consider the electromagnetic scattering of two photons. Assuming the vanishing of the interactions with the momenta, the effective lagrangian for the photons is a series of Lorentz and gauge invariant terms $\mathcal{L}_{\text{eff}} = -\frac{1}{4}F_{\mu\nu}^2 + \mathcal{L}_{\text{U}} + \mathcal{L}_{\text{EH}} + \ldots$ of increasing order in the momenta (derivatives). $\mathcal{L}_{\text{U}}$ is the Uehling interaction [Ueh35] due to the lowest-order vacuum polarization loop where $\alpha = e^2/4\pi$ is the fine structure constant and $\Box \equiv \partial_\mu \partial^\mu$.

$$\mathcal{L}_{\text{U}} = \frac{\alpha}{60\pi m^2} F_{\mu\nu} \Box F^{\mu\nu} \tag{2.1}$$

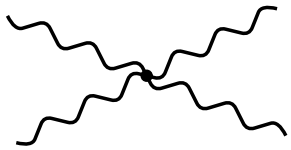

Figure 2.1: Lowest order diagram with effective lagrangian contributing to photon-photon scattering.

This term is can be eliminated when no matter is present due to the free field equation of motion $\Box F_{\mu\nu} = 0$. To fourth order in the momenta, the most general Lorentz and gauge invariant lagrangian with quartic interactions in the photon field is the Euler-Heisenberg lagrangian [HE36]

$$\mathcal{L}_{\text{EH}} = \left(\frac{\alpha}{m^2}\right)^2 \left[c_1(F_{\mu\nu}F^{\mu\nu})^2 + c_2(F_{\mu\nu}\tilde{F}^{\mu\nu})^2\right], \tag{2.2}$$

using the field tensor $F_{\mu\nu} = \partial_\mu A_\nu - \partial_\nu A_\mu$ and its dual $\tilde{F}_{\mu\nu} = \frac{1}{2}\epsilon_{\mu\nu\alpha\beta}F^{\alpha\beta}$. Were the underlying theory not known or not manageable, one would then calculate the scattering amplitude (figure 2.1) and compare with experiment to fix the constants c_1 and c_2. In this case however, the underlying theory is QED and the amplitude to order $\mathcal{O}(p^4)$ can be calculated exactly (figure 2.2) yielding the values $c_1 = 1/90$ and $c_2 = 7/360$. Loosely speaking, what we've done is to shrink the box in diagram 2.2 to a point, that is, replaced the short distance interactions of the box by an effective contact interaction. The next order correction is then furnished by the p^6 contributions of the one-loop diagrams with (2.2) and the tree diagrams of the p^6 lagrangian. In renormalizing the loop diagrams using the calculated one-loop divergencies, the scale then comes into play.

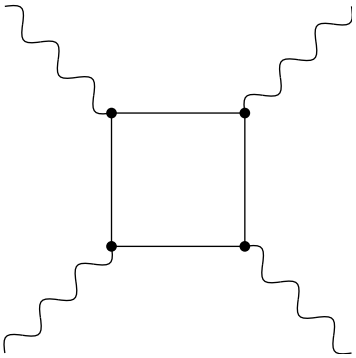

Figure 2.2: Charged particle box diagram contributing to photon-photon scattering.

2.4 Chiral Goldstone bosons

The 8 (3) lightest pseudo-scalar mesons are usually regarded as the Goldstone bosons of spontaneously broken approximate SU(3) (SU(2)) chiral symmetry:

$$G = \mathrm{SU}(N)_{\mathrm{L}} \times \mathrm{SU}(N)_{\mathrm{R}} \longrightarrow H = \mathrm{SU}(N)_{\mathrm{V}}, \tag{2.3}$$

where N is either 3 or 2. The motivation for this is the empirical fact that the mesons are much lighter than other hadrons and that no corresponding scalar meson octet (triplet) exists. The starting point for chiral phenomenology is thus the Goldstone theorem, which we shall now discuss. The Noether currents following from global invariance under G are

$$J^a_{i\mu} = \bar{q}_i \gamma_\mu \frac{\sigma_a}{2} q_i, \qquad (i = \mathrm{L}, \mathrm{R}; \quad a = 1, \ldots, N^2 - 1), \tag{2.4}$$

where σ are the two or three dimensional matrices generating SU(2) or SU(3) with $\langle \sigma_a \sigma_b \rangle = 2\delta_{ab}$. $\langle\rangle$ indicate a trace. The corresponding Noether charges $Q^a_i = \int \mathrm{d}^3 x J^a_{i\,0}(x)$ satisfy

$$[Q^a_i, Q^b_j] = i\delta_{ij} f_{abc} Q^c_i, \tag{2.5}$$

Generally, the Goldstone theorem [Gol61] states that, given a spontaneously broken symmetry G with Noether current J^μ, there exists a continuous family of massles boson states $|\alpha\rangle$ satisfying

$$\langle \alpha | J^0(x) | 0 \rangle \neq 0. \tag{2.6}$$

The proof [Gol61, Bur00] relies on the assumption of the existence of a field ψ transforming like

$$\delta\psi = i[Q, \psi(x)] \equiv \phi(x), \tag{2.7}$$

where the *ordering parameter* ϕ satisfies

$$\langle 0 | \phi(x) | 0 \rangle \neq 0. \tag{2.8}$$

This last condition implies

$$Q | 0 \rangle \neq 0, \tag{2.9}$$

which, in turn, implies that different states are created from the ground state by the symmetry transformation

$$|0\rangle \to e^{i\alpha Q} |0\rangle \equiv |\alpha\rangle \neq |0\rangle . \tag{2.10}$$

Because of the time independence of Q, these states have the same energy as the ground state (here H is the hamiltonian),

$$\dot{Q} = i[H, Q] = 0 \Rightarrow H |\alpha\rangle = H e^{i\alpha Q} |0\rangle = e^{i\alpha Q} H |0\rangle . \tag{2.11}$$

In QCD, the charges in question are the axial charges

$$Q^a_{\rm A} = Q^a_{\rm R} - Q^a_{\rm L} \qquad (a = 1, \ldots, N^2 - 1). \tag{2.12}$$

It then follows from (2.6) and current conservation, $\partial_\mu J^\mu = 0$, that the Goldstone bosons are pseudo-scalar particles. In QCD, a natural choice for the fields ψ^a are the simplest pseudoscalar operators $\psi = \bar{q}\gamma_5\sigma_a q$ with

$$\left[Q^a_{\rm A}, \psi_b\right] = -\frac{1}{2}\bar{q}\{\sigma_a, \sigma_b\}q. \tag{2.13}$$

Thus, the existence of chiral Goldstone bosons follows from the non-vanishing of the chiral condensates [1],

$$\langle 0|\bar{u}u|0\rangle = \langle 0|\bar{d}d|0\rangle \,[= \langle 0|\bar{s}s|0\rangle]\,. \tag{2.14}$$

Generally, it follows from (2.6) and current conservation [Bur00] that the interactions of the Goldstone bosons vanish with vanishing momenta. Thus, in the chiral limit (vanishing quark masses) the interactions of mesons vanish with their momenta and a dual expansion in quark masses and meson momenta might be feasible. The construction of such lagrangians is the subject of the following section.

2.5 Chiral mesonic lagrangians

Goldstone fields $\varphi = (\varphi_1, \varphi_2, \ldots \varphi_N)$ can be viewed [CWZ69, CCWZ69] as coordinates of the coset space G/H. Their symmetry tranformations are best studied by grouping the fields in a matrix $u(\varphi) \in G/H$ (see [Eck98]). Generally, with $g \in G$, the compensator field $h(g, \varphi) \in H$ is defined by

$$u(\varphi) \overset{g\in G}{\longrightarrow} gu(\varphi) = u(\varphi')h(g, \varphi). \tag{2.15}$$

For $G = \mathrm{SU}(N)_{\rm L} \times SU\mathrm{SU}(N)_{\rm R}$, the left and right-handed transformations are related by parity, and specifically,

$$u(\varphi') = g_{\rm R}u(\varphi)h(g, \varphi)^{-1} = h(g, \varphi)u(\varphi)g_{\rm L}^{-1}, \tag{2.16}$$

$$g = (g_{\rm L}, g_{\rm R}) \in G\,.$$

For practical calculations it is often more convenient to work with $U(\varphi) = u(\varphi)^2$, which has the simpler transformation

$$U(\varphi) \overset{G}{\to} g_{\rm R}U(\varphi)g_{\rm L}^{-1}. \tag{2.17}$$

[1] Notice however, that there is nothing in the arguments presented that precludes a chiral Goldstone mechanism even if the quark condensates vanish.

Proceeding now to the construction of the lagrangians, the symmetries that have to be respected are Lorentz invariance, CP invariance (we are considering only strong interactions) and chiral symmetry broken by small mass terms to be considered on equal footing with the momenta in the expansion. In the chiral limit ($m_i = 0, i = \mathrm{u}, \mathrm{d}, \ldots$) the lowest order lagrangian is constructed by allowing only light meson fields collected in the matrix U, and fields v, a, s, p coupling to external sources, and requiring that the generating functional Z written in terms of the meson fields,

$$e^{iZ(v,a,s,p)} = \langle 0_{\mathrm{out}}|0_{\mathrm{in}}\rangle_{v,a,s,p} = \int [\mathrm{d}U] e^{i\int \mathrm{d}^4x \mathcal{L}^{\mathrm{CHPT}}(U,v,a,s,p)}, \tag{2.18}$$

is as general as allowed when requiring that it has the same symmetries as when written in terms of the quark and gluon fields of the QCD lagrangian,

$$e^{iZ(v,a,s,p)} = \langle 0_{\mathrm{out}}|0_{\mathrm{in}}\rangle_{v,a,s,p} = \int [\mathrm{d}q][\mathrm{d}\bar{q}][\mathrm{d}A_\mu^a] e^{i\int \mathrm{d}^4x \mathcal{L}^{\mathrm{QCD}}(q,\bar{q},A_\mu^a,v,a,s,p)}, \tag{2.19}$$

$$\mathcal{L}^{\mathrm{qcd}} = \mathcal{L}_0^{\mathrm{QCD}} + \bar{q}\gamma^\mu(v_\mu + a_\mu\gamma_5)q - \bar{q}(s - ip\gamma_5)q, \tag{2.20}$$

that is, Lorentz, parity and chiral invariance. Chiral tranformations for the external sources of the QCD lagrangian read

$$\begin{aligned} v'_\mu + a'_\mu &= V_{\mathrm{R}}(v_\mu + a_\mu)V_{\mathrm{R}}^\dagger + iV_{\mathrm{R}}\partial_\mu V_{\mathrm{R}}^\dagger, \\ v'_\mu - a'_\mu &= V_{\mathrm{L}}(v_\mu - a_\mu)V_{\mathrm{L}}^\dagger + iV_{\mathrm{L}}\partial_\mu V_{\mathrm{L}}^\dagger, \\ s' + ip' &= V_{\mathrm{R}}(s + ip)V_{\mathrm{L}}^\dagger. \end{aligned} \tag{2.21}$$

Gauge invariance permits v_μ and a_μ to enter the CHPT lagrangian only as gauge fields in the covariant derivative

$$D_\mu U = \partial_\mu U - i(v_\mu + a_\mu)U + iU(v_\mu - a_\mu), \tag{2.22}$$

or through the field strength tensors associated with $r_\mu = v_\mu + a_\mu$ and $l_\mu = v_\mu - a_\mu$,

$$\begin{aligned} F_{\mu\nu}^r &= \partial_\mu r_\nu - \partial_\nu r_\mu - i[r_\mu, r_\nu], \\ F_{\mu\nu}^l &= \partial_\mu l_\nu - \partial_\nu l_\mu - i[l_\mu, l_\nu]. \end{aligned} \tag{2.23}$$

The fields U and the field strengths are then found to transform like

$$\begin{aligned} U' &= V_{\mathrm{R}} U V_{\mathrm{L}}^\dagger, \\ D_\mu U' &= V_{\mathrm{R}} D_\mu U V_{\mathrm{L}}^\dagger, \\ F_{\mu\nu}^{r\,\prime} &= V_{\mathrm{R}} F_{\mu\nu}^r V_{\mathrm{R}}^\dagger, \\ F_{\mu\nu}^{l\,\prime} &= V_{\mathrm{L}} F_{\mu\nu}^l V_{\mathrm{L}}^\dagger. \end{aligned} \tag{2.24}$$

This enables us to find the lowest order lagrangian in the chiral limit (indicated by a superscript 0):

$$\mathcal{L}_2^0 = \frac{f_\pi^2}{4} \langle D_\mu U D^\mu U^\dagger \rangle + \frac{f_\pi^2}{4} \langle \chi U^\dagger + U \chi^\dagger \rangle , \tag{2.25}$$

with

$$\chi \equiv 2B_0(s + ip), \tag{2.26}$$

and B_0 a constant.

In contrast to quarks, the mesons represented by U are experimentally observed particles. As discussed in section 2.4, the three lightest mesons (π^+, π^-, π^0) have almost equal masses and are considered an SU(2) isospin triplet, whereas the eight lightest $(\pi^+, \pi^-, \pi^0, K^+, K^0, \bar{K}^0, K^-)$ are considered an SU(3) octet. In principle U can be chosen any way one likes as long as it contains the 3 or 8 independent meson fields and

$$\det U(x) = e^{i\theta(x)}, \tag{2.27}$$

where $\theta(x)$ is the winding number density, which is set to 0 henceforth [GL85], but in SU(3), usually, the so-called exponential representation is used:

$$U = e^{\frac{i}{f_\pi} \boldsymbol{\varphi} \cdot \boldsymbol{\sigma}}, \tag{2.28}$$

where $\boldsymbol{\sigma}$ is the triplet or octet of two or three dimensional matrices generating SU(2) or SU(3), $\boldsymbol{\varphi}$ is the corresponding triplet or octet of fields representing the light mesons and $\boldsymbol{\varphi} \cdot \boldsymbol{\sigma}$ is thus hermitean and traceless. The fact that different representations give the same matrix elements for physical processes is called representation independence and was first proved by R. Haag [Haa58]. It states more precisely that if two fields ξ and ξ' are related by $\xi = \xi' F(\xi')$ with $F(0) = 1$, then the same matrix elements result if one uses either $\mathcal{L}(\xi)$ or $\mathcal{L}(\xi' F(\xi'))$.

The lagrangian contains two constants, f_π and B_0. The physical interpretation of these follows from considering appropriate matrix elements. B_0 can be studied by evaluating the quark-antiquark vacuum condensate in CHPT by expanding the generating functional in powers of the external field $s(x)$ around the QCD ground state $s = \mathcal{M}, v = a = p = 0$ ($\mathcal{M}$ is the diagonal quark mass matrix with $m_u, m_d, \ldots$ along the diagonal) and varying the components of s. It follows straightforwardly that

$$\langle 0|\bar{q}\sigma^a q|0\rangle = -f_\pi^2 B_0 \langle \sigma^a \rangle \{1 + \mathcal{O}(\mathcal{M})\}. \tag{2.29}$$

f_π can be evaluated by considering the vacuum to meson matrix element of the axial current, which evaluates to

$$\langle 0|A_\mu^k|\varphi^j(\boldsymbol{p})\rangle = i f_\pi p_\mu \delta^{kj}. \tag{2.30}$$

This justifies identifying f_π with the pion decay constant.

Expanding s around $\mathcal{M}$ instead of 0 amounts to accounting for the approximate nature of chiral symmetry (in QCD due to the light but non-vanishing quark masses). We will denote this by dropping the superscript 0 on $\mathcal{L}_2$. For technical details, see section 5.2. The meson masses, being small, will be counted as $\mathcal{O}(p^2)$ in the energy expansion, which is then a dual expansion in external momenta squared and the light quark masses which slightly, but explicitly break chiral symmetry.

Due to the power counting theorem of Weinberg [Wei79], higher loop Feynman amplitudes correspond to higher orders in the momentum and mass expansion. The amplitudes contain divergences that are absorbed by renormalization of constants of the higher order lagrangians. The next to leading order lagrangian reads [GL85]

$$\begin{aligned}\mathcal{L}_4 = \; & L_1 \langle D_\mu U^\dagger D^\mu U\rangle^2 + L_2 \langle D_\mu U^\dagger D_\nu U\rangle \langle D^\mu U^\dagger D^\nu U\rangle \\ & + L_3 \langle D_\mu U^\dagger D^\mu U D_\nu U^\dagger D^\nu U\rangle \\ & + L_4 \langle D_\mu U^\dagger D^\mu U\rangle \langle \chi^\dagger U + \chi U^\dagger\rangle \\ & + L_5 \langle D_\mu U^\dagger D^\mu U(\chi^\dagger U + U^\dagger \chi)\rangle + L_6 \langle \chi^\dagger U + \chi U^\dagger\rangle^2 \\ & + L_7 \langle \chi^\dagger U - \chi U^\dagger\rangle^2 + L_8 \langle \chi^\dagger U \chi^\dagger U + \chi U^\dagger \chi U^\dagger\rangle \\ & - iL_9 \langle F_{\mathrm{R}}^{\mu\nu} D_\mu U D_\nu U^\dagger + F_{\mathrm{L}}^{\mu\nu} D_\mu U^\dagger D_\nu U\rangle \\ & + L_{10} \langle U^\dagger F_{\mathrm{R}}^{\mu\nu} U F_{\mathrm{L}\mu\nu}\rangle + H_1 \langle F_{\mathrm{R}\mu\nu} F_{\mathrm{R}}^{\mu\nu} + F_{\mathrm{L}\mu\nu} F_{\mathrm{L}}^{\mu\nu}\rangle \\ & + H_2 \langle \chi^\dagger \chi\rangle .\end{aligned} \tag{2.31}$$

L_i are coupling constants to be renormalized through

$$L_i^r = L_i + \frac{\Gamma_i}{(32\pi)^2}\left\{\frac{2}{D-4} - \log(4\pi) + \gamma - 1\right\}. \tag{2.32}$$

It is understood that in SU(2) U is a 2×2 matrix and in SU3) a 3×3 matrix. As already discussed, the L_i^r are a priori unknown, but can be obtained if enough experimental data is available, allowing predictions for other experiments. The scale dependence of the counter-terms must cancel the scale dependence of the one-loop generating functional (see below) and therefore takes the form

$$L_i^r(\mu_2) = L_i^r(\mu_1) + \frac{\Gamma_i}{(4\pi)^2}\log\frac{\mu_1}{\mu_2}. \tag{2.33}$$

The standard procedure to obtain the beta functions Γ_i is to calculate the divergent part of the one-loop generating functional $Z_{\mathrm{one-loop}}$ using heat-kernel methods [GL85]. For technical details, see section 5.2.

2.6 Pion-pion scattering

$\pi\pi$ scattering is the most important theoretical laboratory of low energy hadron physics. It is formally a very clean process and provides a testbed for our understanding of the way the left-right symmetry of QCD vacuum is spontaneously broken in nature. The way this breakdown, responsible for the very existence of the pions, is realized depends on the value of the crucial ordering parameter, the quark anti-quark vacuum condensate. Due to their Goldstone nature, the pions are the lightest hadrons, their kinematics is simple since they have spin 0, and they make up an SU(2) isospin triplet. Moreover the $\pi\pi$ scattering process displays full crossing symmetry and is unitary up to the $K\overline{K}$ threshold [2] at about 1 GeV. Unfortunately, experimentally, $\pi\pi$ scattering is not a very clean process because of the volatility of the pions. Sources of data were mentioned in the introduction (chapter 1). The $\pi\pi$ scattering amplitude to next-to-leading order was first calculated in [GL84]. In the context of the present work the process is important in that the pion (meson) (re)scattering is the main subject of coming chapters. In particular, the phase-shift is what we will need later for the analysis of final state interactions in $K \to \pi\pi$ decay.

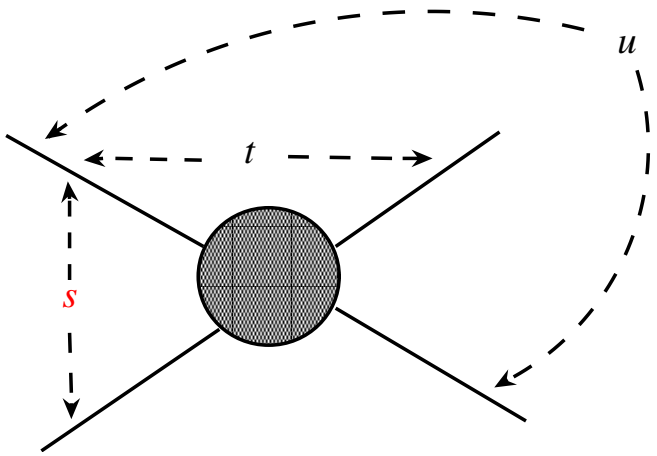

Figure 2.3: Kinematical channels of pion-pion scattering.

The amplitude T is defined by

$$\begin{aligned}&\langle\pi^m(p_4)\pi^l(p_3)\text{ out}|\pi^i(p_1)\pi^k(p_2)\text{ in}\rangle = \\ &\langle\pi^m(p_4)\pi^l(p_3)\text{ in}|\pi^i(p_1)\pi^k(p_2)\text{ in}\rangle \\ &+i(2\pi)^4\delta^{(4)}(P_\text{f}-P_\text{i})T^{ik;lm}(s,t,u),\end{aligned} \tag{2.34}$$

[2] The 4π state is heavily phase-space suppressed and we neglect it.

where

$$\begin{aligned} |\pi^1(m_{\pi^\pm},\vec{p})\rangle &= -\tfrac{1}{\sqrt{2}}\left(|\pi^+(m_{\pi^\pm},\vec{p})\rangle + |\pi^-(m_{\pi^\pm},\vec{p})\rangle\right), \\ |\pi^2(m_{\pi^\pm},\vec{p})\rangle &= \tfrac{i}{\sqrt{2}}\left(\langle\pi^+(m_{\pi^\pm},\vec{p})| - |\pi^-(m_{\pi^\pm},\vec{p})\rangle\right), \\ |\pi^3(m_{\pi^0},\vec{p})\rangle &= |\pi^0(m_{\pi^0},\vec{p})\rangle\,. \end{aligned} \tag{2.35}$$

Neglecting $m_u - m_d$ (see [GL84] for a discussion of the justification of this), there is full isospin symmetry ($m_{\pi^\pm} = m_{\pi^0}$) and thus full crossing symmetry:

$$\begin{aligned} T^{ik;lm}(s,t,u) &= \delta^{ik}\delta^{lm}A(s,t,u)+ \\ &\quad \delta^{il}\delta^{km}A(t,s,u)+ \\ &\quad \delta^{im}\delta^{kl}A(u,t,s), \end{aligned} \tag{2.36}$$

with s,t,u the usual Mandelstam variables

$$s = (p_1+p_2)^2,\quad t = (p_2+p_3)^2,\quad u = (p_2+p_4)^2\,. \tag{2.37}$$

Equation (2.36) defines A.

The amplitude $A(s,t,u)$, indexed with cartesian isospin indices i_1,i_2,i_3,i_4 of the 4 pions, reads (see section 5.4 and the notebook of appendix B for the calculation):

$$\begin{aligned} &A^{i_1,i_2,i_3,i_4}(s,t,u) = \delta_{i_1,i_2}\delta_{i_3,i_4}\Big[(s-m_\pi^2)/f_\pi^2 - \\ &(-21m_\pi^4 + 8m_\pi^2 s + 10s^2 + 3t^2 - 4tu + 3u^2)/(288 f_\pi^4\pi^2) + \\ &4(4(L_3 - 2L_4 - L_5 + 2L_6 + L_8)m_\pi^4 - 2(2L_3 - 2L_4 - L_5)m_\pi^2 s + \\ &L_3 s^2 + 2L_1(-2m_\pi^2 + s)^2 + L_2(8\,m_\pi^4 - 4m_\pi^2 s + s^2 - 2tu))/f_\pi^4 - \\ &(-7m_\pi^4 + 4m_\pi^2 s + 3s^2 + (t-u)^2)\log(m_\pi^2/\mu^2)/(96 f_\pi^4\pi^2) + \\ &(3(s^2 - m_\pi^4)\bar{J}_{m_\pi^2,m_\pi^2}(s) + \\ &(2m_\pi^4 - m_\pi^2(s + 3t - 3u) + t(t-u))\bar{J}_{m_\pi^2,m_\pi^2}(t) + \\ &(2m_\pi^4 + u(-t+u) - m_\pi^2(s - 3t + 3u))\bar{J}_{m_\pi^2,m_\pi^2}(u))/(6 f_\pi^4)\Big] + \\ &\delta_{i_1,i_4}\delta_{i_2,i_3}\Big[s \leftrightarrows t\Big] + \\ &\delta_{i_1,i_3}\delta_{i_2,i_4}\Big[s \leftrightarrows u\Big], \end{aligned} \tag{2.38}$$

where $\bar{J}$ is the Chew-Mandelstam function. We observe: 1) the divergent pieces drop as they should. Analogously, using (2.33), the amplitude is scale independent. 2) The amplitude is

fully crossing symmetric as it should be. 3) The bulk of the next-to-leading order correction comes from the non-analytic contributions ($\bar{J}$'s).

We define the partial wave amplitude T_l by

$$T_l(s) = \frac{1}{2}\int_{-1}^{1} \mathrm{d}z T(s,z) P_l(z), \tag{2.39}$$

where z is the cosine of the scattering angle and P_l is a Legendre polynomial. We moreover define the scattering length a_l^I and effective range b_l^I by

$$\mathrm{Re}T_l\left(q^2\right)/32\pi = q^{2l}\left(a_l + b_l q^2 + \ldots\right), \quad q^2 = s/4 - m_\pi^2. \tag{2.40}$$

With the values of the L_i's m_π and f_π of [JFDH92] we then get the s-wave scattering lengths of table 2.1[3].

	Leading order	Counter-terms	$O(p^4)$ Polynomial	log's	$\bar{J}$'s	Sum
a_0^0	0.16	0.015	-0.010	0.034	0.015	0.21 ± 0.01
a_0^2	-0.045	0.0015	-0.00095	0.0032	0.0013	-0.040 ± 0.002

Table 2.1: Contributions to s-wave $\pi\pi$ scattering lengths at renormalization scale $\mu = m_\rho = 770$ MeV.

[3]The experimental input used is:
$f_\pi = 93.3\,\mathrm{MeV}$, $m_\pi = 139.57\,\mathrm{MeV}$, $L_1 = 0.6510^{-3}$, $L_2 = 1.8910^{-3}$, $L_3 = -3.0610^{-3}$, $L_4 = 0$, $L_5 = 2.310^{-3}$, $L_6 = 0$, $L_8 = 1.210^{-3}$ at renormalization scale $\mu = m_\rho = 770$ MeV.
The values are chosen so as to get agreement with [GL84]. The value of f_π is the one used there; the value of the L_i's are those of of [JFDH92]; the value of m_π is the mass of the charged pion according to [GAA+00] (it is not given in [GL84]). Notice that the L_i's correspond to the counter-terms in the basis with of a matrix representation like the one used in [GL85] but with 2×2 SU(2) matrices. In [GL84] a different basis is used. The slight difference of the one-loop results there as compared to the ones given here arises because the SU(3) values of the L_i's have been used, thus neglecting the logarithms in the transition to SU(2), and because of numerical rounding errors.

Chapter 3

Charged pion-pion scattering

This chapter contains the calculation of the EM corrections to $\pi\pi$ scattering in CHPT. After a few introductory remarks on motivation, the introduction of virtual photons in CHPT is described. Then, the renormalization of the next-to-leading order lagrangian is derived, correcting a few minor misprints in the literature, and, finally, the amplitude is calculated and numerical scattering lengths to order e^2p^2 are given.

3.1 Introduction

As pointed out by Cirigliano, Donoghue and Golowich in [CDG00c], one missing ingredient in the full understanding of the FSI in K$\to 2\pi$ is the EM corrections to charged $\pi\pi$ scattering. This is the main motivation for the calculation presented here. Other points nevertheless deserve mention: 1) As mentioned in the introduction, the scattering lengths a_0^0 and a_0^2 may soon be measured with high precision (also within a few percent) if the DIRAC collaboration measures the energy difference between the 2S and 2P levels of pionium. 2) The corrections are expected to be of the same order of magnitude as the next-to-next-to leading order strong corrections, $\sim$ a few percent, and thus necessary for the extraction of the strong phase-shifts δ_0^0 and δ_0^2. 3) The calculation provides a nice check of the calculational package *PHI* (see chapter 5).

3.2 Virtual photons

Including virtual photons to leading order in CHPT was first touched upon by Ecker *et al.* in ref. [EGPdR89] and later systematically developed by Urech (for SU(3)) in [Ure95] and almost simultaneously by Neufeld and Rupertsberger in [NR96]. The SU(2) case as well as the calculation of the $\pi^0\pi^0 \to \pi^0\pi^0$ amplitude was done by Meissner, Müller and Steininger in

[MMS97]. Knecht and Urech calculated the $\pi^+\pi^- \to \pi^0\pi^0$ amplitude, and while writing this, the calculation of Knecht and Nehme of the $\pi^+\pi^- \to \pi^+\pi^-$ amplitude appeared [KN02].

To preserve chiral invariance, the coupling to the photon field is realized through the covariant derivative introducing two chiral spurions (additional external fields) Q_L, Q_R,

$$\begin{aligned} &D_\mu U \to d_\mu U = \\ &\partial_\mu U - i(v_\mu + Q_R A_\mu + a_\mu)U + iU(v_\mu + Q_L A_\mu - a_\mu), \end{aligned} \tag{3.1}$$

where A is the photon field. The spurions allow constructing additional chiral invariant terms which must be added to the lagrangians; e.g. to (2.25) we add

$$\mathcal{L}_2^{\mathrm{EM}} = -\tfrac{1}{4}F^{\mu\nu}F_{\mu\nu} - \tfrac{1}{2a}(\partial \cdot A)^2 + C\,\langle Q_R U Q_L U^\dagger \rangle\,. \tag{3.2}$$

3.3 Isospin breaking

The kinematics of the $\pi\pi$ scattering were discussed in section 2.6 in the strong case, where there is isospin symmetry, full crossing symmetry and thus only 3 independent isospin channels.

When EM interactions are switched on, although we still neglect $m_u - m_d$, the charged and neutral pions acquire a mass difference already to leading order and instead of one amplitude for the description of all $\pi\pi$ scattering processes we need 5:

$$\begin{aligned} T^{00;00} &= \tfrac{1}{3}(T^0)_{\mathrm{str}} + \tfrac{2}{3}(T^2)_{\mathrm{str}} + \Delta T^{00;00} \\ T^{+0;+0} &= \tfrac{1}{2}(T^2)_{\mathrm{str}} + \Delta T^{+0;+0} \\ T^{+-;00} &= -\tfrac{1}{3}(T^0)_{\mathrm{str}} + \tfrac{1}{3}(T^2)_{\mathrm{str}} + \Delta T^{+-;00} \\ T^{+-;+-} &= \tfrac{1}{3}(T^0)_{\mathrm{str}} + \tfrac{1}{6}(T^2)_{\mathrm{str}} + \Delta T^{+-;+-} \\ T^{++;++} &= (T^2)_{\mathrm{str}} + \Delta T^{++;++} \end{aligned} \tag{3.3}$$

If one-photon exchange Born terms are subtracted off, the crossing formula (2.36) is still valid, but isospin is violated anyway (because of the mass shift). The numerical shifts in the

scattering lengths were calculated by Knecht and Urech [KU98]:

$$\begin{aligned}
\Delta a_0(00;00) &= -\frac{\Delta_\pi}{32\pi F^2} \quad (-6.4\%)\\
\Delta a_0(+0;+0) &= \frac{\Delta_\pi}{32\pi F^2} \quad (+6.4\%)\\
\Delta a_0(+-;00) &= -\frac{\Delta_\pi}{32\pi F^2} \quad (-2.1\%)\\
\Delta a_0(+-;+-) &= \frac{\Delta_\pi}{16\pi F^2} \quad (+6.4\%)\\
\Delta a_0(++;++) &= \frac{\Delta_\pi}{16\pi F^2} \quad (+6.4\%)
\end{aligned} \tag{3.4}$$

Defining

$$\begin{aligned}
a_0^0 &\equiv (a_0^0)_{\text{str}} + 5\,\Delta_\pi 32\pi F^2 = 0.166\\
a_0^2 &\equiv (a_0^2)_{\text{str}} + \Delta_\pi 16\pi F^2 = -0.042,
\end{aligned} \tag{3.5}$$

we get

$$\begin{aligned}
a_0(00;00) &= \tfrac{1}{3}a_0^0 + \tfrac{2}{3}a_0^2 - \Delta_\pi 8\pi F^2\\
a_0(+0;+0) &= \tfrac{1}{2}a_0^2\\
a_0(+-;00) &= -\tfrac{1}{3}a_0^0 + \tfrac{1}{3}a_0^2\\
a_0(+-;+-) &= \tfrac{1}{3}a_0^0 + \tfrac{1}{6}a_0^2\\
a_0(++;++) &= a_0^2
\end{aligned} \tag{3.6}$$

As observed in [KU98], two effects can be discerned: 1) An overall shift of the two scattering lengths a_0^0, a_0^2. 2) An explicit isospin breaking correction to $a_0(00;00)$.

3.4 Divergent one-loop generating functional

The calculation of the generating functional proceeds along the same lines as the purely strong case (see chapters 2.5 and 5.2) but now with the modified covariant derivative (3.1) and the extra terms (3.2). In the end we set $Q_L = Q_R = Q$ and Q is expanded around $\begin{pmatrix} Q_u & & \\ & Q_d & \\ & & Q_s \end{pmatrix}$.

The physical fields must now be expanded around the solution to the EOM $\bar{U} = u^2, \bar{A}$, of

the extended lagrangian,

$$\begin{aligned} U &= u e^{i\sqrt{2}\epsilon/F} u = u\left(\mathbb{1} + i\sqrt{2}\tfrac{\epsilon}{F} - \tfrac{\epsilon^2}{F} + \cdots\right) u, \\ \epsilon &= \xi^i \sigma^i, \\ A_\mu &= \bar{A}_\mu + \xi_\mu. \end{aligned} \tag{3.7}$$

The complete calculation is done in a notebook in appendix B. Because a few misprints in the existing literature were found, we give here our result for SU(2)

$$\begin{aligned} &\tfrac{1}{12}\,\mathrm{Tr}\left(\hat{\Gamma}^{\mu\nu}\hat{\Gamma}_{\mu\nu}\right) + \tfrac{1}{2}\,\mathrm{Tr}\left(\hat{\sigma}^2\right) = \\ &\tfrac{1}{12}\langle\, d^\mu U^\dagger d_\mu U\,\rangle^2 + \tfrac{1}{6}\langle d^\mu U^\dagger d^\nu U\,\rangle\langle\, d_\mu U^\dagger d_\nu U\,\rangle \\ &-\tfrac{1}{32}\langle\, \chi^\dagger U + U^\dagger\chi\,\rangle^2 + \tfrac{1}{2}\langle\, d^\mu U^\dagger d_\mu\chi + d^\mu\chi^\dagger d_\mu U\,\rangle \\ &-\tfrac{1}{6}\langle\, G^{\mathrm{R}}_{\mu\nu} U G^{L\,\mu\nu} U^\dagger\,\rangle - \tfrac{i}{6}\langle\, G^{\mathrm{R}}_{\mu\nu} d^\mu U d^\nu U^\dagger + G^{\mathrm{L}}_{\mu\nu} d^\mu U^\dagger d^\nu U\,\rangle \\ &+\tfrac{1}{2}\langle\,\chi^\dagger\chi\,\rangle - \tfrac{1}{12}\langle\, G^{\mathrm{R}}_{\mu\nu} G^{R\,\mu\nu} + G^{\mathrm{L}}_{\mu\nu} G^{L\,\mu\nu}\,\rangle + \\ &\mathrm{Re}(\det\chi) + \tfrac{1}{6}\langle\, Q\,\rangle^2 F^{\mu\nu} F_{\mu\nu} \\ &-\tfrac{3F^2}{4}\langle\, d_\mu U^\dagger d_\mu U\,\rangle\langle\, Q^2_{\mathrm{R}} + Q^2_{\mathrm{L}}\,\rangle + \left(\tfrac{3}{4} - Z\right) F^2\langle\, d^\mu U^\dagger d_\mu U\,\rangle\langle\, Q\,\rangle^2 \\ &+2ZF^2\langle\, d^\mu U^\dagger d_\mu U\,\rangle\langle\, Q_{\mathrm{R}} U Q_{\mathrm{L}} U^\dagger\,\rangle \end{aligned} \tag{3.8}$$

$$
\begin{aligned}
&-\tfrac{3F^2}{4}\left(\langle\, d^\mu U^\dagger Q_{\rm R} U\,\rangle\langle\, d_\mu U^\dagger Q_{\rm R} U\,\rangle + \langle\, d^\mu U^\dagger Q_{\rm L} U^\dagger\,\rangle\langle\, d_\mu U Q_{\rm L} U^\dagger\,\rangle\right)\\
&+2ZF^2\langle\, d^\mu U^\dagger Q_{\rm R} U\,\rangle\langle\, d_\mu U Q_{\rm L} U^\dagger\rangle - \tfrac{F^2}{8}\langle\chi^\dagger U + U^\dagger\chi\,\rangle\langle\, Q_{\rm R}^2 + Q_{\rm L}^2\,\rangle\\
&-ZF^2\langle\chi^\dagger U + U^\dagger\chi\,\rangle\langle\, Q\,\rangle^2 + \left(\tfrac{1}{4}+2Z\right)F^2\langle\chi^\dagger U + U^\dagger\chi\,\rangle\langle\, Q_{\rm R} U Q_{\rm L} U^\dagger\,\rangle\\
&+\left(\tfrac{1}{8}-Z\right)F^2\langle\,(\chi U^\dagger - U\chi^\dagger) Q_{\rm R} U Q_{\rm L} U^\dagger + (\chi^\dagger U - U^\dagger\chi) Q_{\rm L} U^\dagger Q_{\rm R} U\,\rangle\\
&+\tfrac{F^2}{4}\langle\, d_\mu U^\dagger[(c_{\rm R}^\mu Q_{\rm R}), Q_{\rm R}]U + d_\mu U[(c_{\rm L}^\mu Q_{\rm L}), Q_{\rm L}]U^\dagger\,\rangle\\
&+\left(\tfrac{3}{2}+3Z+12Z^2\right)F^4\langle\, Q_{\rm R} U Q_{\rm L} U^\dagger\,\rangle^2 - \tfrac{3F^4}{2}\langle\, Q_{\rm R} U Q_{\rm L} U^\dagger\,\rangle\langle\, Q_{\rm R}^2 + Q_{\rm L}^2\,\rangle\\
&-\left(3Z+12Z^2\right)F^4\langle\, Q_{\rm R} U Q_{\rm L} U^\dagger\,\rangle\langle\, Q\,\rangle^2 + \left(\tfrac{3}{8}-\tfrac{3Z}{4}+Z^2\right)F^4\langle\, Q_{\rm R}^2 + Q_{\rm L}^2\,\rangle^2\\
&+\left(\tfrac{3Z}{2}-2Z^2\right)F^4\langle\, Q_{\rm R}^2 + Q_{\rm L}^2\,\rangle\langle\, Q\,\rangle^2 - \tfrac{1}{4}Z^2F^4\langle\, Q_{\rm R}^2 - Q_{\rm L}^2\,\rangle^2 + 4Z^2F^4\langle\, Q\,\rangle^4,
\end{aligned}
$$

where $\hat{\Gamma}$ and $\hat{\sigma}$ are the usual heat-kernel quantities (see e.g. [KU98] or [GL85]) and the covariant derivatives of the sources $Q_{\rm L}(x)$ and $Q_{\rm R}(x)$ are

$$
c_\mu^I Q_I = \partial_\mu Q_I - i[G_\mu^I, Q_I], \quad I = {\rm R}, {\rm L}\,, \tag{3.9}
$$

whereas $G_{\mu\nu}^{\rm R}$ and $G_{\mu\nu}^{\rm L}$ are the field strength tensors of $G_\mu^{\rm R}$ and $G_\mu^{\rm L}$, respectively,

$$
G_{\mu\nu}^I \;=\; \partial_\mu G_\nu^I - \partial_\nu G_\mu^I - i\left[G_\mu^I, G_\nu^I\right]\,, \qquad\qquad I = {\rm R}, {\rm L}. \tag{3.10}
$$

The only differences as compared to [KU98] are: 1) The term

$$
\frac{F^2}{4}\langle\, d_\mu U^\dagger Q_{\rm R} U(c_{\rm L}^\mu Q_{\rm L}) + d_\mu U Q_{\rm L} U^\dagger (c_{\rm R}^\mu Q_{\rm R})\,\rangle \tag{3.11}
$$

is not present, because when specializing to SU(2) it cancels with the term

$$
\frac{F^2}{4}\langle\, d_\mu U(c_{\rm L}^\mu Q_{\rm L}) U^\dagger Q_{\rm R} + d_\mu U^\dagger (c_{\rm R}^\mu Q_{\rm R}) U Q_{\rm L}\,\rangle, \tag{3.12}
$$

which is not present in the SU(N) result of [KU98]. 2) the factor $\frac{1}{4}$ on the second last term.

3.5 One-loop amplitudes

Again, the full calculation is done in a notebook in appendix B. The full result for $\pi^+\pi^- \to \pi^+\pi^-$ is given in appendix C. Notice that:

- The expressions in section C.1.1 are in terms of unrenormalized pion decay constant f.
- The $\mathcal{O}(e^4)$ contributions are expected to be small and are not included here. The evaluation of these contributions will be presented elsewhere.
- The soft photon diagrams do not contribute to the scattering lengths, but should be included in a full calculation of the amplitude. The evaluation of these contributions will also be presented elsewhere.

The values of the corrections to the strong $\pi^+\pi^- \to \pi^+\pi^-$ scattering length a_0^{+-+-} are given in table 3.1[1]. Notice the following:

- The corrections given are with respect to the strong scattering length evaluated using the neutral pion mass.
- Here, the expressions used are in terms of the renormalized pion decay constant f_π .
- The renormalization scale used is $\mu = m_\rho = 770$ MeV.
- The value $\frac{1}{16\pi^2}$ has been used for the $k_i(\mu = m_\rho)$.
- The error estimate comes from varying this to $-\frac{1}{16\pi^2}$ and from the errors on the pion mass and decay constant.

[1]The experimental input used is:
$e = \sqrt{4\pi/137}$, $f_\pi = 92.4\,\text{MeV}$, $m_{\pi^+} = 139.57\,\text{MeV}$, $m_{\pi^0} = 134.976\,\text{MeV}$, $\bar{l}_1 = -2.3$, $\bar{l}_2 = 6.0$, $\bar{l}_3 = 2.9$ at renormalization scale $\mu = m_\rho = 770$ MeV.
These values are the same as those used in [KN02]. The basis used for the strong counter-term lagrangian is that of [GL84] but expressed in terms of 2×2 matrices, following [KU98].

	Leading order	Counter-terms	$O(p^4)$ Polynomial	log's	$\bar{J}$'s	C_0's	Sum
$10^3 \Delta a_0^{+-+-}$	5.9	0.74	12	-0.85	-15	0.001	2.6 ± 2

Table 3.1: EM corrections to the scattering length a^{+-+-}.

Chapter 4

Final state interactions in non-leptonic kaon decays

The process studied in this chapter is $K\to\pi\pi$. For this purpose the general theory of dispersion relations and mesonic final-state interactions (FSI) is discussed, following the approach of Omnès, and a short introduction to soft pions is given. Finally, the theory is applied to $K\to\pi\pi$. For the same purpose, the full one-loop CHPT expressions of $K\to\pi$ and $K\to\pi\pi$ with a momentum carrying weak lagrangian have been worked out using the software presented in chapter 5.

4.1 Introduction

The $K\to\pi\pi$ amplitude has been the subject of numerous studies over the years, the main challenge being either to explain the $\Delta I = 1/2$ rule or to provide a reliable estimate of ε'/ε [BBG86, BBG87b, BBG87a, KMW91, BEFL98a, BEFL98b, BP99, BP00, HKS99, HKPS00, Lel01]. Among these attempts, the lattice approach is in principle the most rigorous as the weak matrix elements are calculated from first principles in a truly non-perturbative way. However, the inclusion of FSI is problematic. The calculation of the $K\to\pi\pi$ amplitude, e.g., proceeds by calculating the $K\to\pi$ amplitude on the lattice and using CHPT at tree level to obtain the physical decay amplitude [BDS+85]. As is well known, the latter step induces a sizable uncertainty in the final result, commonly estimated to be around 30%, the typical size of next-to-leading order (NLO) corrections in chiral SU(3). To discuss the relation between the $K\to\pi\pi$ and the $K\to\pi$ amplitude, it is necessary to allow the weak Hamiltonian to carry momentum. Then the former amplitude becomes a function of the usual three Mandelstam variables s, t and u, and is identified with the physical decay amplitude at the point $s = m_K^2$, $t = u = m_\pi^2$. At the

so-called soft-pion point (SPP), where the momentum of one of the two pions is sent to zero, this amplitude is related to the $K \to \pi$ amplitude, up to $\mathcal{O}(m_\pi^2)$ corrections. The problem is how to extrapolate the amplitude from the SPP to the physical point. The only working method proposed so far has been to use CHPT at tree level [BDS+85] - using the one-loop relation does not solve the problem because a number of unknown low energy constants appear [BPP98].

In section 4.2 the physical motivation for our calculation is briefly reviewed.

In sections 4.3, 4.4 and 4.5 the dispersive machinery is set up and discussed using the isosinglet pion scalar form factor (SFF) and the $K \to 2\pi$ amplitude to leading order (LO).

Truong [Tru88], and more recently Pallante and Pich [PP00], have stressed the importance of FSI in $K\to \pi\pi$, for the $\Delta I = 1/2$ rule and ε'/ε, respectively. In estimating these effects they rely on a dispersion relation for the $K\to \pi\pi$ amplitude with the kaon off-shell. While the method provides a quick and simple estimate of the effect of FSI, it is not trivial to promote it to a systematic and rigorous calculation. The problems related to the formulation and the use of dispersion relations for an off-shell amplitude are touched upon in section 4.5. For a full discussion, see [BCKO01b].

In section 4.6 the soft pion theorem is introduced in general form and specialized to the case of $K \to 2\pi$ needed for the following sections.

In section 4.7 a dispersive framework for the $K\to \pi\pi$ amplitude is set up. In section 4.8 it is shown that by solving numerically the dispersion relations one can do the extrapolation in a controlled manner. The unitarity corrections due to rescattering of the pions in the final state, and those due to πK (virtual) rescattering in the t- and u-channel, can be accurately accounted for by solving the dispersion relations. These effects, which also appear to one loop in CHPT, are not the only sources of possible large corrections to tree level: Two subtraction constants appear which may also suffer from large $\mathcal{O}(m_K^2)$ corrections. The soft-pion theorem provides the means to determine one of the two subtraction constants, up to terms of order m_π^2. The other constant (the derivative in s of the amplitude at the SPP) is unfortunately not yet determined with the same accuracy, and at present can be estimated only with tree-level CHPT. A better determination of this constant is the core of the problem. Once solved, the $K\to \pi\pi$ amplitude can be obtained with substantially smaller uncertainties than at present.

Finally, outlook and conclusions are given in section 4.9.

4.2 Kaon phenomenology and FSI

The two main puzzles of kaon CP phenomenology are the $\Delta I = 1/2$ rule and the large experimental value of ε'/ε.

The $\Delta I = 1/2$ rule, that the $I = 2$ $K\to 2\pi$ amplitude $\mathcal{A}^2$ is heavily suppressed compared to

$\mathcal{A}^0$, stems from the experimental fact that

$$\frac{\Gamma(K^0 \to \pi^0\pi^0)}{\Gamma(K^+ \to \pi^+\pi^0)} \approx 200. \tag{4.1}$$

One can attempt a naive analysis based using lowest order W^+ exchange diagrams as in figs. 4.1 and 4.2. This approximation is known as naive factorization. As seen from fig. 4.2, $\Gamma(K^0 \to \pi^0\pi^0)$ should be expected to be suppressed. The experimental evidence for the contrary, signals large corrections due to the strong interaction. That these corrections are due

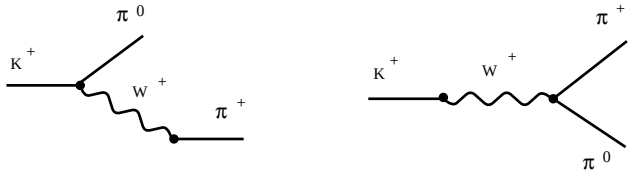

Figure 4.1: The two naive W^+-exchange diagrams for $K^+ \to \pi^+\pi^0$.

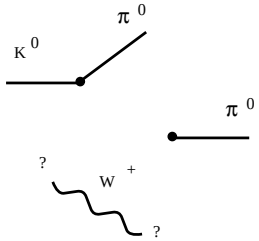

Figure 4.2: No simple W^+-exchange diagram is possible for $K^0 \to \pi^0\pi^0$.

to FSI is indicated by the large phase-shift difference of the $\mathcal{A}^0$ and $\mathcal{A}^2$ amplitudes: Large imaginary parts can arise through large contributions from mesonic rescattering diagrams.

If there were no CP violation, the CP eigenstates,

$$|K^{0\pm}\rangle \equiv \frac{1}{\sqrt{2}}\left(|K^0\rangle \pm |\bar{K}^0\rangle\right), \tag{4.2}$$

would be mass eigenstates and would decay only into CP even states like 2π and CP odd states like 3π respectively. Moreover, Watson's final state theorem (see section 4.5) would be exact (up to unitarity) and we would have

$$\mathcal{A}^0 = A^0 e^{i\delta_0^0}, \quad \mathcal{A}^2 = A^2 e^{i\delta_0^2}, \tag{4.3}$$

where δ_l^I is the isospin I, angular momentum l, $\pi\pi$ scattering phase-shift and $A = |\mathcal{A}|$.

However, CP *is* violated, K and $\overline{\mathrm{K}}$ mix, and the mass eigenstates are

$$|K_{\substack{\mathrm{L}\\\mathrm{S}}}\rangle = \frac{1}{1+|\overline{\varepsilon}|^2}\left(|\mathrm{K}^{0\mp}\rangle + \overline{\varepsilon}\,|\mathrm{K}^{0\pm}\rangle\right). \tag{4.4}$$

Moreover, Watson's final state theorem (which relies on T invariance) is not exact and

$$\mathcal{A}^0 = A^0 e^{i\xi^0} e^{i\delta_0^0}, \quad \mathcal{A}^2 = A^2 e^{i\xi^2} e^{i\delta_0^2}. \tag{4.5}$$

The violation of CP is usually expressed in terms of the parameters ε and ε',

$$\begin{aligned} \frac{\langle\pi^+\pi^-|\,\mathcal{H}_{\mathrm{W}}\,|\mathrm{K_L}\rangle}{\langle\pi^+\pi^-|\,\mathcal{H}_{\mathrm{W}}\,|\mathrm{K_S}\rangle} &\equiv \varepsilon + \varepsilon', \\ \frac{\langle\pi^0\pi^0|\,\mathcal{H}_{\mathrm{W}}\,|\mathrm{K_L}\rangle}{\langle\pi^0\pi^0|\,\mathcal{H}_{\mathrm{W}}\,|\mathrm{K_S}\rangle} &\equiv \varepsilon - 2\varepsilon', \end{aligned} \tag{4.6}$$

where $\mathcal{H}_{\mathrm{W}}$ is the weak hamiltonian and

$$\begin{aligned} \varepsilon &= \overline{\varepsilon} + i\xi^0, \\ \varepsilon' &= \frac{ie^{i\left(\delta_0^2-\delta_0^0\right)}}{\sqrt{2}}\left|\frac{A^2}{A^0}\right|\left(\xi^2-\xi^0\right). \end{aligned} \tag{4.7}$$

We observe that ε' has the phase [1] $\delta_0^2 - \delta_0^0$ and that ε'/ε depends on four different decay rates. Since the treatment of FSI is the same for all four, we shall consider only $\mathrm{K_s} \to \pi^0\pi^0$.

The experimental world average of ε'/ε is [B$^+$88, B$^+$93, G$^+$93, AH$^+$99, F$^+$99] $(19.3 \pm 2.4)\ 10^{-4}$. In contrast hereto, the Standard Model calculations [Jam99, Bur99, B$^+$00, BBL96, BJLW92, BJLW93, BJL93, CFG$^+$99, C$^+$98, CFMR94, CFMR93, CM01a] yield a considerably lower number; typically around $7.0 \cdot 10^{-4}$.

The claim in [PP01, PP00] is that this discrepancy is remedied if the strong final state rescattering of the pions is taken into account in the calculation of the $\mathrm{K} \to 2\pi$ decay constant $\mathcal{A}^I$, not only through the rescattering phase in (4.3), but also through the inclusion of higher-order corrections to A^I. To display the correction explicitly, it is factored out:

$$\mathcal{A}^I \equiv \left(m_{\mathrm{K}}^2 - m_\pi^2\right)\mathcal{R}^I(m_{\mathrm{K}}^2, s_0)A^I(s_0)e^{i\delta_0^I}, \tag{4.8}$$

[1] The phase-shifts were worked out in CHPT by Gasser and Meissner in [GM91b]; they found that although CHPT should in principle not be very reliable at the kaon mass, for this particular difference, higher order corrections largely cancel.

where A^I is now the Standard Model result with no FSI corrections and s_0 is the subtraction point used for the dispersive evaluation of the FSI corrections (to be discussed in the following chapters).

For an overview of the experimental status and the many calculational intricacies including FSI related to the $\Delta I = 1/2$ rule and ε'/ε, see ref. [BEF01, Ber00, Ber02] and references therein. Other corrections to $K \to \pi\pi$ that are potentially important for the understanding of these phenomena are isospin breaking EM effects, which have been discussed in a series of papers by Cirigliano, Donoghue and Golowich [CDG00a, CDG00b, CDG00b]. These authors set up a full framework for evaluating EM FSI in the absence of isospin symmetry. They find no sizeable shift in the theoretical prediction for ε'/ε, but do find that the uncertainties of $\mathcal{A}^I$ are enhanced by 0.6% and 4% for $I = 0$ and $I = 2$ respectively which translates into $\sim 4\%$ for $\mathcal{A}^{K_s \to 2\pi^0} = \sqrt{\frac{2}{3}}\mathcal{A}^0 - \frac{2}{\sqrt{3}}\mathcal{A}^2$. Notice that in our treatment of FSI, we assume isospin symmetry. A complete treatment of all corrections would be desirable.

4.3 Off-shell matrix elements in CHPT

Mesonic physical scattering amplitudes and decay rates are on-shell Green's functions calculable in CHPT using functional differentiation of Feynman diagram techniques considering only the meson fields collected in the matrix U. In order to continue these amplitudes beyond the physical values of the momenta, one must consider not the Green's functions of the meson fields, but instead the Green's functions of external pseudo-scalar sources coupled to the meson fields [GL84, GL85]. Other familiar examples of Green's functions involving source fields include the scalar and vector form factors. In SU(2) CHPT the SFF F_s is defined by

$$\begin{aligned} \langle \varphi^b(p')| \bar{u}u + \bar{d}d \,|\varphi^a(p)\rangle &= \langle \varphi^b(p'), s|\varphi^a(p)\rangle \\ &\equiv \delta_{ab} F_s(s), \end{aligned} \tag{4.9}$$

where s is the usual Mandelstam variable and s is the scalar isosinglet external source. With the two pions on the mass-shell, to order $\mathcal{O}(p^4)$ we find in SU(2) by straightforward evaluation

of Feynman diagrams (see appendix B) with the two first chiral lagrangians (See chapter 2).

$$\begin{aligned} F_s(s) = -2B_0 - \tfrac{B_0}{f_\pi^2}\Big[& -2s/(16\pi^2) \\ & +2s\bar{J}(s,m_\pi^2) - m_\pi^2\bar{J}(s,m_\pi^2)+ \\ & s(8(2L_4+L_5) - 2\log(m_\pi^2/\mu^2)/(16\pi^2))+ \\ & m_\pi^2(-32(2L_4+L_5-2(2L_6+L_8)) - (2\log(m_\pi^2/\mu^2)+1)/(16\pi^2))\Big], \end{aligned} \tag{4.10}$$

where s is the usual Mandelstam variable.

Exactly the same can of course be done for the SFF in SU(3),

$$\begin{aligned} \langle\varphi^b(p')|\,\bar{u}u+\bar{d}d+\bar{s}s\,|\varphi^a(p)\rangle &= \langle\varphi^b(p'),\mathrm{s}|\varphi^a(p)\rangle \\ &\equiv F_s^{ab}(s). \end{aligned} \tag{4.11}$$

Here the general result $F_s^{ab}(t)$ has a more complicated isospin structure (see appendix B) and it is better written for fixed isospins, e.g. $a=b=3$:

$$\begin{aligned} F_s^{33}(s) = -2B_0 - \tfrac{B_0}{f_\pi^2}\Big[& -3s/(16\pi^2) \\ & +s(\bar{J}(s,m_K^2)+2\bar{J}(s,m_\pi^2)) \\ & -m_\pi^2(-1/3\bar{J}(s,m_\eta^2)+\bar{J}(s,m_\pi^2)) \\ & -4m_K^2(8(L_4-2L_6)+\log(m_\eta^2/\mu^2)/(144\pi^2))- \\ & s(24L_4+8L_5+(9\log(m_K^2/\mu^2)+18\log(m_\pi^2/\mu^2))/(144\pi^2))- \\ & 2m_\pi^2(16(2L_4+L_5-4L_6-2L_8)+ \\ & (-3+\log(m_\eta^2/\mu^2)-9\log(m_\pi^2/\mu^2))/(144\pi^2))\Big], \end{aligned} \tag{4.12}$$

where we have neglected isospin breaking and set $m_{K^\pm} = m_{K^0}$. We observe that the non-polynomial contributions which stem from the meson loop pick up additional contributions

from the kaon and the eta when going to from SU(2) to SU(3). The numerical [2] difference is displayed in fig. 4.3. E.g. at $s = m_K^2$ the difference is $\sim 1\%$.

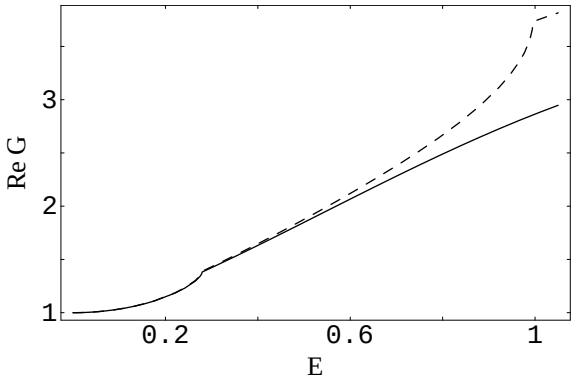

Figure 4.3: Real part of the next-to-leading order isosinglet pion scalar form factor $G(s) \equiv F(s)/F(0)$ as function of the energy $E = \sqrt{s}$ in units of GeV. The solid line is SU(2), the dashed line is SU(3).

The central quantity to be discussed later is the off-shell kaon decay rate. We define (SU(N) indices are suppressed)

$$\begin{aligned}\tau(k^2, p_1^2, p_2^2) \equiv i \int \mathrm{d}^4x \int \mathrm{d}^4y_1 \int \mathrm{d}^4y_2\, e^{ik\cdot x} e^{ip_1\cdot y_1} e^{ip_2\cdot y_2} \\ \left\langle 0 \left| T\left(j_K^\dagger(x) j_{\pi,1}(y_1) j_{\pi,2}(y_2) e^{i(\mathcal{L}^S)} \mathcal{L}^W \right) \right| 0 \right\rangle,\end{aligned} \tag{4.13}$$

where j_K is a source coupling to the kaon field and $j_{\pi,1}$ is a source coupling to one of the pion fields and $j_{\pi,2}$ is a source coupling to the other, $\mathcal{L}_S$ is the strong CHPT lagrangian [GL85] and $\mathcal{L}^W$ is the weak CHPT lagrangian $\mathcal{L}^8_{W,\Delta S=1}$ of [EKW93]. τ is a three-point Green's function with general momenta k, p_1, p_2, not necessarily on the mass-shell. Putting p_1, p_2 on the mass-shell, we define

$$A(k^2) \equiv X \lim_{\substack{p_1^2 \to m_\pi^2 \\ p_2^2 \to m_\pi^2}} (k^2 - m_K^2)(p_1^2 - m_\pi^2)(p_2^2 - m_\pi^2)\tau(k^2, p_1^2, p_2^2), \tag{4.14}$$

X is a factor, depending on the choice of source field, such that the residue at $k^2 = m_K^2$ is the decay rate $\mathcal{A}$,

$$A(m_K^2) = \mathcal{A}. \tag{4.15}$$

[2] The experimental input used is:
$f_\pi = 93.3\,\mathrm{MeV}$, $m_\pi = 139.57\,\mathrm{MeV}$, $m_K = 497.672\,\mathrm{MeV}$, $m_\eta = 547.30\,\mathrm{MeV}$.

In a Feynman diagram calculation of the (on-shell) decay constant, one needs of course only calculate the diagrams without the source field j_K coupling directly to the pions. To calculate the *off-shell* function $A(k^2)$, it is necessary to include *all* relevant diagrams. If this is not done, the function is not well-defined and higher order corrections are not finite. The form of the so calculated off-shell function $A(k^2)$, depends on the choice of the source field j_K. Staying within mesonic CHPT there are at least two possible choices: A pseudo-scalar field P and an axial-vector field A^μ, both with the same quantum numbers as the kaon.

To illustrate the point we calculate the lowest order form of A, using the leading weak lagrangian of [EKW93],

$$\begin{aligned} \mathcal{L}^8_{W,2,\Delta S=1} &= c_2 \langle \lambda_6 D_\mu U^\dagger D^\mu U\rangle + c_5 \langle \lambda_6 \left({}^\dagger\chi + \chi^\dagger U\right)\rangle, \\ D_\mu &= \partial_\mu U - i r_\mu U + i U l_\mu, \\ \chi &= 2B_0(s+ip), \end{aligned} \tag{4.16}$$

with s, p, v, a the scalar, pseudo-scalar, vector and axial-vector external fields respectively and s expanded around the quark mass matrix. For the source field coupled to the kaon taken to be a pseudo-scalar field P_{K_s} and an axial-vector field $A^\mu_{K_s}$ respectively, we get

$$\begin{aligned} A^{P_{K_s}\to 2\pi^0}(k^2) &= \tfrac{1}{i\sqrt{2}}\tfrac{-2i}{3f_\pi^3 m_K^2}(c_2 3m_K^2(k^2-m_\pi^2) - \\ &\quad c_5(k^2-m_K^2)(m_\pi^2+2m_K^2)), \end{aligned} \tag{4.17}$$

$$A^{A^\mu_{K_s}\to 2\pi^0}(k^2) = \frac{1}{i\sqrt{2}}\frac{-ic_2}{f_\pi^3}(k^2-2m_\pi^2+m_K^2), \tag{4.18}$$

with slopes

$$\tfrac{\partial}{\partial k^2}A^{P_{K_s}\to 2\pi^0}(k^2) = \tfrac{1}{i\sqrt{2}}\tfrac{-2i}{3f_\pi^3 m_K^2}(c_2 3m_K^2 - c_5(m_\pi^2+2m_K^2)), \tag{4.19}$$

$$\frac{\partial}{\partial k^2}A^{A^\mu_{K_s}\to 2\pi^0}(k^2) = \frac{1}{i\sqrt{2}}\frac{-ic_2}{f_\pi^3}. \tag{4.20}$$

In the on-shell limit the two expressions of course become identical. Whichever source field is chosen, A will satisfy (4.15). Away from $k^2 = m_K^2$, $A(k^2)$ will have quite differing shapes, depending on the choice of source field. As will be elaborated in the next sections, it is possible to use analyticity to determine $A(m_K^2)$, *provided* $A(k^2)$ is known (better) at some other $k^2 = s_0$.

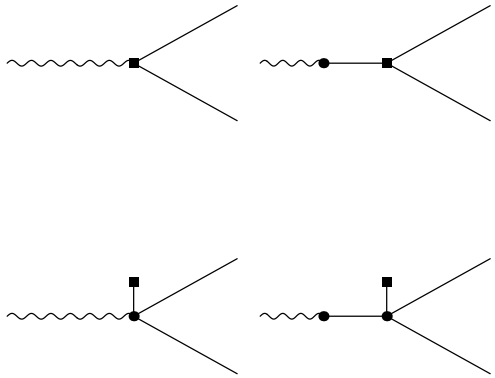

Figure 4.4: Lowest order Feynman diagrams for an off-shell 'kaon source' decaying into two pions.

4.4 Dispersion theory

4.4.1 Elastic unitarity, analyticity and crossing

Unitarity is the assumption that the S matrix is unitary:

$$S^{\dagger}S = 1. \tag{4.21}$$

This implies a relation for the amplitude T defined by

$$S_{fi} = \delta_{fi} + i\,(2\pi)^4\,\delta^4\left(P_f - P_i\right)T_{fi}. \tag{4.22}$$

Elasticity is the assumption that no other states couple to the initial state. Elastic unitarity for $\pi\pi \to \pi\pi$ partial wave amplitudes T_l has a *very* simple form (in contrast to crossing):

$$\begin{gathered} \mathrm{Im}T_l = \rho|T|^2, \mathrm{Im}T_l^{-1} = -\rho, \\ \rho = \sqrt{1 - 4m_\pi^2/s}. \end{gathered} \tag{4.23}$$

It is valid for physical values of the momenta. Since it is a non-linear relation in T, it can be used to evaluate the higher-order corrections or FSI corrections to T. Elastic unitarity for a three-point amplitude F with spinless initial state and $\pi\pi$ final state reads

$$\mathrm{Im}F(s) = \rho(s)T_0^*(s)F(s) \tag{4.24}$$

As for any process with only a $\pi\pi$ final state, solving it with some low order F as input provides a means of evaluating a certain class of higher order corrections to F; the so-called FSI or unitarity corrections coming from the interactions of the two pions: (4.24) allows the resummation of the final state diagrams to *all* orders, but does not tell us anything about the contributions from diagrams where the initial particle or source couples via higher order vertices to the two final pions. That is, given enough information on the $\pi\pi$ amplitude, we can resum all contributions from the right-hand blob of the "cut" diagram of fig. 4.5. For the left-hand vertex we must provide the input, e.g. using CHPT to some order. Contributions that cannot be "cut" in this way are not addressed by this method. For the case of the $I = 0$ s-wave it is known [GM91a] that the final state interactions are very strong and dominate the higher order corrections.

Crossing symmetry (or just crossing) entails the following: With the corresponding choice of momenta and quantum numbers $p_1, p_2, \ldots$, *one* amplitude $T(p_1, p_2, \ldots)$ describes the processes in all channels obtained by interchanging the particles (and changing the sign of the amplitude appropriately).

Analyticity is the assumption that a scattering or decay amplitude T is an analytic function of Lorentz invariant variables, e.g. the Mandelstam variables s, t, u, except for the cuts and singularities demanded by kinematics and resonance poles, unitarity and crossing. E.g. for the case of $\pi\mathrm{K} \to \pi\mathrm{K}$, the amplitude $T(s,t,u)$ is said to be *su*-crossing symmetric; it describes $\pi\mathrm{K} \to \pi\mathrm{K}$ in both the *s*- and *u*-channel and $\pi\pi \to \bar{\mathrm{K}}\mathrm{K}$ scattering in the *t*-channel with the variables in the regimes of fig. 4.6. Between the physical regions *analytic continuation* has to be used.

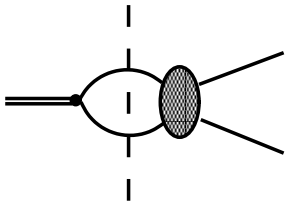

Figure 4.5: "Cut" unitarity diagrams for a three-point amplitude.

4.4.2 Dispersion relations for scattering amplitudes

Consider some scattering process $1 + 2 \to 3 + 4$. It is convenient to specialize to the center of mass system and define the magnitude of the initial and final three-momenta q, q' and cosine

of the scattering angle z. One then has

$$\begin{aligned} s &= \left(\sqrt{q_{(s)}^2 + m_1^2} + \sqrt{q_{(s)}^2 + m_2^2}\right)^2 = \left(\sqrt{q'^2_{(s)} + m_3^2} + \sqrt{q'^2_{(s)} + m_4^2}\right)^2, \\ t &= \left(\sqrt{q'^2_{(s)} + m_3^2} - \sqrt{q_{(s)}^2 + m_2^2}\right)^2 - q_{(s)}^2 - q'^2_{(s)} + 2q_{(s)}q'_{(s)}z_{(s)}, \\ u &= \left(\sqrt{q'^2_{(s)} + m_3^2} - \sqrt{q_{(s)}^2 + m_1^2}\right)^2 - q_{(s)}^2 - q'^2_{(s)} - 2q_{(s)}q'_{(s)}z_{(s)}, \end{aligned} \tag{4.25}$$

with solutions

$$\begin{aligned} q_{(s)}^2 = \frac{\left[s-\left(m_1+m_2\right)^2\right]\left[s-\left(m_1-m_2\right)^2\right]}{4s}, \quad q'^2_{(s)} = \frac{\left[s-\left(m_3+m_4\right)^2\right]\left[s-\left(m_3-m_4\right)^2\right]}{4s}, \\ z_{(s)} = \frac{s(t-u)-\left(m_1^2-m_2^2\right)\left(m_3^2-m_4^2\right)}{4sq_{(s)}q'_{(s)}}, \end{aligned} \tag{4.26}$$

and similarly in the other channels (denoted by the subscript). From these equations one easily finds the regions of the physical processes in the three crossed channels. For the case of πK scattering these regions are displayed in fig. 4.6.

Dispersion relations are useful tools in relating the different energy regimes of amplitudes. Their application relies on the assumption of certain analyticity properties of the amplitudes, namely that the amplitudes have no other singularities than the ones arising from the singularities due to the kinematical right-hand cut and the exchange of particles in the direct and crossed channels. E.g. for elastic scattering of two particles of masses m_1 and m_2, su-crossing implies that the u-channel cut at $u > (m_1 + m_2)^2$ translates into an s-channel cut at $u < (m_1 - m_2)^2$ since $s + t + u = 2m_2^2 + 2m_2^2 \Rightarrow s - 2q^2(1 - z) + u = 2m_1^2 + 2m_2^2$. For partial waves, similar considerations show that poles in crossed channels give singularities on the cuts of the s-channel. For elastic scattering of two particles with different masses, the cut structure of the partial waves is displayed in fig. 4.7. Since the singularity structure is known, one can use Cauchy's theorem for the amplitude T_l to write

$$T_l(s) = \frac{1}{2\pi i}\int_{\mathrm{C}} \frac{T\,(s')\,\mathrm{d}s'}{s' - s}, \tag{4.27}$$

where C is some integration contour enclosing the singularities. If one further assumes sufficiently fast fall-off of T_l, contributions from circles at infinity can be dropped leaving the contour enclosing the singularities.

For the case of elastic $\pi\pi$ scattering, as we have seen in section 2.6, the scattering amplitude $T_l^I(s,t,u)$ displays full crossing symmetry and has only a left- and a right-hand cut, $[-\infty, s_{\mathrm{L}}]$ and $[s_{\mathrm{R}}, \infty]$ respectively. In the case of fixed t, $s_{\mathrm{L}} = -t, s_{\mathrm{R}} = 4m_\pi^2$. For partial waves, $s_{\mathrm{L}} =$

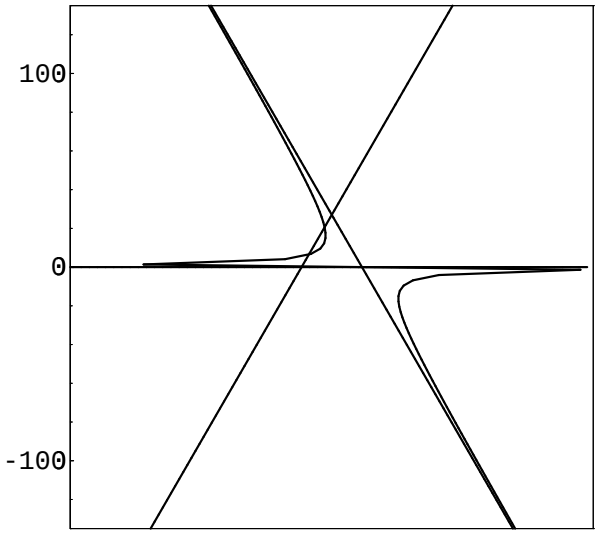

Figure 4.6: Kinematical boundaries of the Mandelstam variables, s, t, u in units of MeV^2 for elastic pion kaon scattering.

$0, s_R = 4m_\pi^2$. If T does not fall of sufficiently fast towards infinity (4.27) must be modified: Assuming that T_l^I approaches a constant at infinity, a *subtraction* at $s = s_0$ must be made,

$$\begin{aligned} T_l^I(s) &= T_l^I(s_0) + \\ &\frac{s-s_0}{\pi}\int_{-\infty}^{s_L}\frac{\mathrm{Im}T_l^I(s')}{(s'-s)(s'-s_0)}\mathrm{d}s' + \frac{s-s_0}{\pi}\int_{s_R}^{\infty}\frac{\mathrm{Im}T_l^I(s')}{(s'-s)(s'-s_0)}\mathrm{d}s', \end{aligned} \tag{4.28}$$

where we have used the following property of the amplitude:

$$\mathrm{Im}T(s) - \mathrm{Im}T(s^*) = 2\mathrm{Im}T(s). \tag{4.29}$$

This dispersion relation (with $I = l = 1$), with simple resonance form input in the crossed channels, was used in the sixties in the failed attempts, referred to in section 2.1, to use dispersion relations for dynamical calculations. This failure indicated that the left-hand cut structure needed to reproduce the physical amplitude was more subtle than what could be parameterized with a few resonances. A much more successful program was the use of dispersion relations in conjunction with experimental data as a way of analytically continuing the amplitudes beyond the experimentally accessible regions. In particular, the set of coupled dispersion equations

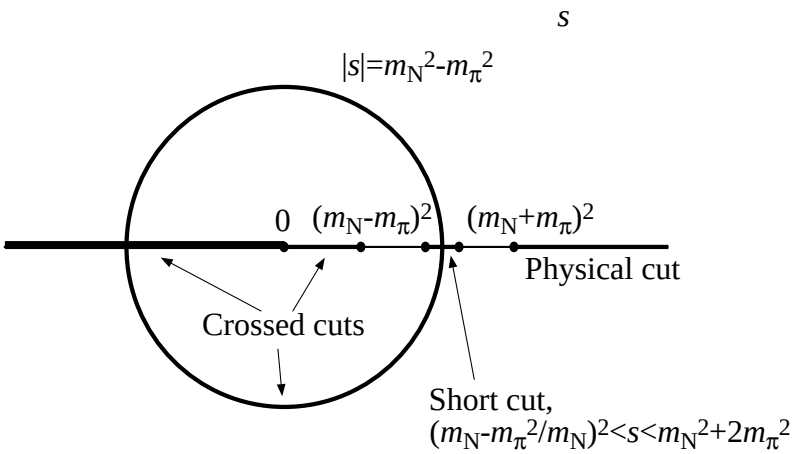

Figure 4.7: Singularities in the complex plane for the elastic scattering of two different masses.

known as the Roy equations were used to get the threshold parameters of $\pi\pi$ scattering. This method has recently been reapplied by Colangelo et al., using also the strictures from CHPT to calculate the current state of the art $\pi\pi$ phases and scattering lengths [ACGL01] (these are the phases we use in our analysis of K$\to 2\pi$ in section 4.8).

4.4.3 Dispersion relations for form factors

The main complication with a dispersive treatment of $\pi\pi$ scattering is the left-hand cut. For three-point amplitudes like form factors or decay amplitudes the situation is simpler; there are no physical crossed channel processes to produce cuts and we have only the kinematical right-hand cut at $s > (m_1 + m_2)^2$. The simplest three-point amplitude with a 2π final state we can think of is the SFF. One appealing property of the form factor of any current operator O, $\int \mathrm{d}x \langle\pi|O(x)|\pi\rangle$, is, that for large q, it will probe only a small region of space around the pion and will vanish for $q \to \infty$. This means that in principle we need not perform any subtractions. Another appealing quality of the SFF is, that although it is not directly measurable [3], a two-loop CHPT calculation [GM91a] as well as a full dispersive coupled channel analysis [DGL90] is available in the literature, providing what in principle replaces rather exact data. From this we know that there are no subthreshold zeros to worry about. Also, the one-loop expression (see below - and appendix B for a check of the calculation) is rather simple.

[3] It is one of the matrix elements needed to describe the decay of a light Higgs boson into two pions [DGL90].

We may write an unsubtracted dispersion relation,

$$F_s(s) = \frac{1}{\pi}\int_{s_R}^{\infty} \frac{\mathrm{Im}F_s(s')}{s'-s}\mathrm{d}s', \tag{4.30}$$

where $s_R = 4m_\pi^2$. The question here is then how to get $\mathrm{Im}F_s$ on the (right-hand) cut. This is the subject of the next section, where we shall consider a systematic way of resumming the chiral series using unitarity [4].

4.5 The Omnès method

4.5.1 General theory

Consider a three-point amplitude F like the SFF or the $K \to \pi\pi$ amplitude. Assume analyticity, elastic unitarity and that only one subtraction is needed. Then

$$\begin{aligned} F(s+i\epsilon) \equiv F(s) &= F(s_0) + \tfrac{1}{\pi}\int \mathrm{d}s' \left(\tfrac{\mathrm{Im}F(s')}{(s'-s)} - \tfrac{\mathrm{Im}F(s')}{(s'-s_0)}\right) \\ &= F(s_0) + \tfrac{s-s_0}{\pi}\int \mathrm{d}s' \tfrac{\mathrm{Im}F(s')}{(s'-s)(s'-s_0)}, \end{aligned} \tag{4.33}$$

where s_0 is an arbitrary subtraction point. Inserting a complete set of states, $\mathrm{Im}F$ can be identified with the spectral function σ [Omn58, Mus53, Bar65],

$$\mathrm{Im}F(s) = \sigma(s) = \frac{1}{2}\sum_n \left\langle \pi\pi; s \left| \mathcal{F}^\dagger \right| n \right\rangle \langle n|\mathrm{K}; s\rangle\,, \tag{4.34}$$

[4] An alternative approach is the so-called inverse amplitude method: Perturbative elastic unitarity, as satisfied by CHPT, reads

$$\mathrm{Im}F^{(0)} = 0, \mathrm{Im}F^{(2)} = \rho T_0^{0\,(2)}, \ldots\,. \tag{4.31}$$

Using this together with exact elastic unitarity and chiral expansion of T_0^0/F one gets the [0,1], [0,2], ... Padé approximants of F,

$$\begin{aligned} F_{[0,1]}(s) &= \tfrac{1}{1-F^{(2)}(s)}, \\ F_{[0,2]}(s) &= \tfrac{1}{1-F^{(2)}(s)+F^{(2)}(s)^2-F^{(4)}(s)}, \ldots\,. \end{aligned} \tag{4.32}$$

Gasser and Meissner showed in [GM91a] that if one expands these amplitudes in p the coefficients on the chiral logs come out wrong as compared to the true chiral expansion. What this means is that the Padé approximants do not resum the chiral series and are therefore of no help in evaluating the constants of the chiral lagrangians. They can be seen as a CHPT inspired parameterization of the form factor.

where $\mathcal{F}$ is the scattering operator, all states are "in" states and n is a state which couples to both the final and initial state. Below the first inelastic threshold the only such state is $\pi\pi$ (see footnote 2 in section 2.6), wherefore

$$\begin{aligned} \mathrm{Im}F(s) &= \rho(s)T_0^*(s)F(s) \\ &= \rho(s)T_0(s)F^*(s) \\ &= e^{i\delta(s)}\sin(\delta(s))F^*(s), \end{aligned} \tag{4.35}$$

where δ is the $\pi\pi$ scattering phase-shift. This leads to the famous Omnès equation [Omn58, Mus53, Bar65]

$$F(s) = F(s_0) + \frac{s-s_0}{\pi}\int_{4m_\pi^2}^{\infty} \mathrm{d}s' \frac{\tan\delta(s')\mathrm{Re}F(s')}{(s'-s)(s'-s_0)}. \tag{4.36}$$

The solution reads [Omn58, Mus53, Bar65]

$$\begin{aligned} F(s) &= P(s)\exp\left\{\tfrac{s-s_0}{\pi}\int_{4m_\pi^2}^{\infty}\mathrm{d}s'\tfrac{\delta(s')}{(s'-s)(s'-s_0)}\right\} \\ &\equiv P(s)\,\Omega_{s_0}(s). \end{aligned} \tag{4.37}$$

The twice subtracted solution reads

$$\begin{aligned} F(s) &= P(s)\exp\left\{\tfrac{F'(s_0)\,(s-s_0)}{F(s_0)}\right\}\exp\left\{\tfrac{(s-s_0)^2}{\pi}\int_{4m_\pi^2}^{\infty}\mathrm{d}s'\tfrac{\delta(s')}{(s'-s)(s'-s_0)^2}\right\} \\ &\equiv P(s)\exp\left\{\tfrac{F'(s_0)\,(s-s_0)}{F(s_0)}\right\}\Omega_{s_0}^{(2)}(s). \end{aligned} \tag{4.38}$$

Since we assume that there are no other singularities than the cut, $P(s)$ is an arbitrary polynomial factor. F has the phase of T_0. This is known as Watson's final state theorem. If $F(s)$ happens to be vanish linearly at $s = s_0$, a small modification is necessary; the zero must be factored out:

$$F(s) = (s-s_0)\overline{F}(s), \tag{4.39}$$

and the same method applied to $\overline{F}$, giving

$$F(s) = (s-s_0)\overline{P}(s)\Omega_{s_0}(s). \tag{4.40}$$

If the subtraction polynomial $P(s)$ can be determined, $F(s)$ is known everywhere. We can then distinguish two cases:

1) $F(s_0) \neq 0$.

$$\begin{aligned} P(s) &= P(s_0) + P'(s_0)(s - s_0) \\ &= F(s_0) + (F'(s_0) - F(s_0)\Omega'_{s_0}(s_0))(s - s_0) \end{aligned} \tag{4.41}$$

2) $F(s_0) = 0$.

$$\overline{P}(s) = F'(s_0) \tag{4.42}$$

In either case the input is $F(s_0)$ and $F'(s_0)$.

4.5.2 The SFF

As mentioned, the SFF is well under control both from a chiral and an "experimental" point of view. To get an understanding of the FSI it is instructive to rewrite the one-loop expression (4.10) as

$$\Gamma(s) \equiv F_s(s)/F_s(0) = 1 + cs + \frac{s^2}{\pi}\int_{4m_\pi^2}^{\infty} \mathrm{d}s' \frac{\delta_0^{0\,(2)}(s')}{s'^2(s' - s)} + \mathcal{O}(s^3), \tag{4.43}$$

where c is a constant related to the L_i's $\sim \ln m_\pi^2$, which can be fixed from the scalar radius of the pion. $\delta_0^{0\,(2)}$ is the LO $\pi\pi$ phase-shift in the s-wave, $I = 0$ channel

$$\begin{aligned} \delta_0^0(s) &= \delta_0^{0\,(2)}(s) + \delta_0^{0\,(4)}(s) + \ldots, \\ \delta_0^{0\,(2)}(s) &= \tfrac{\pi\sigma(s)}{32\pi^2 f_\pi^2}(2s - m_\pi^2), \end{aligned} \tag{4.44}$$

with $\sigma(s) = \sqrt{1 - 4m_\pi^2/s}$. Since there is no zero of Γ at $s = 0$ and only one subtraction is needed, we can use (4.37) with $s_0 = 0$ and $P(s) = 1$. In practise one then needs to cut off the integral at some value Λ^2 high enough that the result depends very little on the precise value. In fig. 4.8 this is displayed, using a cut-off $\Lambda = 1.4$GeV and the phase-shift of [CGL01a], together with the three first orders of CHPT and the "true form factor" [DGL90] referred to in section 4.4.3. At $s = m_K^2 = 0.498\,\mathrm{GeV}$ the chiral series looks as follows:

$$\begin{aligned} &1\ (\mathrm{LO}) \ \rightarrow\ 1.62\ (\mathrm{NLO}) \ \rightarrow\ 1.67\ (\mathrm{NNLO}) \\ &\rightarrow\ 1.42\ (\text{"true value"}). \end{aligned} \tag{4.45}$$

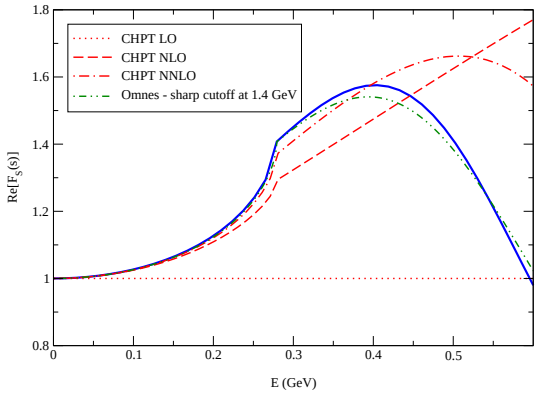

Figure 4.8: Scalar form factor: Comparison of the CHPT calculation to leading, next-to-leading and next-to-next-to-leading order and the dispersive one (see legenda). The solid curve is the "true form factor", see text.

We observe that the bending of the "true form factor" is reproduced by CHPT only at next-to-next-to-leading order (NNLO) and then shifted right. This, however, can be easily understood by observing that

$$\mathrm{Re}\Gamma(s) \sim \cos\delta(s) \sim 1 - \frac{\delta(s)^2}{2} + \ldots, \tag{4.46}$$

and that, since the phase is a quantity of order p^2 in the chiral expansion, the negative part, responsible for the bending down, starts at NNLO and will thus have sizeable contributions from even higher orders.

From the previous paragraphs, we conclude that FSI can indeed shift the leading order result substantially, $\sim 50\%$, and that this effect is primarily carried by the one-loop correction, but that higher orders can modify the one-loop prediction by another $\sim 15\%$.

4.5.3 $\mathbf{K} \to 2\pi$

Armed with the knowledge that FSI are indeed important for three-point amplitudes with s-wave $\pi\pi$ final state, we proceed now to the decay $\mathrm{K} \to 2\pi$. Ignoring for the moment that the constant c_5 of the LO weak chiral lagrangian and the constants of the NLO weak chiral lagrangian are largely unknown, at small values of s, CHPT is reliable and can be used for determining A and the slope of A; we shall use the two amplitudes defined in (4.17) and (4.18). The two CHPT amplitudes have zeros at rather unsuitable values of s: The right-and side of

(4.17) has a zero at

$$\frac{c_2 3m_\pi^2 m_K^2 + c_5 m_K^2(2m_K^2 - m_\pi^2)}{c_2 3m_K^2 + c_5(2m_K^2 - m_\pi^2)} \equiv s_0^P, \tag{4.47}$$

dependent on c_5. The right-hand side of (4.18) has a zero at

$$2m_\pi^2 - m_K^2 \equiv s_0^A, \tag{4.48}$$

Using (4.17), (4.47) and (4.39), *setting* c_5 *to zero* and subtracting at $s_0 = m_\pi^2$, we get [5]

$$\left|A\left(m_K^2\right)\right|/c_2 = 823\,\text{GeV}^{-1}. \tag{4.49}$$

This is the result of [PP00]. Subtracting instead at $s_0 = 0$, we get

$$\left|A\left(m_K^2\right)\right|/c_2 = 941\,\text{GeV}^{-1}. \tag{4.50}$$

This is the result of [PP01]. If c_5 is not set to zero, but instead to e.g. $0.1\,c_2$ and the subtraction is made at $s_0 = s_0^P$, we get

$$\left|A\left(m_K^2\right)\right|/c_2 = 875\,\text{GeV}^{-1}. \tag{4.51}$$

Using (4.18) and (4.48) and subtracting at $s_0 = m_\pi^2$, we get

$$\left|A\left(m_K^2\right)\right|/c_2 = 477\,\text{GeV}^{-1}. \tag{4.52}$$

It is seen that using the (pseudo-scalar) off-shell amplitude (4.17), modifies the result of [PP00] by 6 % with $c_5 = 0.1\,c_2$. It is also seen that using the (axial-vector) off-shell amplitude (4.18), gives a result which differs from the result of [PP00] by 58 %. In this case, it should be noted that the difference is due to the term proportional to $\Omega'(m_\pi^2)$ which is of one order higher in the chiral expansion than the rest.

These simple examples spotlight the perils of using (weak) CHPT for fixing subtraction constants in a dispersive treatment of $K \to 2\pi$: In contrast to the case of the SFF, there is no observable quantity which can be used for fixing the subtraction constants; that is, the coupling constants of the weak chiral lagrangians are largely unknown, even those of the LO lagrangian. Moreover, the off-shell CHPT amplitudes are not uniquely defined and cannot be used to fix subtraction constants in a dispersive representation. In other words, $A^{K\to\pi\pi}(s)$ is ill-suited for dispersive treatment because the subtraction point must be made in an off-shell region where it is ambiguous.

In section 4.7 an alternative method is proposed which avoids this problem. First however, we need to introduce some additional tools.

[5] The experimental input used is:
$f_\pi = 92.4\,\text{MeV}$, $m_\pi = 139.57\,\text{MeV}$, $m_K = 495.67\,\text{MeV}$ and the phase-shift analysis of [AMP87]. The value of f_π is the one used in [PP01].

4.6 The soft pion theorem for non-leptonic kaon decays

4.6.1 Allowing the weak lagrangian to carry momentum

The generating functional reads

$$W[j_V, j_A, j_s, j_p] = \int [\mathrm{d}U] e^{i\int \mathrm{d}x(\mathcal{L}^{\mathrm{S}}+\mathcal{L}^{\mathrm{W}}+V_\mu j_V^\mu+\ldots)}. \tag{4.53}$$

Since the weak coupling is indeed very weak, we need keep only linear terms in $\mathcal{L}^{\mathrm{W}}$,

$$\begin{aligned} &W[j_V, j_A, j_s, j_p] = \\ &\qquad \int [\mathrm{d}U] e^{i\int \mathrm{d}x(\mathcal{L}^{\mathrm{S}}+V_\mu j_V^\mu+\ldots)}(1 + i\int \mathrm{d}x \mathcal{L}^{\mathrm{W}} + \ldots). \end{aligned} \tag{4.54}$$

We may view $\mathcal{L}^{\mathrm{W}}$ like any other operator whose expectation values can be calculated from W. To this end we couple it to a source, i.e. allow it to carry momentum q. The CP conserving $\Delta S = 1$ weak CHPT lagrangian $\mathcal{L}^{\mathrm{W}}$, which we are considering, can be viewed as the sixth component of an isoscalar operator octet, and can thus be coupled to a multiplet of external sources j^i_{W}. To achieve this we substitute $\lambda_6 \to j^i_{\mathrm{W}}\lambda_i$. Thus instead of (4.16) we shall use

$$\overline{\mathcal{L}}_{\mathrm{W},2} = c_2 \langle j^i_{\mathrm{W}}\lambda_i D_\mu U^\dagger D^\mu U\rangle + c_5 \langle j^i_{\mathrm{W}}\lambda_i \left(^\dagger\chi + \chi^\dagger U\right)\rangle . \tag{4.55}$$

There is of course no field in nature corresponding to j^i_{W}, that is, the Green's functions with $q^\mu \neq 0$ are well-defined but unphysical objects. Setting $q^\mu = 0$ is the physical limit.

The amplitudes we shall need for our discussion of the soft pion theorem are the $\mathrm{K_l} \to \pi^0$ and $\mathrm{K_s} \to \pi^0\pi^0$ amplitudes, both with a momentum carrying weak lagrangian. More precisely, we define

$$\Xi(q^2) \equiv \frac{1}{(-2f_\pi B_0)^2} \lim_{\substack{k^2\to m_{\mathrm{K}}^2 \\ p^2\to m_\pi^2}} (k^2 - m_{\mathrm{K}}^2)(p^2 - m_\pi^2)\xi^{63}(k^2, p^2, q^2), \tag{4.56}$$

with

$$\begin{aligned} &\xi^{63}(k^2, p^2, q^2) \equiv \\ &i\int \mathrm{d}^4x \int \mathrm{d}^4y \int \mathrm{d}^4z\, e^{ik\cdot x}e^{ip\cdot y}e^{iq\cdot z} \left\langle 0 \left| \mathrm{T}\left\{P^{6\dagger}(x)P^3(y)\overline{\mathcal{L}}^{\mathrm{W}}(z)\right\}\right| 0\right\rangle , \end{aligned} \tag{4.57}$$

and

$$\begin{aligned} &T^+(s,t,u,q^2) \equiv \\ &\frac{1}{(-if_\pi p^\mu)(-2f_\pi B_0)^2} \lim_{\substack{k^2\to m_{\mathrm{K}}^2 \\ p_1^2\to m_\pi^2 \\ p_2^2\to m_\pi^2}} (k^2-m_{\mathrm{K}}^2)(p_1^2-m_\pi^2)(p_2^2-m_\pi^2)\tau_\mu^{733}(s,t,u,k^2,p_1^2,p_2^2,q^2), \end{aligned} \tag{4.58}$$

with

$$\begin{aligned} &\tau_\mu^{733}(s,t,u,k^2,p_1^2,p_2^2,q^2) \equiv i\int \mathrm{d}^4x \int \mathrm{d}^4y_1 \int \mathrm{d}^4y_2 \int \mathrm{d}^4z \\ &e^{ik\cdot x}e^{ip_1\cdot y_1}e^{ip_2\cdot y_2}e^{iq\cdot z}\left\langle 0\left|\mathrm{T}\left\{A_\mu^{7+}(x)P^3(y_1)P^3(y_2)\overline{\mathcal{L}}^{\mathrm{W}}(z)\right\}\right|0\right\rangle \end{aligned} \tag{4.59}$$

and s,t,u the usual Mandelstam variables

$$s=(p_1+p_2)^2,\quad t=(q+p_1)^2,\quad u=(q+p_2)^2\,, \tag{4.60}$$

where all momenta considered incoming, related by $s+t+u=2m_\pi^2+m_{\mathrm{K}}^2+q^2$, with q the momentum carried by the weak Hamiltonian. From now on we set $q^2=0$ (but $q^\mu\neq 0$ in general).

4.6.2 The soft pion theorem

First we consider a general matrix element involving a soft pion [LSZ55],

$$\begin{aligned} \langle\pi^i(p)B|O(0)|A\rangle &= i\int \mathrm{d}^4x e^{ip\cdot x}(\Box+m_\pi^2)\langle B|T\pi^i(x)O(0)|A\rangle \\ &= \int \mathrm{d}^4x e^{ip\cdot x}(-p^2+m_\pi^2)\langle B|T\left\{\pi^i(x)O(0)\right\}|A\rangle\,, \end{aligned} \tag{4.61}$$

where A and B denote two arbitrary ensembles of particles, π^i a pion with isospin index i, which is to be taken off-shell, $p\to 0$, and O is some operator. According to the Haag theorem (see section 2.5), we can make the PCAC choice

$$\pi^i=\frac{1}{f_\pi m_\pi^2}\partial^\mu A_\mu^i, \tag{4.62}$$

where A^i_μ is the isospin i axial-vector current operator. From the above two equations follows

$$\begin{aligned}
&\left\langle \pi^i(p)\, B|O(0)|A\right\rangle = i\tfrac{m_\pi^2-p^2}{f_\pi m_\pi^2}\int \mathrm{d}^4x e^{ip\cdot x}\left\langle B|T\left\{\partial^\mu A^i_\mu(x)O(0)\right\}|A\right\rangle \\
&= i\tfrac{m_\pi^2-p^2}{f_\pi m_\pi^2}\int \mathrm{d}^4x e^{ip\cdot x} \\
&\quad \left\langle B|\theta(x_0)\partial^\mu A^i_\mu(x)O(0) - \theta(-x_0)O(0)\partial^\mu A^i_\mu(x)|A\right\rangle \\
&= i\tfrac{m_\pi^2-p^2}{f_\pi m_\pi^2}\int \mathrm{d}^4x e^{ip\cdot x} \\
&\quad \left(\partial^\mu\left\langle B|T\left\{A^i_\mu(x)O(0)\right\}|A\right\rangle - \delta(x_0)\left\langle B|\left[A^i_0(x), O(0)\right]|A\right\rangle\right) \\
&= i\tfrac{m_\pi^2-p^2}{f_\pi m_\pi^2}\int \mathrm{d}^4x e^{ip\cdot x} \\
&\quad \left(-ip^\mu\left\langle B|T\left\{A^i_\mu(x)O(0)\right\}|A\right\rangle - \delta(x_0)\left\langle B|\left[A^i_0(x), O(0)\right]|A\right\rangle\right),
\end{aligned} \tag{4.63}$$

where we have used integration by parts and the fact that the derivative of the Heavyside step function θ is the Dirac delta function δ. We now take the limit $q^\mu \to 0$ by first setting $\boldsymbol{q} = 0$ and then letting $q_0 \to 0$, whereby we get the soft pion theorem,

$$\begin{aligned}
\langle \pi^i(p=0)\, B|O(0)|A\rangle &= -\tfrac{i}{f_\pi}\langle B|\left[Q^i_5, O(0)\right]|A\rangle + i\lim_{p^\mu\to 0} p^\mu R^i_\mu, \\
R^i_\mu &= -\tfrac{i}{f_\pi}\int \mathrm{d}^4x e^{ip\cdot x}\langle B|T\left\{A^i_\mu(x)O(0)\right\}|A\rangle .
\end{aligned} \tag{4.64}$$

The last term vanishes unless R^i_μ has a singularity at $q^\mu = 0$. This is the case e.g. for the matrix elements considered in K_{l4} decays as noted by Weinberg in [Wei66]. The soft pion theorem is exact at the SPP, $p_\mu = 0$, and relates one state $|B\rangle$ to another state $|\pi^i_{p_\mu=0}B\rangle$ obtained by the addition of a zero-energy Goldstone pion. When going away from the SU(2) chiral symmetry limit to the real world, $q^2 = m_\pi^2$, corrections of order m_π^2 can be expected [GL84].

Now we want to apply the soft pion theorem to the case of $\mathrm{K_s} \to 2\pi^0$. For the amplitude

$T^+(s,t,u,q^2)$ of (4.58) we get

$$\begin{aligned} T^+(s=m_\pi^2, t=m_K^2, u=m_\pi^2, q^2=0) &= \left\langle \phi^3 | \mathcal{H}_W^6(0) | \phi^7\phi^3 \right\rangle \\ = -\tfrac{i}{f_\pi}\left\langle 0 \left| \left[Q_5^3, \mathcal{H}_W^6(0)\right] \right| \phi^7\phi^3 \right\rangle &= -\tfrac{i}{f_\pi}\left\langle 0 \left| \left[Q_5^3, \mathcal{H}_W^7(0)\right] \right| \phi^6\phi^3 \right\rangle \\ = -\tfrac{1}{2f_\pi}\left\langle 0 | \mathcal{H}_W^6(0) | \phi^6\phi^3 \right\rangle &= -\tfrac{1}{2f_\pi}\Xi(q^2), \end{aligned} \tag{4.65}$$

where we have used the fact that $\mathcal{H}_W^i(0)$ is an SU(3) octet and obeys the algebra

$$\left[Q_5^i, \mathcal{H}_W^j(0)\right] = i f_{ijk} \mathcal{H}_W^k(0). \tag{4.66}$$

(4.65) can be considered accurate up to $\mathcal{O}(m_\pi^2)$ because it is based on the soft pion theorem. In contrast hereto, the CHPT prediction at the physical point, $q^2 = 0, s = m_K^2, t = m_\pi^2, u = m_\pi^2$, suffers from $\mathcal{O}(m_K^2)$ corrections. Moreover $T^+(s,t,u)$ is well-suited for dispersive treatment because the continuation from the SPP to the physical point is done in the on-shell region where it is well-defined.

We have checked the that the relation (4.64) is satisfied by the CHPT amplitudes of section C.2.

4.7 Crossed channel dispersion equations

Since the weak Hamiltonian has the quantum numbers of the kaon, and the pions are in an isospin zero state, $T^+(s,t,u)$ is analogous to the $t \leftrightarrows u$ even combination of the KK$\to \pi\pi$ scattering amplitude (the notation is borrowed from ref. [Lan78]). Like in that case, one can show that if one neglects the imaginary parts of d-waves and higher in all channels, then the analytic structure of the amplitude simplifies and it can be decomposed into a combination of functions of a single variable (for the Kπ scattering case see [AB01]):

$$\begin{aligned} T^+(s,t,u) &= M_0(s) + \tfrac{1}{3}\left[N_0(t) + N_0(u)\right] + \tfrac{2}{3}\left[R_0(t) + R_0(u)\right] \\ &+ \tfrac{1}{2}\left[\left(s - u - \tfrac{m_\pi^2\Delta}{t}\right)N_1(t) + \left(s - t - \tfrac{m_\pi^2\Delta}{u}\right)N_1(u)\right], \end{aligned} \tag{4.67}$$

where $\Delta = m_K^2 - m_\pi^2$. Notice that the terms proportional to N_1 drop out in the physical decay amplitude:

$$\begin{aligned} \mathcal{A}_{K\to\pi\pi} &= T^+(m_K^2, m_\pi^2, m_\pi^2) = \\ &= M_0(m_K^2) + \tfrac{2}{3}\left[N_0(m_\pi^2) + 2R_0(m_\pi^2)\right]. \end{aligned} \tag{4.68}$$

Each of the single variable functions appearing in equation (4.67) is analytic in the complex plane except for a cut starting at $4m_\pi^2$ for M_0 and at $(m_K + m_\pi)^2$ for the remaining ones. These functions are defined to have the discontinuity on the positive real axis identical to that of a specific partial wave: M_0 to the $I = 0$ S-wave in the s-channel, whereas in the t-channel, N_0 and N_1 to the $I = 1/2$ s- and p-wave respectively, and R_0 to the $I = 3/2$ s-wave [6]. Below the inelastic threshold, the elastic unitarity condition for these functions reads

$$\begin{aligned} \mathrm{disc}M_0(s) &= \sin\delta_0^0(s)e^{-i\delta_0^0}\left[M_0(s) + \hat{M}_0(s)\right], \\ \mathrm{disc}N_l(s) &= \sin\delta_l^{1/2}(s)e^{-i\delta_l^{1/2}}\left[N_l(s) + \hat{N}_l(s)\right], \\ \mathrm{disc}R_0(s) &= \sin\delta_0^{3/2}(s)e^{-i\delta_0^{3/2}}\left[R_0(s) + \hat{R}_0(s)\right], \end{aligned} \tag{4.69}$$

where δ_0^0 is the $\pi\pi$ phase-shift, whereas those with half-integer isospin are the πK phase-shifts.

The "hat functions" denote contributions from the other channels contributing via angular

[6] We disregard the imaginary part of the $I = 3/2$ p-wave in the t-channel because it is phenomenologically very small and vanishes in the chiral expansion up to order p^6.

averages (to be specified below). They are defined by

$$\begin{aligned}
\hat{M}_0(s) &= \left[s\Sigma_1 - 2m_{\rm K}^2 m_\pi^2 - \tfrac{1}{4}(m_{\rm K}^4 + 3s^2)\right]\langle\tilde{N}_1\rangle + 2s|\mathbf{p}||\mathbf{q}|\langle z\tilde{N}_1\rangle \\
&\quad +4|\mathbf{p}|^2|\mathbf{q}|^2\langle z^2\tilde{N}_1\rangle + \tfrac{2}{3}(\langle N_0\rangle + 2\langle R_0\rangle), \\
\hat{N}_0(t) &= \langle M_0\rangle_s + y(t)\langle M_1\rangle_s - r(t)\langle zM_1\rangle_s + \tfrac{1}{3}\left(4\langle R_0\rangle_u - \langle N_0\rangle_u\right) \\
&\quad -\tfrac{1}{8}w(t)\langle\tilde{N}_1\rangle_u - \tfrac{1}{4}v(t)\langle z\tilde{N}_1\rangle_u + \tfrac{1}{8}r^2(t)\langle z^2\tilde{N}_1\rangle_u, \\
\hat{N}_1(t) &= \tfrac{2}{r(t)}\left\{\langle zM_0\rangle_s + y(t)\langle zM_1\rangle_s - r(t)\langle z^2M_1\rangle_s\right. \\
&\quad +\tfrac{1}{3}\left(4\langle zR_0\rangle_u - \langle zN_0\rangle_u\right) - \tfrac{1}{8}w(t)\langle z\tilde{N}_1\rangle_u \\
&\quad \left.-\tfrac{1}{4}v(t)\langle z^2\tilde{N}_1\rangle_u + \tfrac{1}{8}r^2(t)\langle z^3\tilde{N}_1\rangle_u\right\} \\
\hat{R}_0(t) &= \langle M_0\rangle_s - \tfrac{1}{2}y(t)\langle M_1\rangle_s + \tfrac{1}{2}r(t)\langle zM_1\rangle_s + \tfrac{1}{3}\left(\langle R_0\rangle_u + 2\langle N_0\rangle_u\right), \\
&\quad +\tfrac{1}{4}w(t)\langle\tilde{N}_1\rangle_u + \tfrac{1}{2}v(t)\langle z\tilde{N}_1\rangle_u - \tfrac{1}{4}r^2(t)\langle z^2\tilde{N}_1\rangle_u,
\end{aligned} \tag{4.70}$$

where

$$\begin{gathered}
\tilde{N}_1(t) = N_1(t)/t,\ \Sigma = m_{\rm K}^2 + m_\pi^2, \\
\Sigma_1 = \Sigma + m_\pi^2,\ y(t) = \Sigma_1 - 3t - \tfrac{m_\pi^2\Delta}{t}, \\
\rho_{\pi K}(t) = \sqrt{\left(1 - (m_{\rm K} + m_\pi)^2/t\right)\left(1 - (m_{\rm K} - m_\pi)^2/t\right)}, \\
r(t) = (t - m_\pi^2)\rho_{\pi K}(t),\ v(t) = \left(t - \tfrac{m_\pi^2\Delta}{t}\right)r(t), \\
w(t) = 3t^2 - 4t\Sigma_1 + 5m_\pi^4 + \Sigma^2 - \tfrac{m_\pi^4\Delta^2}{t^2}.
\end{gathered} \tag{4.71}$$

$\langle\rangle$ indicate angular averages defined by

$$\begin{aligned}
\langle z^n X\rangle(s) &= \tfrac{1}{2}\int_{-1}^{1} {\rm d}z z^n X(\Sigma_1/2 - s/2 + 2|\mathbf{p}||\mathbf{q}|z), \\
\langle z^n X\rangle_v(t) &= \tfrac{1}{2}\int_{-1}^{1} {\rm d}z z^n X(v(t,z)),\quad v = s, u,
\end{aligned} \tag{4.72}$$

where

$$|\mathrm{p}|^2 = \tfrac{s}{4} - m_\pi^2,\ |\mathrm{q}|^2 = \tfrac{s}{4}\left(1 - \tfrac{m_K^2}{s}\right)^2, \qquad s + u = \Sigma_1 - t,\ s - u = \tfrac{m_\pi^2 \Delta}{t} + r(t)z. \tag{4.73}$$

In the definition of the "hat functions" the function M_1 appears. This function is analogous to M_0 in the case of the $I = 1$ p-wave in the s-channel, and is necessary to describe the $T^+(s,t,u)$ in full generality, for all channels (including the $t \leftrightarrows u$ odd, $I = 1$ s-channel). It does not contribute directly to the physical decay process: Its indirect (and small) contribution via the angular average in the dispersion relation is a consequence of crossing symmetry.

If one is only interested in the low-energy region, neglecting the inelastic channels is a good approximation. Then the solution of the dispersion relation for each of the functions is well approximated by the Omnès function times a polynomial [Omn58]. It is therefore convenient to write the dispersion relation for the functions divided by the corresponding Omnès function (see [AL96] for a detailed discussion of this point, although in a different framework) in the following form:

$$\begin{aligned}
M_0(s) &= \Omega_0^0(s,s_0)\Big\{a + b(s-s_0) + \\
&\qquad \tfrac{(s-s_0)^2}{\pi}\int_{4m_\pi^2}^{\Lambda_1^2} \frac{\sin\delta_0^0(s')\hat{M}_0(s')\mathrm{d}s'}{|\Omega_0^0(s',s_0)|(s'-s)(s'-s_0)^2}\Big\}, \\
N_0(s) &= \Omega_0^{1/2}(s)\left\{\tfrac{s^2}{\pi}\int_{(m_K+m_\pi)^2}^{\Lambda_2^2} \frac{\sin\delta_0^{1/2}(s')\hat{N}_0(s')\mathrm{d}s'}{|\Omega_0^{1/2}(s')|(s'-s)s'^2}\right\}, \\
N_1(s) &= \Omega_1^{1/2}(s)\left\{\tfrac{s}{\pi}\int_{(m_K+m_\pi)^2}^{\Lambda_2^2} \frac{\sin\delta_1^{1/2}(s')\hat{N}_1(s')\mathrm{d}s'}{|\Omega_1^{1/2}(s')|(s'-s)s'}\right\}, \\
R_0(s) &= \Omega_0^{3/2}(s)\left\{\tfrac{s^2}{\pi}\int_{(m_K+m_\pi)^2}^{\Lambda_2^2} \frac{\sin\delta_0^{3/2}(s')\hat{R}_0(s')\mathrm{d}s'}{|\Omega_0^{3/2}(s')|(s'-s)s'^2}\right\}.
\end{aligned} \tag{4.74}$$

$\Omega_I^I(s)$ is the Omnès function [Omn58], defined by

$$\begin{aligned}
\Omega_0^0(s,s_0) &= \exp\left\{\tfrac{(s-s_0)}{\pi}\int_{4m_\pi^2}^{\tilde{\Lambda}_1^2} \mathrm{d}s' \tfrac{\delta_0^0(s')}{(s'-s_0)(s'-s)}\right\}, \\
\Omega_I^I(s) &= \exp\left\{\tfrac{s}{\pi}\int_{(m_K+m_\pi)^2}^{\tilde{\Lambda}_2^2} \mathrm{d}s' \tfrac{\delta_I^I(s')}{s'(s'-s)}\right\}, \quad I = \tfrac{1}{2}, \tfrac{3}{2}.
\end{aligned} \tag{4.75}$$

All functions are subtracted at $s = 0$ except for M_0, for which the subtraction point s_0 is left unspecified. In the following we use $s_0 = m_\pi^2$. The fact that only M_0 depends on subtraction constants does not have any deep reason: The splitting of polynomial terms of T^+ between

the various functions M_0, $N_{0,1}$ and R_0 is arbitrary, and we have merely used this freedom to remove them from the latter three. The final result does not depend on this choice [AL96]. All the dispersive integrals above have been cut off at energies $\Lambda_{1,2}$ and $\tilde{\Lambda}_{1,2}$ - numerical values will be given below.

4.8 Solving the equations

If the $\pi\pi$ and Kπ phase-shifts, the cutoffs $\Lambda_{1,2}$, and the subtraction constants a and b are given, the dispersion relations (4.74) can be solved numerically. Such a solution gives the amplitude $T^+(s,t,u)$ at any point (provided it is far enough from the inelastic thresholds) of the Mandelstam plane, in particular at the physical point. The crucial new input here are the two subtraction constants. The phase-shifts are known with sufficient accuracy, whereas the choice of the cutoffs is dictated by the inelastic thresholds. Before proceeding we have to discuss how these two subtraction constants can be determined. If they could be calculated with better accuracy than the physical amplitude itself, it would represent a clear advantage for our method.

For one of the two subtraction constants this is the case. The soft-pion theorem relates the amplitude at the SPP to the K$\to\pi$ amplitude up to terms of order m_π^2. We can therefore write

$$-\frac{1}{2f_\pi}\mathcal{A}_{K\to\pi} = a + \frac{1}{3}\left[N_0(m_K^2) + 2R_0(m_K^2)\right] + O(m_\pi^2), \tag{4.76}$$

which shows that a is indeed directly related to a quantity that is calculable (more easily than the decay amplitude itself), e.g. on the lattice. The relation (4.76) illustrates the strength of the soft-pion theorem: Although the process involves a kaon, the relation is based on the use of the $SU(2)$ symmetry, and therefore suffers from corrections of order m_π^2 only.

The key to the problem is the calculation of b. This constant is related to the derivative in s of the amplitude T^+ at the SPP. The calculation of b requires the evaluation of the physical amplitude T^+ at an unphysical point, via analytic continuation. While this is easy to do with an analytical method like CHPT, it is practically impossible with a numerical method like the lattice method. However there is a Ward identity that relates this derivative to a Green's function which is directly calculable:

$$\frac{\partial}{\partial s}T^+(s,\Sigma-s,m_\pi^2)_{|s=m_\pi^2} = \frac{1}{2}C(m_\pi^2,m_K^2,m_\pi^2) + O(m_\pi^2), \tag{4.77}$$

where $C(s,t,u)$ is an amplitude defined by

$$\frac{i}{f_\pi}\int \mathrm{d}x e^{ip_1x}\langle\pi(p_2)|T\mathcal{H}_W^{1/2}(0)A^\mu(x)|K(q_1)\rangle = ip_1^\mu B + iq_1^\mu C + iq_2^\mu D\,, \tag{4.78}$$

where $A^\mu(x)$ is the axial current that couples to the pion removed from the outgoing state. By making the momentum p_2 soft, one can also derive a soft-pion theorem which relates the four-point function in equation (4.78) to a three-point function. Unfortunately the function C cannot be singled out from this relation.

We are not aware of any attempts to calculate b. In order to illustrate our method we proceed by fixing b at a certain value and then varying it within a fairly wide range. To fix the central value and the range we use CHPT as a guide. At leading order, CHPT dictates the following relation between a and b:

$$b = \frac{3a}{m_K^2 - m_\pi^2}\left(1 + X + O(m_K^4)\right). \tag{4.79}$$

The size of the correction is at the moment unknown, but nothing prevents it from being of order m_K^2: $X = m_K^2/(16\pi^2 F_K^2)x$, with x expected to be of order one. An explicit calculation in CHPT (see section C.2) yields[7]:

$$\begin{aligned} x \;=\; & \tfrac{383}{9} - \tfrac{8021}{54}\log\tfrac{4}{} + \tfrac{1}{3}\log\tfrac{m_K^2}{m_\pi^2} \\ & -\tfrac{8}{3}(\bar{N}_5 + 2\bar{N}_7 - \bar{N}_9 - 4\bar{N}_{10} - 4\bar{N}_{11}) \\ & +2(\bar{N}_{19} - \bar{N}_{20}) - \tfrac{4}{3}(2\bar{N}_{21} + \bar{N}_{22} + 2\bar{N}_{23}) + O\left(\tfrac{m_\pi^2}{m_K^2}\right), \end{aligned} \tag{4.80}$$

where $\bar{N}_i = 16\pi^2 N_i^r(m_K)$ are the renormalized low-energy constants introduced in [EKW93]. Since we lack information on many of the constants, the CHPT calculation (4.80) does not allow us to do more than an order of magnitude estimate for b. In our numerical study we have used $X = \pm 30\%$. The normalization of the amplitude is irrelevant here, and we have fixed it at $T^+(m_\pi^2, m_K^2, m_\pi^2) = 1$. For the cutoffs we have used $\Lambda_1 = 1$ GeV, $\Lambda_2 = 1.3$ GeV, and $\tilde{\Lambda}_i = 1.05\Lambda_i$. Our results [8] are shown in fig. 4.9, where we have plotted $|T^+(s, \Sigma - s, m_\pi^2)|$ versus s, comparing our numerical solution of the dispersion relations to the CHPT leading order formula. The latter is what has been used so far whenever a number for the K$\to \pi\pi$ matrix element extracted from the lattice has been given. Our treatment shows that large corrections with respect to leading-order CHPT are to be expected. One source of large corrections is the Omnès factor due to $\pi\pi$ rescattering in the final state [PP00, Tru88]. The other potentially dangerous source is represented by X, the next-to-leading order correction to the relation (4.79) between a and b. The latter could (depending on the sign) in principle double, or to a large

[7] We have dropped the contribution coming from the weak mass term - more on this below.

[8] The experimental input used is:
$m_\pi = 139.57\,\text{MeV}$, $m_K = 497.672\,\text{MeV}$, $m_\eta = 547.30\,\text{MeV}$, the $\pi\pi$ phase-shifts from [ACGL01], the scattering lengths determined in [CGL00], and the πK phase-shifts from [JOP00].

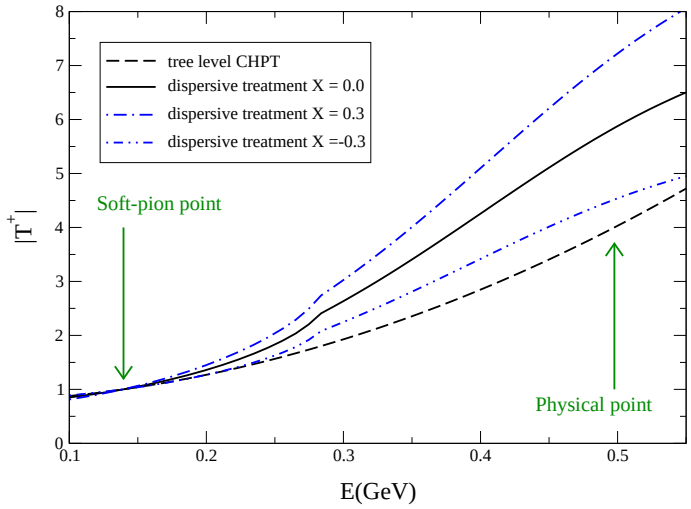

Figure 4.9: The function $|T^+(s,t,u)|$ plotted *vs.* $E = \sqrt{s}$ along the line of constant $u = m_\pi^2$. The result of our numerical study for different values of X are compared to tree level CHPT.

extent reabsorb the correction due to FSI. The dependence on X is well described by the following linear formula:

$$\frac{|\mathcal{A}(\mathrm{K}\to\pi\pi)|}{|\mathcal{A}^{\text{LO CHPT}}(\mathrm{K}\to\pi\pi)|} = 1.5\,(1+0.76X)\,, \tag{4.81}$$

after having normalized both amplitudes to $T^+(m_\pi^2, m_\mathrm{K}^2, m_\pi^2) = 1$. The evaluation of the uncertainties to be attached to the numbers in equation (4.81) is in progress. At the moment, however, the main source of uncertainty is the fact that X is largely unknown.

One of the outcomes of the present analysis is that the effects embodied in the functions $N_{0,1}$ and R_0 have turned out to be very small: If we drop them altogether, the numbers in equation (4.81) change from 1.5 to 1.4 and from 0.76 to 0.75. Notice that these effects are in principle of order m_K^2, as can be seen in equation (4.76), and that they are not a priori negligible. On the other hand this result is very much welcome, because the size of these functions depends both on the πK phases (which are less well known than the $\pi\pi$ ones) and on the choice of the cutoff Λ_2, which may induce large uncertainties.

4.9 Results and discussion

We have set up a dispersive framework for the K→ $\pi\pi$ amplitude that allows evolving the amplitude from the soft-pion point (where it is given by the $K \to \pi$ amplitude) to the physical point, taking into account all the main physical effects. As we have pointed out, this evolution is on safe ground only if a second input is made available: The derivative of the amplitude at the soft-pion point, which, to the best of our knowledge, has not been calculated so far. We have calculated this second subtraction constant to NLO in CHPT. Given the presence of unknown low-energy constants, we cannot use this expression for more than an order of magnitude estimate. Our numerical work, however, shows that the amplitude at the physical point depends strongly on the value of the slope at the SPP, see fig. 4.9 and related discussion in the text. A non-perturbative calculation of the second subtraction constant b is necessary in order to obtain an accurate result with this method. We have provided a Ward identity which might be useful in this respect.

Lattice calculations of the K→ $\pi\pi$ amplitude made so far [Lel01] rely on tree-level CHPT to relate the calculated $K \to \pi$ matrix elements to the physical decay amplitude. The method proposed here improves this scheme by combining input from the lattice with dispersion relation techniques, thereby providing a fully consistent treatment of FSI in K→ $\pi\pi$. Given the two subtraction constants, the dispersion relations can be solved numerically to good accuracy. Recently, a direct calculation of the K→ $\pi\pi$ matrix element on the lattice has been proposed in ref. [LL01] - this method does not rely on CHPT. Other lattice methods, which also do not rely on the evaluation of the K → π amplitude, have also been proposed [D$^+$98]. Each of these methods presents different technical problems in its practical implementation [Gol00], and it is difficult to predict which one will lead to a reliable calculation of the K → $\pi\pi$ amplitude. We hope that the present work will stimulate further efforts to calculate the subtraction constants a and b, either on the lattice, or by other non-perturbative methods.

Chapter 5

Computerized quantum field theory

This chapter contains an introduction to the automatized Feynman diagram calculations used in the previous chapters. This includes some historical notes and a short review of other computerization methods as well as some simple explicit examples of using the *MATHEMATICA* package *FEYNCALC* coauthored by the author.

5.1 Introduction

Loop calculations in renormalizable theories

In recent years, a great deal of work has been invested by various groups in the automatization of Feynman diagram calculations (see [HS99] for a review). The focus has mainly been on perturbative QCD [GW73a, GW74, GW73b, Pol73], the electro-weak part of the Standard Model [Gla61, Wei67a, Sal68] and supersymmetric extensions [WZ74, VA73] of it. Electro-weak calculations are at the two-loop level for correlators (e.g. [WSB94, FHWW00]), but essentially still at one-loop level (e.g. [BMR72, DH98, DP01]) for vertex and scattering diagrams. Experiments are however reaching a level of precision demanding higher order calculations and some have already been done, e.g. the muon anomalous moment to two loops [CKM96] (see [CM01b] for an update on the muon anomalous magnetic moment and [GR01] for a general review of two-loop calculations), but a general method like [tHV79, PV79] is still lacking; thus some integrals have to be done numerically. In QED loop calculations are of course much simpler and of older date. The two-loop vacuum polarization was calculated in 1955 [KS55], the two-loop electron self energy in 1962 [Sab62], the anomalous magnetic moment [Sch49] to two loops in 1957 [Pet57], the full two-loop three-point function in 1972 [BMR72] and two-loop Bhabha scattering in 2000 [BDG01]. The QED contributions to the quark mass and

wavefunction renormalization have by now been calculated to three loops on the mass-shell [MvR00] and the anomalous magnetic moment of the electron has been calculated analytically to three loops [LR97] and numerically up to five loops [Kin96, CM99]. QCD calculations are at two loops for correlator ([FJTV99]) diagrams and some vertex diagrams (e.g $Z_0 \to b\bar{b}$ in the large top mass limit [FTJR92] or the matrix element of the current current operator in $b \to s\gamma$ [GHW96, BCMU01]) but are reaching three loops [CKS96, MvR00] and are at four loops for the beta function [vRVL97] whereas scattering diagrams are at the two-loop level (see [GTY00, Glo01] for an overview). One challenge in QCD and electro-weak calculations is the enormeous number of Feynman diagrams arising from the many different particles and couplings. In the proposed supersymmetric extensions of the standard model this problem is all the more acute (see e.g. [HW01, HHRW01, HS01]). The physical motivation for such calculations is of course that they are necessary to match the precision of experiments. More generally, these detailed checks are necessary because even though the Standard Model has not so far been in disagreement with experiment, it is generally considered unsatisfying as a final theory and the only obvious way to look for a new theory is to find disagreement between the old theory and experiments and explain these via extensions of the old theory.

Loop calculations in CHPT

Loop calculations in CHPT are necessary because of the level of accuracy direct low energy scattering experiments are reaching [G$^+$01, P$^+$01, Pan99, LMGPNP], but also because CHPT is used as an ingredient in the calculation of important parameters of the Standard Model like quark masses and the quark vacuum condensate [GL82, CGL01b], CKM matrix elements [KM73, BBJR92] and ε'/ε [PP00, PP01, BCKO01a]. Many processes in CHPT have by now been calculated at the two-loop level [GM91a, BCT98, BCE$^+$97, ABT00a, ABT00b, BGS, Bur96, GK95, GK98, DK00]. In one-loop SU(2) mesonic CHPT, the main challenge is not the number of Feynman diagrams, but rather the complexity of the counter-term lagrangian. When going to SU(3) and/or two loops however, the number of Feynman diagrams also becomes an issue. Notice that one feature distinguishing effective theories like CHPT from traditionally renormalizable theories is that there is no restriction on the number of legs in vertices (ruling out, for our purposes, all Feynman diagram generating software I know of except for *FeynArts*).

Purpose and features of the package *PHI*

As is clear from the preceding, loop calculations and in particular more or less computerized loop calculations is a very active line of research in most field theories. Indeed, the precision of high energy experiments like the ones at SLC and LEP 1 spurred computational projects like

MADGRAPH [SL94], GRACE [Y+00], COMPHEP [P+99], *FEYNARTS* [Hah01] and *FEYNCALC* [RMD91, MBD91b, KEM, Merb, WMSBb, MS98, MO00] of which all but the first one is still in more or less active development. With the next generation of experiments like the ones at LEP 2 and LHC, some authors argue that it would be desirable to have more collaboration and standardization between the different projects. Recently a proposal [DKR02] for standardizing the definition of a field theoretical model has appeared. The proposal is far from perfect or complete, but in my opinion a step in the right direction. If all projects would follow such a standard, it would mean that the definition of a model could be written down by one group in form of an XML [Con] file, immediately processed and used for calculations of amplitudes and sent to other groups that could also immediately process it and use it for calculations of amplitudes with their different computational software. Of course, to be of real use, such a standard would have to be accompanied by a standard for the notation of amplitudes. Also recently a proposal [Tka02] for converging on a common programming language and further modularization or componentization of the computational software developed has appeared. One benefit of this would be the easy reuse of code (e.g. a fast algorithm for the evaluation of Dirac traces). While nice, I don't think this idea has many chances of being adopted generally.

Notice one point: In all the computational projects mentioned except, despite good intentions, the specification of a model is a non-trivial undertaking and indeed all projects, except for *FEYNCALC*, deal exclusively with the Standard Model and/or minimal supersymmetric extensions of the Standard Model.

Originally, the *MATHEMATICA* package *FEYNCALC* was developed for calculating one-loop Feynman diagrams in the electro-weak Standard Model. The input was raw integral expressions which can be written by hand or, when too many, produced by e.g. the Feynman diagram generator *FEYNARTS* [KEM, HPV99, Hah01]. The output was expressions written in terms of Passarino-Veltman functions [tHV79, PV79]. This implied implementing kinematical tensor structures, Dirac algebra etc. Later, general aspects were developed further and some two-loop formalism was also implemented by the original author in connection with perturbative QCD calculations [MvN96], and recently (see previous chapters and [BCKO01a]), *FEYNCALC* has also been used for some calculations in CHPT.

PHI is a *MATHEMATICA* [Wol00] package for Feynman diagram computations in CHPT. It is an extension of *FEYNCALC* and can be used to automatize the most cumbersome tasks in the calculation of amplitudes.

The motivation for writing *PHI* was the lack of software for quickly and systematically implementing a quantum field theoretic model; for example an effective model like the various CHPT models mentioned above which have a more complicated power counting than models which simply expand Green's functions perturbatively in a coupling constant. However, the

package is general enough that other models can easily be specified as demonstrated with the simple example of QED (see appendix B). Given the many effective models that already exist and the many new ones that keep coming, it is the hope of the author that this software might be of use also outside the realm of CHPT.

The main features of *PHI* are:

- A set of basic objects are provided that can be composed and manipulated to form CHPT lagrangians.
- The most common CHPT lagrangians are included and new ones can easily be defined.
- The lagrangians can be expanded in terms of pion (meson) fields, with SU(2) (SU(3)) flavour traces being done automatically.
- External sources can be switched off and on.
- Compatibility with *FeynArts* for generation of Feynman diagrams and amplitudes including counter-terms. Power counting and storing of Feynman rules is systematized.

The idea is to allow writing up a calculation starting with a lagrangian and ending up with an amplitude, all within the framework of *FeynCalc*. This write-up is then to be transparent and intelligible to others, since all the lengthy standard manipulations are done automatically by using functions provided by the package. The remaining sections of this chapter describe the elements of such calculations. This description relies on the *FeynCalc* framework, from which, here, only the necessary variables and functions are briefly described. The full zoo of variables and functions is described in [MO00]. For a full description of the sub-package *PHI*, see appendices B and A. Let me mention here that the modular structure of *PHI* would make the implementation of a standardized model definition like mentioned above fairly easy. Let me also mention that although there are no conceptual obstacles, with the current speed of computers *FeynCalc*/*PHI* is not well suited for multi-loop calculations, its main strength being the relative ease of implementing and trying out new models.

Notice that the typeset expressions in the present chapter are not just how the results look after LaTeX'ing it etc. It is exactly what one sees on the screen after evaluating the *Mathematica* code. This is because *FeynCalc* by default gives the output in **`TraditionalForm`** for which it has a lot of formatting rules defined. To obtain plain text output, one can either change *Mathematica*'s default output format or apply **`InputForm`** to the result. Obtaining LaTeX output is illustrated in some of the notebooks in appendix B; alternatively one can of course use the *Mathematica* built-in LaTeX utilities.

5.2 Working with quantum fields

Notation

A generic field ϕ is written **QuantumField[ϕ]**. When doing functional or space-time differentiation, an extra argument should be supplied: **QuantumField[ϕ][r]**, where **r** is a momentum or space-time variable. Depending on which kind of field is to be represented, additional information can be supplied to **QuantumField**.

- If ϕ represents a vector field, it may be given an argument with head **LorentzIndex**: **QuantumField[ϕ, LorentzIndex[μ]][x]**.
- If ϕ is part of an SU(N) isospin multiplet, it may be given an argument with head **SUNIndex**: **QuantumField[ϕ, SUNIndex[j]][x]**.
- If ϕ represents a fermion, its adjoint field $\bar{\phi} = \phi^\dagger \gamma^0$ is represented by **DiracBar[ϕ]** (*PHI* [1]).
- Optionally (*PHI*), instead of a symbol ϕ, one may use **Particle[q]**, where **q** is some particle name, e.g. **Pion**.

QuantumFields can be composed and manipulated arithmetically with **+**, **-** and *****, and space-time derivatives may be taken via the functions **FieldDerivative** and **CovariantFieldDerivative** (*PHI*) [2]. E.g.

$$\partial_\mu(\phi_\pi(x)^2) \tag{5.1}$$

is represented by

```
FieldDerivative[QuantumField[Particle[Pion]][x]^2,
  x, LorentzIndex[μ]]
```

On polynomials of **QuantumField**s, functional derivatives may be performed with respect to the **QuantumField**s. E.g.

$$\partial_\phi \phi^2 \tag{5.2}$$

is calculated by

[1] Here and in the following the *PHI* in parentesis indicates a *FeynCalc* symbol/function that is available only on loading *PHI* (see appendix A for how to do this.)

[2] This implementation of space-time differentiation is designed to work with the *PHI* extensions. The original *FeynCalc* space-time differentiation operators are **RightPartialD, LeftPartialD, LeftRightPartialD, ExpandPartialD**.

```
FunctionalD[QuantumField[φ]^2, QuantumField[φ]]
```

QuantumFields may be grouped in SU(N) matrices or multiplets via the heads **IsoVector**, **UMatrix** and **UVector**. E.g. the SU(N) construction

$$\overrightarrow{\overline{\psi}}_{\mathrm{N}}\gamma^{\mu}u\partial_{\mu}u^{\dagger}\overrightarrow{\psi}_{\mathrm{N}}, \tag{5.3}$$

where u is some $N \times N$ field matrix, is represented by

```
UVector[QuantumField[DiracBar[Particle[Nucleon]]]][x].
DiracGamma[LorentzIndex[μ]].
NM[UMatrix[SMM][x],
  FieldDerivative[Adjoint[UMatrix[SMM][x]], x,
    LorentzIndex[μ]]].
UVector[QuantumField[Particle[Nucleon]]][x]
```

The *MATHEMATICA* **Dot** is used for multiplication of Dirac matrices and the multiplication of SU(N) matrices with SU(N) vectors, whereas **NM** (*PHI*) is used for multiplication of SU(N) matrices. Many operations through *FEYNCALC*/*PHI* functions can be performed on expressions like the one above. For more information see [MO00] and appendices B and A. To illustrate the use of **QuantumField**s we shall now consider two examples from CHPT. Notice that in CHPT a condensed notation is used and objects like **MM[x]** and **SMM[x]** actually contain **QuantumField**s. For an explanation of the notation, see appendix A.

Example: Chiral equations of motion and meson mass eigenstates

As a specific example of using **QuantumField**s we shall now consider the equations of motion of CHPT as derived in [GL85] (see chapter 2 for definitions of the variables used in the following). The equation of motions are obtained by adding a perturbation ξ to φ, that is, perturb U around the ground state $\overline{U}$,

$$U = \overline{U}e^{\frac{i}{F_{\pi}}\xi\cdot\sigma}, \tag{5.4}$$

and keeping only the terms linear in the perturbation. First we tell *PHI* to not expand the chiral quantities U, u, χ, D_{μ}; next we input U as given by (5.4), calling it **up**, replace **MM[x]** in the predefined lagrangian (2.25) with **up**, discard other than terms linear in the perturbation, do some reduction and write out dot products with indices and finally do the functional differentiation

```
SetOptions[#, Explicit -> False] & / MM, SMM,
  UChi, CovariantFieldDerivative;
```

```
up = NM[UMatrix[U][x],
  UFieldMatrix[QuantumField[Particle[
  UPerturbation]][x], ExpansionOrder -> 1,
  DropOrder -> 1, Constant ->
  DecayConstant[PhiMeson]]] // NMExpand;

lag = ArgumentsSupply[Lagrangian[ChPT3[2]], x] /.
  MM[x, ___] -> up /.
  CovariantFieldDerivative -> FieldDerivative;

s = DiscardTerms[lag, Retain ->
  Particle[UPerturbation] -> 1] // Simplify;

s1 = s // SurfaceReduce[#,
  UFields -> UPerturbation] & // Simplify;

s2 = s1 // IsoIndicesSupply // IndicesCleanup //
  CycleUTraces // Simplify;

dsdpi = FunctionalDerivative[s2,
  QuantumField[Particle[UPerturbation],
  SUNIndex[i1]][p1]] // SUNReduce // Simplify
```

yielding

$$\langle\left(\partial_\mu\partial_\mu\overline{U}^\dagger\overline{U} - \overline{U}^\dagger\partial_\mu\partial_\mu\overline{U} + \overline{U}^\dagger\chi - \chi^\dagger\overline{U}\right)\sigma^i\rangle\,, \tag{5.5}$$

which is to be set to zero. Due to the constraint $\det U = 1$ this implies[3]

$$\partial_\mu\partial_\mu\overline{U}^\dagger\overline{U} - \overline{U}^\dagger\partial_\mu\partial_\mu\overline{U} + \overline{U}^\dagger\chi - \chi^\dagger\overline{U} - \frac{1}{n}(\langle\overline{U}^\dagger\chi - \chi^\dagger\overline{U}\rangle) = 0, \tag{5.6}$$

where n is the order of the gauge group SU(n) (2 or 3). Writing out $\overline{U}$ in terms of $\overline{\varphi}\cdot\boldsymbol{\sigma}$ and diagonalizing the mass terms with matrices satisfying

$$\langle\sigma_p\sigma_{p'}^\dagger\rangle = 2\delta_{pp'}, \tag{5.7}$$

[3]More precisely: The fact that we can write the perturbation as $e^{\boldsymbol{\xi}\cdot\boldsymbol{\sigma}}$ stems from the condition $\det U = 1$ or $\langle\log U\rangle = 0$ and implies that we end up with an equation of the form $\langle A\sigma^i\rangle = 0 \Leftrightarrow \langle A\sigma^i - \frac{1}{n}\langle A\rangle\sigma^i\rangle = 0$ since the last term is 0.

one obtains in SU(3) (see the notebook in appendix B for the calculation)

$$\begin{aligned}
\sigma_{\pi^+} &= -\sqrt{\tfrac{1}{2}}(\sigma^1 + i\sigma^2) \quad , \quad \sigma_{\pi^-} = -\sqrt{\tfrac{1}{2}}(\sigma^1 - i\sigma^2), \\
\sigma_{\mathrm{K}^+} &= -\sqrt{\tfrac{1}{2}}(\sigma^4 + i\sigma^5) \quad , \quad \sigma_{\mathrm{K}^-} = -\sqrt{\tfrac{1}{2}}(\sigma^4 - i\sigma^5), \\
\sigma_{\mathrm{K}^0} &= -\sqrt{\tfrac{1}{2}}(\sigma^6 + i\sigma^7) \quad , \quad \sigma_{\bar{\mathrm{K}}^0} = -\sqrt{\tfrac{1}{2}}(\sigma^6 - i\sigma^7),
\end{aligned} \tag{5.8}$$

$$\sigma_{\pi^0} = \cos(\varepsilon)\sigma^3 + \sin(\varepsilon)\sigma^8 \quad , \quad \sigma_\eta = \cos(\varepsilon)\sigma^8 - \sin(\varepsilon)\sigma^3,$$

$$\tan(2\varepsilon) = \frac{\sqrt{3}}{2}\frac{m_\mathrm{d} - m_\mathrm{u}}{m_\mathrm{s} - \frac{m_\mathrm{u}+m_\mathrm{d}}{2}}, \tag{5.9}$$

and, using (2.29), to lowest order in the masses, the eigenvalues

$$\begin{aligned}
m^2_{\pi^\pm} &= (m_\mathrm{u} + m_\mathrm{d})B_0, \\
m^2_{\mathrm{K}^\pm} &= (m_\mathrm{u} + m_\mathrm{s})B_0, \\
m^2_{\mathrm{K}^0} &= m^2_{\bar{\mathrm{K}}^0} = (m_\mathrm{d} + m_\mathrm{s})B_0, \\
m^2_{\pi^0} &= (m_\mathrm{u} + m_\mathrm{d})B_0 - \tfrac{4}{3}(m_\mathrm{s} - \tfrac{m_\mathrm{u}+m_\mathrm{d}}{2})B_0 \sin^2(\varepsilon)/\cos(2\varepsilon), \\
m^2_\eta &= \tfrac{2}{3}(\tfrac{m_\mathrm{u}+m_\mathrm{d}}{2} + 2m_\mathrm{s})B_0 + \tfrac{4}{3}(m_\mathrm{s} - \tfrac{m_\mathrm{u}+m_\mathrm{d}}{2})B_0 \sin^2(\varepsilon)/\cos(2\varepsilon).
\end{aligned} \tag{5.10}$$

Example: Chiral one-loop divergencies

Again, we shall derive a well-known result following [GL85]. First we write the lagrangian (2.25) in a notation more convenient for our purpose,

$$\mathcal{L}_2 = \frac{F_\pi^2}{4}\left(\langle u_\mu u_\mu\rangle + \langle \chi_+\rangle\right), \tag{5.11}$$

with

$$\chi_+ \equiv u^\dagger \chi u^\dagger + u\chi^\dagger u, \;\; u_\mu \equiv i u^\dagger D_\mu U u^\dagger. \tag{5.12}$$

and then perturb U around the ground state $\overline{U}$,

$$U = \overline{u} e^{\frac{i\sqrt{2}}{F_\pi}\boldsymbol{\xi}\cdot\boldsymbol{\sigma}}\overline{u}, \tag{5.13}$$

keeping only the terms quadratic in the perturbation. This can be achieved with the following sequence of commands:

```
lag = 1/4 DecayConstant[Pion]^2 (UTrace[
  NM[USmall[LorentzIndex[μ1][x],
  USmall[LorentzIndex[μ1][x]] +
  UChiPlus[x]])

lag0 = lag //
  UPerturb[#, ExpansionOrder -> {0, 2}] & //
  NMExpand // Expand //
  DiscardTerms[#, Retain ->
  {Particle[UPerturbation] -> 2}] & //
  CycleUTraces // Simplify

s0 = -lag0 // IsoIndicesSupply //
  IndicesCleanup // Expand //
  CycleUTraces // Simplify
```

s0 is now minus the terms of the lagrangian quadratic in the perturbation.

The next steps are: 1) Go to Euclidean space-time ($x_\nu y^\nu \to -x_\nu y^\nu$). 2) Write **s0** as a quadratic form $(\xi, \mathcal{D}\xi)$,

$$\int \mathrm{d}x \mathcal{L}_2^{\mathrm{ChPT}} = \bar{Z}_2 - \frac{1}{2}F^2\,(\xi, \mathcal{D}\xi)\,, \tag{5.14}$$

with

$$\begin{aligned} \mathcal{D}^{ab}\xi^b &= -d_\nu d_\nu \xi^a + \hat{\sigma}^{ab}\xi^b, \\ d_\nu \xi^a &= \partial_\nu \xi^a + \hat{\Gamma}_\nu^{ab}\xi^b, \end{aligned} \tag{5.15}$$

$\hat{\sigma}$ hermitean, and $\hat{\Gamma}$ anti-hermitean. 3) Identify $\hat{\sigma}$ and $\hat{\Gamma}$. 4) Calculate $Z_{\text{one loop}}$,

$$\begin{aligned} e^{iZ_{\text{one loop}}} &= \int \mathrm{d}\mu[\xi] e^{(i/2)F^2(\xi, D\xi)}, \\ Z_{\text{one loop}} &= \tfrac{1}{2} i \log\det D \\ &= \ldots\ - \tfrac{1}{16\pi^2}\tfrac{1}{D-4}\int d^4x\ \mathrm{Sp}\left(\tfrac{1}{12}\hat{\Gamma}_{\mu\nu}\hat{\Gamma}^{\mu\nu} + \tfrac{1}{2}\hat{\sigma}^2\right) + \ldots. \end{aligned} \tag{5.16}$$

All of this is done in a notebook in appendix B. In particular step 3) is accomplished by the following reasoning:
Assume that

$$\begin{aligned}(\xi, \mathcal{D}\xi) &= \xi^a(-\delta^{ab}\partial_\nu\partial_\nu - \hat{\Gamma}^{aj}_\nu\hat{\Gamma}^{jb}_\nu - \delta^{aj}(\partial_\nu\hat{\Gamma}^{jb}_\nu) \\ &\quad -2\delta^{aj}\hat{\Gamma}^{jb}_\nu\partial_\nu + \hat{\sigma}^{ab})\xi^b \\ &\equiv A + B + C + D + E\end{aligned} \tag{5.17}$$

- C drops due to anti-hermiticity.
- Find double derivative term A.
- Find $(B + E)$ by setting derivatives to 0.
- Find $D = (\xi, \mathcal{D}\xi) - (B + E) - A$ and $\hat{\Gamma}$ by setting $\partial_\nu\xi, \xi \to 1$.
- Calculate $B = \xi^a\hat{\Gamma}^{aj}_\nu\hat{\Gamma}^{jb}_\nu\xi^b$.
- Calculate $E = (B + E) - B$ and $\hat{\sigma}$ by setting $\partial_\nu\xi, \xi \to 1$.
- Symmetrize $\hat{\sigma}$ and anti-symmetrize $\hat{\Gamma}$ and check that $A + B + C + D + E$ is indeed equal to the original $(\xi, \mathcal{D}\xi)$.

The idea governing the way such calculations are done in the present work is that general and to some extent trivial but tedious operations such as using the completeness relations for SU(N) generators, the Cayley-Hamilton / Newton formulae and equations of motion relations are relegated to functions defined in the package *FeynCalc*.

5.3 Lagrangians and Feynman rules

FeynCalc has some lagrangians predefined: The QCD lagrangian, **`Lagrangian["QCD"]`**, some twist-2 operator product expansion lagrangians [MO00], many of the CHPT lagrangians (*PHI*) (see appendix A) like e.g. the leading strong lagrangian **`Lagrangian[ChPT2[2]]`**, and the two leading QED lagrangians (*PHI*) **`Lagrangian[QED[1]]`** and **`Lagrangian[QED[2]]`**. To get a Feynman rule from a lagrangian, functional differentiation must be done. Functional differentiation is implemented through the functions **`FunctionalDerivative`** and **`FeynRule`**. The former is a lower level function which we have already used, the latter additionally does some reduction. In the following, a few elementary applications of **`FeynRule`** will be considered.

Example: The QED 3-vertex

One does functional differentiation with respect to the three fields on the term

$$eA_\mu \bar{\psi}\gamma^\mu\psi \tag{5.18}$$

from the leading order QED lagrangian **`Lagrangian[QED[1]]`**. In computerized notation, this term reads

```
CouplingConstant[QED[1]]
QuantumField[Particle[Photon], LorentzIndex[μ]].
QuantumField[DiracBar[Particle[Electron]]].
DiracGamma[LorentzIndex[μ]].
QuantumField[Particle[Electron]]
```

and the differentiation is done by issuing

```
FeynRule[Lagrangian[QED[1]],
{QuantumField[Particle[Electron]][p1],
QuantumField[DiracBar[Particle[Electron]]][p2],
QuantumField[Particle[Photon],
  LorentzIndex[μ3]][p3]}]
```

yielding

$$ie\gamma^{\mu 3}. \tag{5.19}$$

Notice that **`FeynRule`** does not write out the momentum conserving $\delta(p_1+p_2+p_3)$. As we shall see later, this is anyway enforced when using the vertex for Feynman diagram calculations.

Example: The weak $W^+W^+W^-W^-$ vertex

We calculate the Feynman rule from the term

$$L_G = -\frac{1}{2}G_j^{\mu\nu}G_j^{\mu\nu}. \tag{5.20}$$

First we introduce some short-hand symbols:

```
q = QuantumField;
l = LorentzIndex;
s = SUNIndex;
p = Particle;
```

Next we define the term (5.20)

```
lg = -1/4*
FieldStrength[l[μ], l[ν], s[i],
  CouplingConstant -> g, Explicit -> True,
  QuantumField -> Particle[G]]
FieldStrength[l[μ], l[ν], s[i],
  CouplingConstant -> g, Explicit -> True,
  QuantumField -> Particle[G]]
```

Transform to the W, $W^\dagger$ fields

```
lg1 =
SUNReduce[SUNSimplify[L], Explicit -> True,
  HoldSums -> False] /.
{q[__, s[3]] -> 0,
q[d___, p[G], l[μ_], s[1]] ->
  1/Sqrt[2](q[d, p[W], l[μ]] + q[d, p[W†], l[μ]]),
q[d___, p[G], l[μ_], s[2]] ->
  1/(Sqrt[2]I)(q[d, p[W], lμ] - q[d, p[W†], l[μ]])} // Calc
```

Getting the Feynman rule is done by

```
mWeak = FeynRule[lg1,
  {q[p[W†], l[μ1]][p1], q[p[W†], l[μ2]][p2],
  q[p[W], l[μ3]][p3], q[p[W], l[μ4]][p4]}] //
Simplify
```

The result reads

$$-ig^2(g^{\mu_1\mu_4}g^{\mu_2\mu_3} + g^{\mu_1\mu_3}g^{\mu_2\mu_4} - 2g^{\mu_1\mu_2}g^{\mu_3\mu_4}). \tag{5.21}$$

Example: The strong 4-gluon vertex

To calculate the Feynman rule we can use a predefined lagrangian and simply evaluate

```
FeynRule[Lagrangian["QCD"],
  q[GaugeField, l[μ1], s[i1]][p],
  q[GaugeField, l[μ2], s[i2]][q],
  q[GaugeField, l[μ3], s[i3]][r],
  q[GaugeField, l[μ4], s[i4]][s]]//
IndicesCleanup // FullSimplify
```

which yields

$$\begin{aligned} &-ig_S^2\Big(g^{\mu_1\mu_2}g^{\mu_3\mu_4}(f_{i_1i_4k_1}f_{i_2i_3k_1}+f_{i_1i_3k_1}f_{i_2i_4k_1})+\\ &g^{\mu_1\mu_3}g^{\mu_2\mu_4}(f_{i_1i_2k_1}f_{i_3i_4k_1}-f_{i_1i_4k_1}f_{i_2i_3k_1})-\\ &g^{\mu_1\mu_4}g^{\mu_2\mu_3}(f_{i_1i_3k_1}f_{i_2i_4k_1}+f_{i_1i_2k_1}f_{i_3i_4k_1})\Big) \end{aligned} \tag{5.22}$$

Example: The 4-pion CHPT vertex

The leading 4-pion CHPT Feynman rule is derived from a predefined lagrangian by evaluating the following:

```
lag = Lagrangian[ChPT2[2]] //
  ArgumentsSupply[#, x,
    ExpansionOrder -> 4, DropOrder -> 4]& //
  DiscardTerms[#, Retain ->
    {Particle[Pion] -> 4}, Method -> Expand]& //
  ExpandU // IsoIndicesSupply //
  IndicesCleanup // Simplify;

mChPT = FeynRule[lag,
  q[p[Pion], SUNIndex[I1]][p1],
  q[p[Pion], SUNIndex[I2]][p2],
  q[p[Pion], SUNIndex[I3]][p3],
  q[p[Pion], SUNIndex[I4]][p4]] // Simplify
```

The reason for the initial sequence of commands issued is that the CHPT lagrangians are stored in the usual condensed notation (see chapter 2) and need to be expanded in the physical fields before applying **FeynRule**. For an explanation of these commands, see appendix A. The

result reads

$$
\begin{aligned}
&\tfrac{-i}{3f_\pi^2} \\
&\Big(\delta_{i_1 i_4}\delta_{i_2 i_3} \\
&(p_1\cdot p_2 + p_1\cdot p_3 - 2p_1\cdot p_4 - 2p_2\cdot p_3 + p_2\cdot p_4 + p_3\cdot p_4 - m_\pi^2) + \\
&\delta_{i_1 i_3}\delta_{i_2 i_4} \\
&(p_1\cdot p_2 - 2p_1\cdot p_3 + p_1\cdot p_4 + 2p_2\cdot p_3 - 2p_2\cdot p_4 + p_3\cdot p_4 - m_\pi^2) + \\
&\delta_{i_1 i_2}\delta_{i_3 i_4} \\
&(2p_1\cdot p_2 - p_1\cdot p_3 - 2p_1\cdot p_4 - p_2\cdot p_3 - p_2\cdot p_4 + 2p_3\cdot p_4 - m_\pi^2)\Big).
\end{aligned}
\tag{5.23}
$$

5.4 Feynman rules and Feynman diagrams

To use calculated Feynman rules for calculating Feynman diagrams we shall employ the following strategy:

i Make a list of all vertices necessary to calculate the given process to the given order in the perturbation expansion.

ii For each vertex calculate the Feynman rule using the procedure outlined in the previous section.

iii Generate the **`Generic`** and **`Classes`** *FeynArts* couplings using the functions provided by *FeynCalc* (*PHI*) and store the files in the directory "HighEnergyPhysics/Phi/CouplingVectors" using a naming convention understood by *FeynCalc* (*PHI*).

iv Use *FeynArts* to generate the raw diagrams to the counter-term order to which we are working and insert the Feynman rules in these diagrams via the model files "Automatic.gen" and "Automatic.mod" (which are provided by *FeynCalc* and which load the couplings stored in the directory "HighEnergyPhysics/Phi/CouplingVectors").

v Use various *FeynCalc* utilities to reduce the result to a human readable form.

The first step is illustrated by the case of $\pi\pi$ scattering in CHPT below. The second step has been discussed in the previous section. In the following we shall discuss the remaining steps one by one.

Regarding step iii: Since *FeynArts* is used for the calculation of Feynman diagrams, we need to convert the vertices generated in *FeynCalc* notation to a form that *FeynArts* understands. The standard way of doing this is to write two model definition files. One called a "generic" model definition file containing the kinematic structure for the couplings and one called a "classes" model definition file containing the isospin/particle structure. This splitting corresponds to the 3 different levels, "generic", "classes" and "particle", at which one can calculate amplitudes with *FeynArts*. These conventions are described in [Hah01]. For our purposes we need not understand these details as we shall deal exclusively with the "classes" level. The way chosen to implement the *FeynCalc* → *FeynArts* communication is to feed the calculated vertices to *FeynArts* through the two model files "Automatic.gen" and "Automatic.mod". These files are really small programs that read settings (propagators etc.) from the active *FeynCalc* (*PHI*) model file and couplings from the directory "HighEnergyPhysics/Phi/CouplingVectors". The coupling files in this directory have been generated with the *FeynCalc* (*PHI*) functions **MomentaCollect**, **GenericCoupling**, **ClassesCoupling** and **CheckF**. To see how this works, we will again consider some examples.

Example: Storing the weak $W^+W^+W^-W^-$ vertex

Consider the vertex **mWeak** from (5.21). First we need to tell *PHI* which monomials we consider kinematical:

```
$ExpansionQuantities =
Union[$ExpansionQuantities, {MetricTensor[__]}];
```

Then we collect these

```
mWeak1 = MomentaCollect[mWeak];
```

Next we generate **mWeak1** the "generic" vector by

```
GenericCoupling[mWeak1]
```

yielding (in **StandardForm**)

```
{MetricTensor[μ1, μ4] MetricTensor[μ2, μ3],
MetricTensor[μ1, μ3] MetricTensor[μ2, μ4],
MetricTensor[μ1, μ2] MetricTensor[μ3, μ4]}
```

and the "classes" vector by

```
ClassesCoupling[mWeak1]
```

yielding (in **StandardForm**)

```
{{(-i g^2}, {-i g^2}, {2 i g^2}}
```

In this particular case (and for all other Standard Model couplings up to next-to-leading order) we need not save the coupling vectors as these are already part of the standard *FeynArts* distribution in the model files "Lorentz.gen" and "SM.mod". The full "classes" vector reads

```
{{(-i g^2, i g^2 (4 dZe - 4 dSW/SW + 4 dZW)},
{-i g^2, i g^2 (-2 dZe + 2 dSW/SW - 2 dZW)},
{2 i g^2, i g^2 (-2 dZe + 2 dSW/SW - 2 dZW)}}
```

If we call the "classes" vector $\vec{G}$, the coupling, that is, the product of the "generic" and the "classes" vector, can be written in a more readable form[4] as

$$\vec{G}_{V_i,V_j,V_k,V_l} \cdot \begin{pmatrix} g^{\mu\nu} g^{\rho\sigma} \\ g^{\mu\rho} g^{\nu\sigma} \\ g^{\mu\sigma} g^{\rho\nu} \end{pmatrix}, \tag{5.24}$$

where

$$G^{(1)}_{V_i,V_j,V_k,V_l} = 2ig^2,\ G^{(2)}_{V_i,V_j,V_k,V_l} = -ig^2,\ G^{(3)}_{V_i,V_j,V_k,V_l} = -ig^2 \tag{5.25}$$

to leading order, and

$$G^{(1)}_{V_i,V_j,V_k,V_l} = ig^2(4dZ_e - 4dS_W/S_W + 4dZ_W), \tag{5.26}$$

$$G^{(2)}_{V_i,V_j,V_k,V_l} = ig^2(-2dZ_e + 2dS_W/S_W - 2dZ_W), \tag{5.27}$$

$$G^{(3)}_{V_i,V_j,V_k,V_l} = ig^2(-2dZ_e + 2dS_W/S_W - 2dZ_W) \tag{5.28}$$

to next-to-leading order ($g = \frac{e}{S_W}$, S_W is sin of the Weinberg angle and dZ_e, dS_W and dZ_W are renormalization constants).

[4] This notation is not what one sees on the screen, it is used simply to make the concepts more intelligible.

Example: Storing the 4-pion CHPT vertex

For renormalizable theories having a "generic" vector which contains the kinematical structures is logical, since no new structures appear in the higher order counter-term lagrangians. For effective theories this is not the case. The way chosen to use *FeynArts* for effective theories is, as mentioned, through the two model files "Automatic.gen" and "Automatic.mod", which set up a "generic" vector containing all the kinematical structures (monomials) up the order we are working. The "classes" vector then keeps track of the power counting by having non-zero entries only for the monomials of the given order. All this requires the environment variable **$VerticesSpecifications** to be set correctly.

Consider now the 4-pion CHPT vertex (5.23). To generate the coupling vectors to be stored, issue:

```
mChPT1 = MomentaCollect[mChPT1];
gChPT = GenericCoupling[mChPT1];
cChPT = ClassesCoupling[mChPT1];
```

These are saved in the directory "HighEnergyPhysics/Phi/CouplingVectors" by

```
CheckF[gChPT, XName[VertexFields ->
  {Pion[0], Pion[0], Pion[0], Pion[0]},
  PerturbationOrder -> 2, PhiModel -> ChPT2] <> ".Gen"];

CheckF[cChPT, XName[VertexFields ->
  {Pion[0], Pion[0], Pion[0], Pion[0]},
  PerturbationOrder -> 2, PhiModel -> ChPT2] <> ".Mod"];
```

The procedure outlined above has been carried out for many CHPT vertices and the resulting files in "HighEnergyPhysics/Phi/CouplingVectors" are part of the standard *FeynCalc* distribution.

We now move on to the initially defined step iv and again consider a simple example.

Example: Møller scattering diagrams

Consider leading-order Møller scattering (see the notebook in appendix B for the full calculation). First, create the topologies:

```
tops = CreateTopologies[0, 2 -> 2,
  Adjacencies -> {3},
```

```
  ExcludeTopologies -> {SelfEnergies, WFCorrections},
  CountertermOrder -> 0];
```

Insert the vertices in the topologies:

```
inserttops = InsertFields[tops,
  Electron[0], Electron[0] -> Electron[0], Electron[0],
  Model -> "Automatic", GenericModel -> "Automatic",
  InsertionLevel -> Classes];
```

Calculate the amplitude:

```
amp = CreateFCAmp[inserttops]
```

Finally, for step v) we shall stick with the simple case of Møller scattering.

Example: Møller scattering postprocessing

The Møller cross-section can be calculated with the following code:

```
squaredAmp = FermionSpinSum[
  (Plus @@ amp)
  (ComplexConjugate[Plus @@ amp /.
    {μ1 -> ν1, μ2 -> ν1}]) /.
  ParticleMass[Photon, ___] -> 0 //
  Expand // Contract] /.  DiracTrace -> Tr //
  DiracSimplify // Contract;

squaredAmp // PropagatorDenominatorExplicit //
MandelstamReduce[#, Masses ->
  ParticleMass[Electron, RenormalizationState[0]],
  ParticleMass[Electron, RenormalizationState[0]],
  ParticleMass[Electron, RenormalizationState[0]],
  ParticleMass[Electron, RenormalizationState[0]],
  MandelstamCancel -> MandelstamU] & // Simplify
```

The result reads

$$\begin{aligned}\Big(16\Big(64\left(m_\psi^0\right)^8 - 16\,(6\,s - t)\left(m_\psi^0\right)^6 + 4\left(13\,s^2 + 3\,t\,s + 3\,t^2\right)\\ \left(m_\psi^0\right)^4 - 4\left(3\,s^3 + 3\,t\,s^2 + 3\,t^2\,s + 2\,t^3\right)\left(m_\psi^0\right)^2 +\\ \left(s^2 + t\,s + t^2\right)^2\Big)\left(e^0\right)^4\Big)\Big/\Big(t^2\left(-4\left(m_\psi^0\right)^2 + s + t\right)^2\Big)\end{aligned} \tag{5.29}$$

Having discussed individually the steps i)-v) of a scattering amplitude calculation, we now briefly sketch the simple example of the calculation of the one-loop diagrams of $\pi\pi$ scattering in CHPT. (again, the full calculation of the one-loop scattering amplitude is contained in a notebook in appendix B).

Example: One-loop pion-pion scattering amplitude in CHPT

Create all topologies with one loop, 4- or 6-leg vertices and no self-energy or wave-function renormalization diagrams; tell *PHI* which field-vertices to use; insert these fields; create the amplitudes:

```
mesonstop =
  CreateTopologies[1, 2 -> 2,
  Adjacencies -> 4, 6,
  ExcludeTopologies -> SelfEnergies, WFCorrections,
  CountertermOrder -> 0];

mins = InsertFields[mesonstop,
  Pion[0, i1], Pion[0, i2] ->
  Pion[0, i3], Pion[0, i4],
  Model -> "Automatic",
  GenericModel -> "Automatic",
  InsertionLevel -> Classes];

amplFC = CreateFCAmp[mins,
  AmplitudeLevel -> Classes, NoSums -> True,
  EqualMasses -> True];
```

Drawing the diagrams is done with

```
Paint[mins];
```

yielding fig. 5.1 The remaining contributions are calculated analogously. After adding everything up and simplifying using the tools provided by *FeynCalc* one gets the result given in section 2.

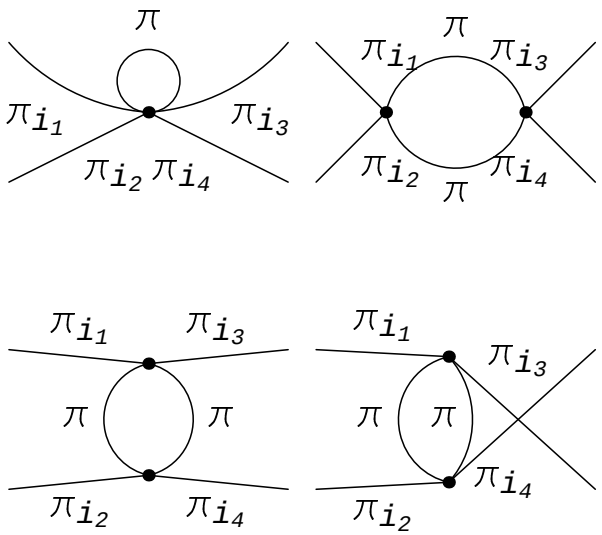

Figure 5.1: One-loop diagrams of pion-pion scattering.

Conclusion

1) The calculation in Chiral Perturbation Theory of various processes, that are important for the understanding of the strong and electro-weak forces at low energies, has been carried out. The approach has been to develop a general calculational machinery which can also be applied to other processes. The resulting computer program has been made publicly available and can be downloaded freely.

Two new calculations were carried out with the computer program:

- The calculation of the one-loop $\pi^+\pi^- \to \pi^+\pi^-$ amplitude in Chiral Perturbation Theory with virtual photons.
- The calculation of the one-loop amplitude of $K \to 2\pi$ with a momentum-carrying weak chiral lagrangian.

The conclusion from the first calculation is that electromagnetic corrections do not alter the strong predictions by more than 5%. Therefore the extraction of the strong scattering lengths a_0^0 and a_0^2 from the DIRAC experiment is on a sound footing. Work is under way to finish the full radiative calculation including $O(e^4)$ corrections. Moreover, the results of the calculation are necessary for a complete treatment of final state interactions in $K \to 2\pi$.

The second calculation allowed an order of magnitude estimate of the subtraction constant b, needed for the analysis of final state interactions in $K \to 2\pi$.

2) Mesonic final-state interactions in $K \to 2\pi$ have been analyzed. This analysis showed that final state interactions do potentially resolve the discrepancy of experimental with theoretical values of ε'/ε, but that at present no conclusive statement can be made, because of the uncertainties due to our ignorance of the weak interaction at low energies. Our framework provides the means of consistently including final state interactions in $K \to 2\pi$, but will remain non-predictive until the slope of the amplitude at the subtraction point has been provided e.g. by a lattice calculation.

From (4.46) and fig. 4.3 it is seen that the contribution of kaon loops is not of the same order of magnitude as the next-to-next-to-leading order contribution to the scalar form factor, but if one aims at a $\sim 1\%$ level of accuracy, one should do a full coupled-channel analysis of the final state interactions, including the KK channel. For $K \to 2\pi$, work in this respect is also under way.

Appendix A

PHI reference manual

This manual should serve both as a quick read for getting started with doing CHPT with *FeynCalc* and as a structured reference. It is, however, not an exhaustive reference for all functions. The full alphabetic reference can be found either with the help system coming with the *FeynCalc* distribution or on the *FeynCalc* web site [MO00]. Examples of applications of these can be found on the *FeynCalc* web-site [MO00].

It is assumed that the reader is familiar with *Mathematica*, in particular with how input is given to *Mathematica* and that the screen output can be chosen to be in either **`StandardForm`** which can be fed back to *Mathematica*, or in **`TraditionalForm`** which looks nice, but cannot be fed back to *Mathematica*. The usual convention is followed: Names starting with a capital letter represent objects provided by the package (built-in).

A.1 Installing and loading the packages

The *Mathematica* package *PHI* is distributed as a subpackage of *FeynCalc*, which is available at [MO00] in form of a compressed archive. Installing *FeynCalc* (and thereby *PHI*) is done by unpacking the archive and moving the resulting directory "HighEnergyPhysics" into either one of the following places:

- The *Mathematica* installation "Applications" directory: Under UNIX/LINUX this would typically be somewhere like "/usr/local/Mathematica/AddOns/Applications/". Under Windows it would typically be "C:\Program Files\Wolfram Research\Mathematica\4.1 \AddOns\Applications". Under MAC OS it would typically be "Macintosh HD:Applications:Wolfram Research:Mathematica:4.1:AddOns:Applications".

- Your local "Applications" directory: Under UNIX/LINUX this is " /.Mathemat-

ica/x/AddOns/Applications/", where the tilde refers to you home directory and the x to your version of *MATHEMATICA* (e.g. 4.0 or 4.1; as of version 4.2 of *MATHEMATICA*, "x/AddOns/" should be left out). Under other architectures there is no such directory.

In order to be able to use *FEYNARTS* together with *FEYNCALC*, one should download *FEYNARTS* from http://www.feynarts.de/. It should simply be extracted in the directory "HighEnergyPhysics". When done installing the packages, *FEYNCALC* can be loaded as described below.

Before loading *FEYNCALC*, one should set configuration variables causing *PHI* and *FEYNARTS* to be loaded. This is done by evaluating the following:

```
$LoadPhi=True;
$LoadFeynArts=True;
```

Then, the first thing to do before a calculation can be undertaken is to specify a model. If needed, lagrangians to be loaded can also be specified. E.g. to specify standard SU(2) CHPT one would have to evaluate the following before loading *FEYNCALC*:

```
$Configuration="ChPT2";
$Lagrangians={"ChPT2"[2],"ChPT2"[4]};
```

After doing this (if often working with the same model, one may want to put the above in the configuration file "PhiStart.m"), one can load *FEYNCALC* in the standard manner with

```
«"HighEnergyPhysics‘FeynCalc‘";
```

A.2 Framework

Consider the basic quantity in CHPT, the $U(x)$ field containing the meson fields φ^i. It is written as **MM[x]**. Below are shown some examples of input and the resulting screen output on evaluation

```
In[1]:= MM
Out[1]= 𝒰

In[2]:= ?MM
```

MM[x] := UFieldMatrix[QuantumField[Particle[Pion]][x]].
MM takes three optional arguments with head RenormalizationState, RenormalizationScheme and ExpansionState respectively. MM[i,x] is the i'th power of MM[x]

```
In[3]:= MM[x]
```

$$\text{Out[3]}= \frac{i\,\vec{\pi}\cdot\vec{\sigma}}{f_\pi}-\frac{\vec{\pi}\cdot\vec{\sigma}\star\vec{\pi}\cdot\vec{\sigma}}{2\,(f_\pi)^2}-\frac{i\left(\vec{\pi}\cdot\vec{\sigma}\star\vec{\pi}\cdot\vec{\sigma}\star\vec{\pi}\cdot\vec{\sigma}\right)}{6\,(f_\pi)^3}+\frac{\vec{\pi}\cdot\vec{\sigma}\star\vec{\pi}\cdot\vec{\sigma}\star\vec{\pi}\cdot\vec{\sigma}\star\vec{\pi}\cdot\vec{\sigma}}{24\,(f_\pi)^4}+\mathbb{Id}$$

```
In[4]:= MM[x, ExpansionOrder → 6, DropOrder → ∞]
```

$$\text{Out[4]}= \frac{i\,\vec{\pi}\cdot\vec{\sigma}}{f_\pi}-\frac{\vec{\pi}\cdot\vec{\sigma}\star\vec{\pi}\cdot\vec{\sigma}}{2\,(f_\pi)^2}-\frac{i\left(\vec{\pi}\cdot\vec{\sigma}\star\vec{\pi}\cdot\vec{\sigma}\star\vec{\pi}\cdot\vec{\sigma}\right)}{6\,(f_\pi)^3}+\frac{\vec{\pi}\cdot\vec{\sigma}\star\vec{\pi}\cdot\vec{\sigma}\star\vec{\pi}\cdot\vec{\sigma}\star\vec{\pi}\cdot\vec{\sigma}}{24\,(f_\pi)^4}+\frac{i\left(\vec{\pi}\cdot\vec{\sigma}\star\vec{\pi}\cdot\vec{\sigma}\star\vec{\pi}\cdot\vec{\sigma}\star\vec{\pi}\cdot\vec{\sigma}\star\vec{\pi}\cdot\vec{\sigma}\right)}{120\,(f_\pi)^5}-\frac{\vec{\pi}\cdot\vec{\sigma}\star\vec{\pi}\cdot\vec{\sigma}\star\vec{\pi}\cdot\vec{\sigma}\star\vec{\pi}\cdot\vec{\sigma}\star\vec{\pi}\cdot\vec{\sigma}\star\vec{\pi}\cdot\vec{\sigma}}{720\,(f_\pi)^6}+\mathbb{Id}$$

```
In[5]:= MM[x, ExpansionOrder → 6, DropOrder → 1]
```

$$\text{Out[5]}= \frac{i\,\aleph\,\vec{\pi}\cdot\vec{\sigma}}{f_\pi}+\mathbb{Id}$$

```
In[6]:= MM[1/2, x, ExpansionOrder → 6, DropOrder → 1]
```

$$\text{Out[6]}= \frac{i\,\aleph\,\vec{\pi}\cdot\vec{\sigma}}{2\,f_\pi}+\mathbb{Id}$$

```
In[7]:= MM[1/2, x, ExpansionOrder → 6, DropOrder → 1]//
        StandardForm
```

```
Out[7]= (i DropFactor[PseudoScalar[2]]
        IsoDot[IsoVector[QuantumField[Particle[PseudoScalar[2]]]][x],
        IsoVector[UMatrix[UGenerator[]]]])/(2 DecayConstant[PseudoScalar[2]])+
        UMatrix[UIdentity]
```

```
In[8]:= $UExpansionCoefficients
```

$$\text{Out[8]= } \left\{1, 1, \frac{1}{2}, \frac{1}{6}, \frac{1}{24}, \frac{1}{120}, \frac{1}{720}, \frac{1}{5040}, \frac{1}{40320}, \frac{1}{362880}, \frac{1}{3628800}\right\}$$

These examples illustrate some general features of *MATHEMATICA*:

- A function may take different numbers of arguments.
- If not supplied, optional arguments are assumed to have default values.
- The special kind of arguments called options and denoted with "→" are always optional.
- Default values for options can be set with **SetOptions**.

They also illustrate some general features of *FEYNCALC* and *PHI*:

- Most built-in quantities have display rules defined so that their output form is typeset (when using **TraditionalForm** as output format type).
- All built-in quantities have descriptions which can be accessed in the standard *MATHEMATICA* way by using the **?** operator.
- The behaviour of some functions is controlled by the setting of environment variables recognizable by the **$** as the first letter. In contrast to options, these are meant to be set once and for all in a calculation session, preferably in the configuration "PhiStart.m" or in the chosen configuration file in the directory "Configurations". When using one of the predefined configurations the user does not have to care about these.

A.3 Building blocks, lagrangians

As we have seen, the most important building block when constructing chiral mesonic lagrangians are the U matrix, the χ matrix and traces and derivatives of these.

MM[x]	the matrix $e^{\frac{i}{F_\pi}\varphi\cdot\sigma}$ collecting the meson fields. Evaluating returns a result in terms of dot products (**IsoDot**) of isovectors (**IsoVector**) of φ with isovectors of the triplet or octet of matrices σ (**UGeneratorMatrix**) generating SU(2) or SU(3)

MM[i, x]	the **i**'th power of **MM[x]**
UChiMatrix[x]	equivalent to **UMatrix[UChi[]][x]**. The matrix χ containing the scalar and pseudoscalar external source fields. Depending on the setting of options, evaluating can return a result either in terms of generator matrices or the unevaluated quark mass matrix (see **UMatrix, UGenerator, QuarkMass**)
UTrace[e]	attempts to calculate the trace of the expression **e**. Only very simple expressions are calculated; that is, terms with one symbolic matrix or explicitly written matrices. Other expressions are returned as **UTrace1[e]**. More complicated expressions can be reduced using **UExpand** or **WriteOutUMatrices**
FieldDerivative[g[x], x, {l1, l2, ...}]	calculates $\frac{\partial}{\partial x_{l1}}\frac{\partial}{\partial x_{l2}}\ldots$ on the expression **g[x]**
CovariantFieldField Derivative[g[x], x, {l1, l2, ...}]	as above but with the vector and axial-vector source field terms included. This is defined in the chosen model configuration file

Building blocks for CHPT lagrangians

These functions are predefined in terms of lower level functions, the most important of which are listed below.

UFieldMatrix[f]	matrix $e^{\frac{i}{F_\pi}\boldsymbol{f}\cdot\boldsymbol{\sigma}}$ of the field $\boldsymbol{f}$

UMatrix[m]	is recognized as an SU(2) or SU(3) matrix (depending on the setting of the option **GaugeGroup**). If **m** is one of the four quantities below an expanded result is returned
UGenerator[]	generic name for the matrices generating SU(2) or SU(3)
UGenerator[i]	the **i**'th generating matrix
UChi[]	the matrix χ
QuarkMass[]	the quark mass matrix
UQuarkCharge[]	the quark charge matrix
QuantumField[f]	**QuantumField[f][x]** represents a quantum field depending on the space-time arguments **x**. **QuantumField[f]** may be given as argument to **IsoVector**
Particle[p]	represents a particle field and may be used as the argument **f** above
IsoVector[v]	represents an SU(2) or SU(3) multiplet with number of entries corresponding to the number of generators
UVector[v]	represents an SU(2) or SU(3) multiplet with number of entries corresponding to the dimension of the representation

Basic functions used internally for defining the above building blocks

ExpansionOrder	the order in the meson fields to which every U matrix is expanded

DropOrder	the maximal order of monomials in the meson fields (e.g. when multiplying two U matrices)
GaugeGroup	the number N of generators of the gauge group SU(N)
UDimension	the dimension of the representation of the gauge group
DiagonalToU	whether a matrix should be written as a linear combination of the generator matrices and the identity matrix
QuarkToMesonMasses	whether the quark masses in the quark mass matrix should be expressed by the meson masses using the mass relations **$QuarkToPionMassesRules** (when **GaugeGroup** is set to 2) or **$QuarkToMesonMassesRules** (when **GaugeGroup** is set to 3)

Options of CHPT building blocks and basic functions

Adjoint[m]	if **m** is a matrix it is adjoint, if it's a scalar (members of **$UScalars**) it's just complex conjugated
Conjugate[s]	complex conjugation of s. The built-in function **Conjugate** has been extended to know about *PHI* objects

Complex conjugation and adjungation

ParticleMass[p]	mass of the particle p
DecayConstant[p]	decay constant of the particle p

UCouplingConstant[m, i]	the **i**'th coupling constant of the model m. The **i** is optional
RenormalizationState[i]	optional argument for constants specifying whether or not a constant is renormalized (**i**=1 corresponds to the former, **i**=0 to the latter)
RenormalizationOrder[i]	optional argument for constants
RenormalizationScheme[i]	optional argument for constants

Constants

As mentioned, not only options, but also environment variables control the behaviour of the defined functions and allow for customization. If for instance one wants to check representation independence (c.f. below (2.27)) one can calculate an amplitude, change **$UExpansionCoefficients** and verify that the result is the same as before.

$QuarkToPionMassesRules	rules for translating from u, d quark masses to pion masses (the default is standard CHPT to lowest order)
$QuarkToMesonMassesRules	rules for translating from u, d, s quark masses to meson masses (the default is standard CHPT to lowest order)
$UExpansionCoefficients	list of coefficients used for expanding the U matrix containing the meson fields (the default is the exponential representation)
$UParticles	list of allowed names for particle and source fields
$ExpansionQuantities	which quantities apart from powers of the momenta should be collected
$SUNBasis	the basis matrices of the representation of the gauge group. Changing them will also change **SU2F, SU3F, SU3D**

$ConstantIsoIndices	isospin indices that are not automatically contracted or summed over

Environment variables controlling the behaviour of CHPT functions

Corresponding to the way fields are grouped, there are several be multiplication operations defined: Single field, isovector and matrix multiplication.

NM	non-commutative multiplication for matrices and/or fields
IsoDot	dot product for isospin vectors
IsoCross	cross product for isospin vectors using the antisymmetric structure constants **SU2F[i,j,k]** or **SU3F[i,j,k]**
IsoSymmetricCross	cross product for isospin vectors using the symmetric structure constants **SU3D[i,j,k]** (0 in SU(2))

Multiplication operators for fields and field multiplets

To manipulate the expressions, a number of utility functions are provided. Which functions should be applied, in which order and with which options, depends on the problem under consideration. Examples are given below.

ExpandU[e]	expands IsoDot products in the expression **e** involving isovectors of generator matrices into products containing at most one generator matrix which can be handled by **UTrace**
DiscardTerms[e, Retain → {p1 → n1, p2 → n2, ...}]	discards all factors of fields that do not contain **n1** particle fields **p1**, **n2** particle fields **p2**, etc.

ArgumentsSupply[e, x, opts]	**ArgumentsSupply** is a function that allows quick entering of lagrangians. That is, an expression **e** can be given without heads for derivatives, Lorentz and isospin arguments and without an extra pairs of empty brackets for scalars. The expression is then returned with space-time argument **x** and options specifications and brackets supplied
UNMSplit[e, x , ops]	returns the expression **e** with **NM** products of **MM** (without arguments) expanded in the meson fields
CycleUTraces[e]	rotates factors in **NM** or dot products inside **UTrace1** until the 'smallest' factor is in front
CommutatorReduce[e]	does some reduction on expressions containing **NM** or dot products
NMExpand[e]	distributes **NM** over **Plus**
WriteOutIsoVectors[e]	writes out isovectors (with head **IsoVector**) in components
WriteOutUMatrices[e]	writes out matrices (with head **UMatrix**) in components
IsoIndicesSupply[e]	replaces dot products of isovectors with contracted indices
SUNReduce[e]	does some reduction on expressions involving isoindices (with head**SUNIndex**)
IndicesCleanup[e]	renames Lorentz and isospin indices in a systematic way

Functions for manipulating lagrangians

After manipulations, the result typically contains functions of isospin indices. These have head

SUNIndex.

SU2Delta[i,j]	SU(2) Kronecker delta function
SU2F[i,j,k]	SU(2) antisymmetric structure constants
SU3Delta[i,j]	SU(3) Kronecker delta function
SU3F[i,j,k]	SU(3) antisymmetric structure constants
SU3D[i,j,k]	SU(3) symmetric structure constants

Isospin functions

As a simple example consider e.g. how the leading order CHPT SU(3) lagrangian (2.25) was used to derive the equations of motion (5.6) for the mesons, diagonalize the mass term and thus calculate the information (5.8) tabulated in **$QuarkToMesonMassesRules**. One point of using some or all of the above functions for manipulating lagrangians is to bring it into a form where Feynman rules can simply be read off. The "reading off" can be done using the function **FeynRule** or the lower level function **FunctionalDerivative**. The task discussed in the next section is then how to generate all necessary Feynman rules (for a given process), store them and use the stored rules for doing loop Feynman diagram calculations.

A.4 Feynman rules, loops and power counting

Consider the CHPT 4-pion Feynman rule. It is derived straight-forwardly with *FeynCalc* as shown below (again an excerpt from a *Mathematica* notebook with the full calculation available at [MO00]). Notice that the predefined lagrangian **Lagrangian[ChPT2[2]]** is preloaded because of the configuration choice described in the beginning of section A.2. It is stored in a compact notation which is expanded by the function **ArgumentsSupply**.

The leading order lagrangian in raw form:

```
In[9]:= Lagrangian[ChPT2[2]]
```

$$\text{Out[9]}= \frac{1}{4}(f_\pi)^2\left(\langle U^\dagger\chi\rangle + \langle\chi^\dagger U\rangle + \left\langle D_\mu(U)^\dagger D_\mu(U)\right\rangle\right)$$

The evaluated lagrangian (external fields have been set to zero in the configuration file):

```
In[10]:= ll = ArgumentsSupply[Lagrangian[ChPT2[2]], x,
          RenormalizationState[0], GaugeGroup → 2,
          ExpansionOrder → 4, DropOrder → 4];
```

Redundant terms are discarded:

```
In[11]:= lll = DiscardTerms[ll, Retain → {Particle[Pion,
          RenormalizationState[0]] → 4}, Method → Expand]//
          Simplify
```

$$\text{Out[11]}= \frac{1}{48\,(f_\pi)^2}\Big(\big\langle \vec{\pi}\cdot\vec{\sigma}\star\vec{\pi}\cdot\vec{\sigma}\star\vec{\pi}\cdot\vec{\sigma}\star\vec{\pi}\cdot\vec{\sigma}\big\rangle\,(m_\pi)^2 - 2\,\big\langle \vec{\pi}\cdot\vec{\sigma}\star\vec{\pi}\cdot\vec{\sigma}\star\partial_\mu(\vec{\pi})\cdot\vec{\sigma}\star\partial_\mu(\vec{\pi})\cdot\vec{\sigma}\big\rangle + \big\langle \vec{\pi}\cdot\vec{\sigma}\star\partial_\mu(\vec{\pi})\cdot\vec{\sigma}\star\vec{\pi}\cdot\vec{\sigma}\star\partial_\mu(\vec{\pi})\cdot\vec{\sigma}\big\rangle + 3\,\big\langle \vec{\pi}\cdot\vec{\sigma}\star\partial_\mu(\vec{\pi})\cdot\vec{\sigma}\star\partial_\mu(\vec{\pi})\cdot\vec{\sigma}\star\vec{\pi}\cdot\vec{\sigma}\big\rangle - \big\langle \partial_\mu(\vec{\pi})\cdot\vec{\sigma}\star\vec{\pi}\cdot\vec{\sigma}\star\vec{\pi}\cdot\vec{\sigma}\star\partial_\mu(\vec{\pi})\cdot\vec{\sigma}\big\rangle + \big\langle \partial_\mu(\vec{\pi})\cdot\vec{\sigma}\star\vec{\pi}\cdot\vec{\sigma}\star\partial_\mu(\vec{\pi})\cdot\vec{\sigma}\star\vec{\pi}\cdot\vec{\sigma}\big\rangle - 2\,\big\langle \partial_\mu(\vec{\pi})\cdot\vec{\sigma}\star\partial_\mu(\vec{\pi})\cdot\vec{\sigma}\star\vec{\pi}\cdot\vec{\sigma}\star\vec{\pi}\cdot\vec{\sigma}\big\rangle\Big)$$

Generator matrices are traced:

```
In[12]:= llle = ExpandU[lll, CommutatorReduce →
          True]//Simplify
```

$$\text{Out[12]}= \frac{1}{24\,(f_\pi)^2}\Big(\big(\vec{\pi}\cdot\partial_\mu(\vec{\pi})\big)^2 + \big(\partial_\mu(\vec{\pi})\cdot\vec{\pi}\big)^2 + \big(\vec{\pi}\cdot\vec{\pi}\big)^2\,(m_\pi)^2 - 2\,\big(\vec{\pi}\cdot\vec{\pi}\star\partial_\mu(\vec{\pi})\cdot\partial_\mu(\vec{\pi})\big) + 3\,\big(\vec{\pi}\cdot\partial_\mu(\vec{\pi})\star\partial_\mu(\vec{\pi})\cdot\vec{\pi}\big) - \partial_\mu(\vec{\pi})\cdot\vec{\pi}\star\vec{\pi}\cdot\partial_\mu(\vec{\pi}) - 2\,\big(\partial_\mu(\vec{\pi})\cdot\partial_\mu(\vec{\pi})\star\vec{\pi}\cdot\vec{\pi}\big)\Big)$$

Indices are supplied:

```
In[13]:= llll = llle//IsoIndicesSupply//IndicesCleanup//
          CommutatorReduce[#, FullReduce →
          True]&//Simplify
```

$$\text{Out[13]}= \frac{(m_\pi)^2\,(\pi^{k1})^2\,(\pi^{k2})^2 - 2\,(\pi^{k2}\,\partial_{\tau 1}\pi^{k1} - \pi^{k1}\,\partial_{\tau 1}\pi^{k2})^2}{24\,(f_\pi)^2}$$

Calculation of the Feynman rule:

```
In[14]:= melsimplified = FeynRule[llll,
         {QuantumField[Particle[PhiMeson],
         SUNIndex[i1]][p1],
         QuantumField[Particle[PhiMeson],
         SUNIndex[i2]][p2],
         QuantumField[Particle[PhiMeson],
         SUNIndex[i3]][p3],
         QuantumField[Particle[PhiMeson],
         SUNIndex[i4]][p4]}]//
         Simplify
```

$$\text{Out[14]}= -\frac{1}{3\,(f_\pi)^2}\Big(i\,\Big(\Big(-(m_\pi)^2 + p_1\cdot p_2 + p_1\cdot p_3 - 2\,p_1\cdot p_4 - 2\,p_2\cdot p_3 + p_2\cdot p_4 + p_3\cdot p_4\Big)\,\delta_{i_1 i_4}\,\delta_{i_2 i_3} +$$

$$\Big(-(m_\pi)^2 + p_1\cdot p_2 - 2\,p_1\cdot p_3 + p_1\cdot p_4 + p_2\cdot p_3 - 2\,p_2\cdot p_4 + p_3\cdot p_4\Big)\,\delta_{i_1 i_3}\,\delta_{i_2 i_4} -$$

$$\Big((m_\pi)^2 + 2\,p_1\cdot p_2 - p_1\cdot p_3 - p_1\cdot p_4 - p_2\cdot p_3 - p_2\cdot p_4 + 2\,p_3\cdot p_4\Big)\,\delta_{i_1 i_2}\,\delta_{i_3 i_4}\Big)\Big)$$

Terms are collected according to momenta:

```
In[15]:= mfacoll = MomentaCollect[melsimplified,
         ParticlesNumber → 4, PerturbationOrder → 2,
         ScalarproductForm → Pair];
```

Coupling vectors are generated and saved:

```
In[16]:= gencoup = GenericCoupling[mfacoll];

In[17]:= classcoup = ClassesCoupling[mfacoll];

In[18]:= CheckF[gencoup, XName[VertexFields →
         {PseudoScalar[2][0], PseudoScalar[2][0],
         PseudoScalar[2][0], PseudoScalar[2][0]},
         PerturbationOrder → 2, PhiModel → ChPT2] <> .Gen];

In[19]:= CheckF[classcoup, XName[VertexFields →
         {PseudoScalar[2][0], PseudoScalar[2][0],
         PseudoScalar[2][0], PseudoScalar[2][0]},
         PerturbationOrder → 2, PhiModel → ChPT2] <> .Mod];
```

The reason for collecting the monomials in the momenta is that this allows splitting in two coupling vectors, one containing the kinematical monomials and one containing the rest. The dot product of these two vectors then gives the full coupling. Although this splitting is of no obvious use here, this is the convention used by *FeynArts* (see [Hah01]). The coupling vectors

are stored in the "Phi" subdirectory "CouplingVectors". From there they can be loaded by the *FeynArts* models "Automatic.gen" and "Automatic.mod".

FunctionalDerivative[lag, {f1,...}]	where {f1,...} is of the form {QuantumField[name, LorentzIndex[mu], ..., SUNIndex[a]][p1],...}, calculates the functional derivative of lag with respect to the field list (with incoming momenta p1, etc.) and does the fourier transform
FunctionalDerivative[lag, {f1,...}]	where {f1,...} is of the form {QuantumField[name, LorentzIndex[mu],...SUNIndex[a]],...}] calculates the functional derivative and does partial integration but omits the x-space delta functions
FeynRule[lag,{f1,...}]	gives the feynmanrule corresponding to the field configuration {f1,...} of the lagrangian lag

Functions for calculating Feynman rules. These are built-in *FeynCalc* functions and are describe here only for completeness

MomentaCollect[f]	collects terms containing the variables given by the setting of the options **MomentumVariablesString** and **ParticlesNumber**

GenericCoupling[f]	constructs the kinematical coupling vector to be used in a generic model file for *FeynArts* from the Feynman rule f. **GenericCoupling** will only work on sums where each term has a monomial in the momenta (and other expansion quantities) as overall factor. Such expressions can usually be obtained with **MomentaCollect**. Also depends on the setting of **$ExpansionQuantities**
ClassesCoupling[f]	constructs the corresponding "Classes" coupling vector
XName[opts]	generates a filename using a simple naming convention
CheckF[exp,fil]	If fil exists, **Get**s fil and returns the loaded expressions. If fil does not exist, evaluates exp, saves it to fil and returns the evaluated exp. If fil ends with ".Gen" or ".Mod", the setting of **Directory** is ignored and fil is saved in the "CouplingVectors" subdirectory of "Phi"

Functions for generating and saving coupling definitions

ParticlesNumber	specifies the number of lines of a vertex
PerturbationOrder	specifies the maximum order in the momentum and/or other perturbative expansion parameters from **$ExpansionQuantities**
ScalarProductForm	specifies the scalarproduct used for the momenta

ExtendedCollect	specifies whether or not to collect terms containing elements from **$ExpansionQuantities**
Directory	specifies the directory used for storing files
ForceSave	whether or not to force evaluation and saving
NoSave	whether or not to save. Overrides the setting of **ForceSave**
VertexFields	list of fields of a vertex
PhiModel	name of the model to be used for naming files
XFileName	name to be used for saving files. If set to **Automatic** the name is generated from the remaining options specifications

Options of functions for generating and saving coupling definitions

Similarly to the 4-pion Feynman rule, any other Feynman rule can be generated using the predefined lagrangians or defining new lagrangians one self. Indeed, this has been done by the author, and *PHI* ships with a number of ready to use coupling vectors (in the directory "CouplingVectors"). Thus, when calculating some amplitude to some order, having all necessary Feynman rules at our disposal, the procedure is to use *FeynArts* for generating all diagrams and calculating the amplitude using the models "Automatic.gen" and "Automatic.mod" included with the *FeynCalc* distribution [MO00]. These are actually small programs that load the coupling vector definitions specified by the variable **$VerticesSpecifications** from the directory "CouplingVectors" inside the *FeynCalc* directory hierarchy. Thus, in order to use the *FeynArts* ChPT couplings distributed with *FeynCalc*, one must have assigned a suitable value to **$VerticesSpecifications** and give

```
Model -> "Automatic",
GenericModel -> "Automatic"
```

as arguments to the *FeynArts* function **InsertFields** (the use of which is documented in [Hah01]).

By default, **$VerticesSpecifications** is set to contain all vertices stored in the directory "HighEnergyPysics/Phi/CouplingVectors" belonging to the current *PHI* model, **$Configuration**, so usually one does not have to worry about setting it. When using vertices from lagrangians belonging to different models, this, however, becomes necessary.

$VerticesSpecifications	variable used by the *FeynArts* model files "Automatic.gen" and "Automatic.mod". It is a list specifying the options of **XName**, and it determines which of the files in the subdirectory "CouplingVectors" of "Phi" are loaded by "Automatic.gen" and "Automatic.mod"

Specifying which vertices to use

The result (diagrams) returned by **InsertFields** can be given to **CreateFCAmp** which then returns the amplitudes corresponding to each diagram. *FeynCalc* provides a number of functions for processing these, i.e. doing loop integrals, reducing isospin (see section A.2), kinematical and Dirac structures, etc. Which functions should be applied and in which order, depends on the specific process. It can be straightforward, but often care must be taken in order not to end with excessively time consuming computations. In appendix B specific examples are given which illustrate this point.

Appendix B

PHI applications

This chapter contains descriptions of calculations made to test the package *PHI* (and *FeynCalc* in general and *FeynArts*). The calculations presented should be seen as attempts at realizing the ideal goal set at the end of section 5.1. Insofar as obtaining publication ready output from calculated amplitudes is by no means straightforward, the goal is not always reached and some of the notebooks do contain rather lengthy and unreadable code, mostly serving the purpose of structuring calculated expressions. Also, certainly, some of the calculations were left when a result was obtained and could use some more cleaning up. Nevertheless, in general, it is the hope that the calculations will serve the interested reader as prototypes for his own calculations with *PHI*.

If you have the CD accompanying this text, the notebooks described in this chapter are available to you from the CD, and should run with the versions of *PHI* and *FeynCalc* also on the CD. Alternatively, the notebooks can be downloaded from [Ore02]. Some of these notebooks will undergo improvement with time, but should run with the version of *FeynCalc* available at the same place. Since they are compressed, they must be uncompressed before they can be opened with *Mathematica*. Assuming the right versions of *PHI* and *FeynCalc* has been installed (see section A.1), the notebooks should run with no further ado, as they load *FeynCalc* in their preambles.

B.1 QED

These notebooks derive textbook results from QED with one lepton, thus testing among other things, the handling of one-loop two-point functions with two propagators and two different masses in the loop, a three-point function with three propagators and two different masses, as well as the handling of spinors.

Møller scattering

Name of file: "Moeller.nb".
Available at: http://www.feyncalc.org/phi/examples/QED/Moeller.nb.gz.
Description: The Møller differential cross section to leading order.

Radiative corrections

Name of file: "QEDRadiativeCorrections.nb".
Available at: http://www.feyncalc.org/phi/examples/QED/QEDRadiativeCorrections.nb.gz.
Description: The photon self-energy, the electron self-energy and the photon-electron-electron vertex correction to one loop in QED.

B.2 CHPT, pions

These notebooks derive some of the classical SU(2) results of Gasser and Leutwyler [GL84] using Feynman diagram techniques for the calculation of amplitudes.

Lagrangians

Name of file: "EOMTricks.nb".
Available at:
http://www.feyncalc.org/phi/examples/ChPT/Pions/EOMTricks.nb.gz.
Description: Useful SU(2) equation of motion relations are derived.

Name of file: "GeneratingFunctional.nb".
Available at:
http://www.feyncalc.org/phi/examples/ChPT/Pions/GeneratingFunctional.nb.gz.
Description: The one-loop generating functional is derived.

Feynman rules

Name of file: "FeynmanRules.nb".
Available at:
http://www.feyncalc.org/phi/examples/ChPT/Pions/FeynmanRules.nb.gz.
Description: The pionic $O(p^2)$ 4,6-vertices and the $O(p^2)$ 4-vertex are calculated and stored.

Name of file: "PSFeynmanRules.nb".

Description: Pionic vertices with external pseudo-scalar and scalar fields are calculated and stored.
Available at:
http://www.feyncalc.org/phi/examples/ChPT/Pions/PSFeynmanRules.nb.gz.

Two-point amplitudes

Name of file: "WaveFunctionFactor.nb".
Available at:
http://www.feyncalc.org/phi/examples/ChPT/Pions/WaveFunctionFactor.nb.gz.
Description: The one-loop pion wave-function and mass renormalization factors are calculated and stored.

Name of file: "DecayConstantFactor.nb".
Available at:
http://www.feyncalc.org/phi/examples/ChPT/Pions/DecayConstantFactor.nb.gz.
Description: The one-loop renormalization of the pion decay constant is calculated and stored.

Name of file: "PionPseudoscalarFactor.nb".
Available at:
http://www.feyncalc.org/phi/examples/ChPT/Pions/PionPseudoscalarFactor.nb.gz.
Description: The two-point pion-pseudo-scalar correlator to one loop is calculated and stored.

Scalar form factor

Name of file: "ScalarFormFactor.nb".
Available at:
http://www.feyncalc.org/phi/examples/ChPT/Pions/ScalarFormFactor.nb.gz.
Description: The pion scalar form factor to one loop.

Pion-pion scattering

Name of file: "PiPiScattering.nb".
Available at:
http://www.feyncalc.org/phi/examples/ChPT/Pions/PiPiScattering.nb.gz.
Description: The one-loop pion-pion scattering amplitude. Partial wave and isospin projections are given.

B.3 CHPT, pions and photons

Amplitudes involving the external vector field of the covariant derivative are calculated.

Feynman rules

Name of file: "FeynmanRules.nb".
Description: Pionic vertices with an external vector field are calculated and stored.
Available at:
http://www.feyncalc.org/phi/examples/ChPT/Pions+Photons/FeynmanRules.nb.gz.

Vector form factor

Name of file: "PhotonFormFactor.nb".
Available at:
http://www.feyncalc.org/phi/examples/ChPT/Pions+Photons/PhotonFormFactor.nb.gz.
Description: The vector form factor to one loop.

Compton scattering

Name of file: "ComptonScattering.nb".
Available at:
http://www.feyncalc.org/phi/examples/ChPT/Pions+Photons/ComptonScattering.nb.gz.
Description: Compton scattering of a pion and an external vector field to one loop.

B.4 CHPT, mesons

These notebooks derive some of the classical SU(3) results of [GL85] as well as a few 3- and 4-point amplitudes.

Lagrangians

Name of file: "EquationsOfMotion.nb".
Available at:
http://www.feyncalc.org/phi/examples/ChPT/Mesons/EquationsOfMotion.nb.gz.
Description: The SU(3) equations of motion are derived.

Name of file: "EOMTricks.nb".

Available at:
http://www.feyncalc.org/phi/examples/ChPT/Mesons/EOMTricks.nb.gz.
Description: Useful SU(2) equation of motion relations are derived.

Name of file: "GeneratingFunctional.nb".
Available at:
http://www.feyncalc.org/phi/examples/ChPT/Mesons/GeneratingFunctional.nb.gz.
Description: The one-loop generating functional is derived.

Feynman rules

Name of file: "FeynmanRules.nb".
Available at:
http://www.feyncalc.org/phi/examples/ChPT/Mesons/FeynmanRules.nb.gz.
Description: The mesonic SU(3) $O(p^2)$ 4,6-vertices and the $O(p^2)$ 4-vertex are calculated and stored.

Name of file: "SFeynmanRules.nb".
Available at:
http://www.feyncalc.org/phi/examples/ChPT/Mesons/PSFeynmanRules.nb.gz.
Description: Mesonic SU(3) vertices with an external scalar field are calculated and stored.

Two-point amplitudes

Name of file: "WaveFunctionFactor.nb".
Available at:
http://www.feyncalc.org/phi/examples/ChPT/Mesons/WaveFunctionFactor.nb.gz.
Description: The one-loop meson SU(3) wave-function and mass renormalization factors are calculated and stored.

Name of file: "DecayConstantFactor.nb".
Available at:
http://www.feyncalc.org/phi/examples/ChPT/Mesons/DecayConstantFactor.nb.gz.
Description: The one-loop renormalization of the pion, kaon and eta-meson decay constants are calculated and stored.

Name of file: "MesonPseudoscalarFactor.nb".
Available at:
http://www.feyncalc.org/phi/examples/ChPT/Mesons/MesonPseudoscalarFactor.nb.gz.
Description: The two-point one-loop correlators of a pseudo-scalar external field with a pion, kaon and an eta-meson are calculated and stored.

Scalar form factor

Name of file: "ScalarFormFactor.nb".
Available at:
http://www.feyncalc.org/phi/examples/ChPT/Mesons/ScalarFormFactor.nb.gz.
Description: The SU(3) meson scalar form factors to one loop.

Meson-meson scattering

Name of file: "MesonMesonScattering-pions.nb".
Available at:
http://www.feyncalc.org/phi/examples/ChPT/Pions/MesonMesonScattering-pions.nb.gz.
Description: The one-loop SU(3) pion-pion scattering amplitudes.
Name of file: "MesonMesonScattering-kaons.nb".
Available at:
http://www.feyncalc.org/phi/examples/ChPT/Pions/MesonMesonScattering-kaons.nb.gz.
Description: The one-loop kaon-kaon scattering amplitudes.

B.5 CHPT, pions and virtual photons

Following [KU98], the EM interaction is incorporated through the inclusion of virtual photons in the lagrangians. The one-loop generating functional is explicitly calculated, making use of the Cayley-Hamilton equations of motion. Also, the amplitude given in appendix C.1.1 is calculated.

Lagrangians

Name of file: "EquationsOfMotion.nb".
Available at:
http://www.feyncalc.org/phi/examples/ChPT/Pions+VirtualPhotons/
EquationsOfMotion.nb.gz.
Description: The SU(2) equations of motion for the pion and the photon are derived.

Name of file: "EOMTricks.nb".
Available at:
http://www.feyncalc.org/phi/examples/ChPT/Pions+VirtualPhotons/
EOMTricks.nb.gz.
Description: Useful equation of motion relations are derived.

Name of file: "GeneratingFunctional.nb".
Available at:
http://www.feyncalc.org/phi/examples/ChPT/Pions+VirtualPhotons/GeneratingFunctional.nb.gz.
Description: The one-loop generating functional with virtual photons is derived.

Feynman rules

Name of file: "FeynmanRules.nb".
Available at:
http://www.feyncalc.org/phi/examples/ChPT/Pions+VirtualPhotons/FeynmanRules.nb.gz.
Description: Feynman rules with virtual photons are calculated and stored.

Two-point amplitudes

Name of file: "WaveFunctionFactor.nb".
Available at:
http://www.feyncalc.org/phi/examples/ChPT/Pions+VirtualPhotons/WaveFunctionFactor.nb.gz.
Description: The one-loop pion wave-function and mass renormalization factors are calculated and stored.

Name of file: "PhotonWaveFunctionFactor.nb".
Available at:
http://www.feyncalc.org/phi/examples/ChPT/Pions+VirtualPhotons/PhotonWaveFunctionFactor.nb.gz.
Description: The one-loop photon wave-function renormalization factor is calculated and stored.

Name of file: "DecayConstantFactor.nb".
Available at:
http://www.feyncalc.org/phi/examples/ChPT/Pions+VirtualPhotons/DecayConstantFactor.nb.gz.
Description: The one-loop renormalization of the pion decay constant with virtual photons is calculated and stored.

Pion pion scattering

Name of file: "PiPiScattering.nb".
Available at:
http://www.feyncalc.org/phi/examples/ChPT/Pions+VirtualPhotons/PiPiScattering.nb.gz.
Description: The one-loop pion-pion scattering amplitude with virtual photons. All channels can be calculated. $O(e^4)$ contributions are also calculated.

B.6 Weak CHPT

The $\Delta S = 1$ lagrangians of [EKW93] are coupled to an external source and used for calculating the amplitudes used given in section C.2.

Feynman rules

Name of file: "FeynmanRules.nb".
Available at:
http://www.feyncalc.org/phi/examples/ChPT/Weak/FeynmanRules.nb.gz.
Description: Feynman rules of mesons and an axial external field using the weak lagrangian are calculated and stored.

Name of file: "SFeynmanRulesA.nb".
Available at:
http://www.feyncalc.org/phi/examples/ChPT/Weak/SFeynmanRulesA.nb.gz.
Description: $O(p^2)$ Feynman rules of mesons and the weak lagrangian lagrangian are calculated and stored.

Name of file: "SFeynmanRulesB.nb".
Available at:
http://www.feyncalc.org/phi/examples/ChPT/Weak/SFeynmanRulesB.nb.gz.
Description: $O(p^4)$ Feynman rules of mesons and the weak lagrangian lagrangian are calculated and stored.

Name of file: "PFeynmanRules.nb".
Available at:
http://www.feyncalc.org/phi/examples/ChPT/Weak/PFeynmanRules.nb.gz.
Description: Feynman rules of mesons, a pseudo-scalar external field and the weak lagrangian are calculated and stored.

Name of file: "S2FeynmanRules.nb".
Available at:
http://www.feyncalc.org/phi/examples/ChPT/Weak/S2FeynmanRules.nb.gz.
Description: Feynman rules of mesons, a scalar external field and the weak lagrangian are calculated and stored.

Two-point amplitudes

Name of file: "ScalarMesonFactor.nb".
Available at:
http://www.feyncalc.org/phi/examples/ChPT/Weak/ScalarMesonFactor.nb.gz.
Description: The two-point one-loop correlators of a scalar external field with a kaon are calculated and stored.

$\mathbf{K} \to \pi$

Name of file: "KSPiAmplitude.nb".
Available at:
http://www.feyncalc.org/phi/examples/ChPT/Weak/KSPiAmplitude.nb.gz.
Description: The three-point function of a kaon, a pion and the weak lagrangian.

Name of file: "KSPiChecks.nb".
Available at:
http://www.feyncalc.org/phi/examples/ChPT/Weak/KSPiChecks.nb.gz.
Description: Various checks and reduction of the expressions of "KSPiAmplitude.nb".

$\mathbf{K} \to 2\pi$

Name of file: "A7PiPiAmplitude.nb".
Available at:
http://www.feyncalc.org/phi/examples/ChPT/Weak/A7PiPiAmplitude.nb.gz.
Description: The one-loop three-point function of an external axial-vector field with the SU(3) index of K_s and two neutral pions.

Name of file: "P7PiPiAmplitude.nb".
Available at:
http://www.feyncalc.org/phi/examples/ChPT/Weak/P7PiPiAmplitude.nb.gz.
Description: The leading order three-point function of an external pseudo-scalar field with the SU(3) index of K_s and two neutral pions.

Name of file: "KSPiPiAmplitude.nb".
Available at:
http://www.feyncalc.org/phi/examples/ChPT/Weak/KSPiPiAmplitude.nb.gz.
Description: The four-point function of a K_s, two neutral pions and the weak lagrangian.

Name of file: "KSPiPiChecksA.nb".
Available at:
http://www.feyncalc.org/phi/examples/ChPT/Weak/KSPiPiChecksA.nb.gz.
Description: Various checks of the expressions of "KSPiPiAmplitude.nb".

Name of file: "KSPiPiChecksB.nb".
Available at:
http://www.feyncalc.org/phi/examples/ChPT/Weak/KSPiPiChecksB.nb.gz.
Description: Reduction of the expressions of "KSPiPiAmplitude.nb".

K → s

Name of file: "KSS2Amplitude.nb.nb".
Available at:
http://www.feyncalc.org/phi/examples/ChPT/Weak/KSS2Amplitude.nb.nb.gz.
Description: The three-point function of a kaon, an external scalar field and the weak lagrangian.

Name of file: "KSS2Checks.nb.nb".
Available at:
http://www.feyncalc.org/phi/examples/ChPT/Weak/KSS2Checks.nb.nb.gz.
Description: Various checks and reduction of the expressions of "KSS2Amplitude.nb".

Appendix C

One-loop amplitudes

C.1 Pion-pion scattering

C.1.1 $\pi^+\pi^- \to \pi^+\pi^-$

Leading order:

$$T^{(2)} = \frac{1}{f^2}(-2m_{\pi^0}^2 + s + t) + \frac{1}{f^2 st}\left\{-2e^2 f^2\left(s^2 + st + t^2 - 2m_{\pi^+}^2(s+t)\right)\right\}. \tag{C.1}$$

Rational contribution from the loops:

$$\begin{aligned} T^{(4)}_{\text{poly}} = & -\frac{4e^4}{288\pi^2 st(s-4m_{\pi^+}^2)(t-4m_{\pi^+}^2)} \\ & (-9344m_{\pi^+}^8 + 8m_{\pi^+}^4(73s^2 + st + 73t^2) + \\ & st(109s^2 + 199st + 109t^2) + \\ & 2336m_{\pi^+}^6 u + 2m_{\pi^+}^2 u(146s^2 + 543st + 146t^2)) - \\ & \frac{1}{288 f^4 \pi^2} \end{aligned} \tag{C.2}$$

$$(280m_{\pi^+}^4 + 198m_{\pi^0}^4 + 23s^2 + 20st + 23t^2 +$$

$$90m_{\pi^0}^2 u - 2m_{\pi^+}^2(324m_{\pi^0}^2 + 17u)) -$$

$$\frac{4e^2}{288f^2\pi^2(s - 4m_{\pi^+}^2)(t - 4m_{\pi^+}^2)}$$

$$(54m_{\pi^0}^2(-4m_{\pi^+}^2 + s)(4m_{\pi^+}^2 - t) - 69stu -$$

$$4m_{\pi^+}^2(51s^2 + 91st + 51t^2 + 292m_{\pi^+}^2 u - 816m_{\pi^+}^4)).$$

Counter-terms:

$$\begin{aligned} T_{\mathrm{CT}}^{(4)} &= \frac{2e^2}{9f^2}\Big[4(-10k_1 - 10k_2 + 18k_3 + 9k_4 + 9l_6)m_{\pi^+}^2 + \\ &\quad 2(10k_1 + 10k_2 + 9(2k_3 - k_4 + 8(k_6 + k_8)))m_{\pi^0}^2 - \\ &\quad (-10k_1 + 26k_2 + 54k_3 + 27k_4 + 27l_6)u\Big] + \\ &\quad \frac{1}{f^4}\Big[4l_3 m_{\pi^0}^4 + 2l_1(-8m_{\pi^+}^4 + s^2 + t^2 + 4m_{\pi^+}^2 u) + \\ &\quad l_2(-32m_{\pi^+}^4 + 3s^2 + 4st + 3t^2 + 12m_{\pi^+}^2 u)\Big] + \\ &\quad \frac{8e^4}{9}\Big[10h_2 + 18k_{14} - 5k_{15} + \\ &\quad \frac{5}{st}((2h_2 - k_{15})(-8m_{\pi^+}^4 + s^2 + t^2 + 2m_{\pi^+}^2 u) - \\ &\quad l_5(-8m_{\pi^+}^4 + s^2 + st + t^2 + 2m_{\pi^+}^2 u))\Big]. \end{aligned} \tag{C.3}$$

Logs:

$$T_{\log}^{(4)} = -\frac{e^4 \log(m_\gamma^2/\mu^2)}{2\pi^2} - \tag{C.4}$$

$$\frac{\log(m_{\pi^+}^2/\mu^2)}{96f^4\pi^2}\Big[8e^2f^2(8m_{\pi^+}^2-9m_{\pi^0}^2+3u)+$$
$$\frac{4e^4f^4}{st}(-8m_{\pi^+}^4+s^2+7st+t^2+2m_{\pi^+}^2u)+$$
$$(64m_{\pi^+}^4+60m_{\pi^0}^4+5s^2+8st+5t^2+$$
$$24m_{\pi^0}^2u-4m_{\pi^+}^2(48m_{\pi^0}^2+u))\Big]-$$
$$\frac{\log(m_{\pi^0}^2/\mu^2)}{32f^4\pi^2}\Big[10m_{\pi^0}^4+s^2+t^2+4m_{\pi^0}^2(u-4m_{\pi^+}^2)\Big].$$

$\overline{J}$'s (see appendix C.4):

$$\begin{aligned}T_{\overline{J}}^{(4)} &= \overline{J}_{m_\gamma^2,m_\gamma^2}(s)4e^4+\overline{J}_{m_\gamma^2,m_\gamma^2}(t)4e^4+ \\ &\frac{\overline{J}_{m_{\pi^0}^2,m_{\pi^0}^2}(s)}{2f^4}(-m_{\pi^0}^2+s)^2+\frac{\overline{J}_{m_{\pi^0}^2,m_{\pi^0}^2}(t)}{2f^4}(-m_{\pi^0}^2+t)^2+ \\ &\frac{\overline{J}_{m_{\pi^+}^2,m_{\pi^+}^2}(u)}{2f^4}(-2e^2f^2-4m_{\pi^+}^2+2m_{\pi^0}^2+u)^2+ \\ &\frac{\overline{J}_{m_{\pi^+}^2,m_{\pi^+}^2}(s)}{6f^4s^2(s-4m_{\pi^+}^2)} \\ &\Big[s^2(s-4m_{\pi^+}^2)(4(6m_{\pi^0}^4-3m_{\pi^0}^2(4m_{\pi^+}^2+s)+ \\ &m_{\pi^+}^2(8m_{\pi^+}^2+2s-t))+s(2s+t))+ \\ &4e^2f^2s(32m_{\pi^+}^6+s^2(6m_{\pi^0}^2-8s-13t)- \\ &16m_{\pi^+}^4(3s+t)+2m_{\pi^+}^2s(-12m_{\pi^0}^2+21s+16t))+ \\ &4e^4f^4(-32m_{\pi^+}^6-28m_{\pi^+}^2s(3s+2t)+ \\ &8m_{\pi^+}^4(15s+2t)+s^2(14s+25t))\Big]+(s\leftrightarrows t)\end{aligned} \tag{C.5}$$

$$\frac{\overline{J}_{m_{\pi^+}^2,m_\gamma^2}(m_{\pi^+}^2)}{3f^2(s-4m_{\pi^+}^2)(t-4m_{\pi^+}^2)}4e^2$$

$$\Big[-8m_{\pi^+}^2 st + 6m_{\pi^0}^2(s-4m_{\pi^+}^2)(t-4m_{\pi^+}^2) -$$

$$80m_{\pi^+}^4 u + 3stu + 6e^2 f^2(-16m_{\pi^+}^4 + s^2 + st + t^2 + 8m_{\pi^+}^2 u)\Big].$$

C_0's (see section C.4):

$$\begin{aligned} T_{C_0}^{(4)} \;=\; & \frac{e^4}{2\pi^2}C_0(s,m_{\pi^+}^2,m_{\pi^+}^2,m_\gamma^2,m_\gamma^2,m_{\pi^+}^2)(s-2m_{\pi^+}^2)+ \\ & \frac{e^4}{2\pi^2}C_0(t,m_{\pi^+}^2,m_{\pi^+}^2,m_\gamma^2,m_\gamma^2,m_{\pi^+}^2)(t-2m_{\pi^+}^2)+ \\ & \frac{1}{16Cf^2\pi^2 s}C_0(s,m_{\pi^+}^2,m_{\pi^+}^2,m_{\pi^+}^2,m_{\pi^+}^2,m_\gamma^2) \\ & (s-2m_{\pi^+}^2)(f^2(-4m_{\pi^+}^4+7m_{\pi^+}^2m_{\pi^0}^2-3m_{\pi^0}^4)s+ \\ & 2Ce^2(4e^2f^2(s+t-2m_{\pi^+}^2)+s(2u-4m_{\pi^+}^2+m_{\pi^0}^2)))+ \\ & \frac{1}{16Cf^2\pi^2 t}C_0(t,m_{\pi^+}^2,m_{\pi^+}^2,m_{\pi^+}^2,m_{\pi^+}^2,m_\gamma^2) \\ & (t-2m_{\pi^+}^2)(f^2(-4m_{\pi^+}^4+7m_{\pi^+}^2m_{\pi^0}^2-3m_{\pi^0}^4)t+ \\ & 2Ce^2(4e^2f^2(-2m_{\pi^+}^2+s+t)+t(-4m_{\pi^+}^2+m_{\pi^0}^2+2u)))- \\ & \frac{1}{16Cf^2\pi^2}C_0(u,m_{\pi^+}^2,m_{\pi^+}^2,m_{\pi^+}^2,m_{\pi^+}^2,m_\gamma^2) \\ & (u-2m_{\pi^+}^2)(f^2(-4m_{\pi^+}^4+7m_{\pi^+}^2m_{\pi^0}^2-3m_{\pi^0}^4)+ \\ & 2Ce^2(-4e^2f^2-4m_{\pi^+}^2+m_{\pi^0}^2+2u)). \end{aligned} \tag{C.6}$$

D_0's (see appendix C.4):

$$
\begin{aligned}
T^{(4)}_{D_0} &= \frac{e^4}{4\pi^2}\Big(\\
&D_0(s, m^2_{\pi^+}, t, m^2_{\pi^+}, m^2_{\pi^+}, m^2_{\pi^+}, m^2_\gamma, m^2_\gamma, m^2_{\pi^+}, m^2_{\pi^+})(t - 2m^2_{\pi^+})^2 + \\
&D_0(s, m^2_{\pi^+}, t, m^2_{\pi^+}, m^2_{\pi^+}, m^2_{\pi^+}, m^2_{\pi^+}, m^2_{\pi^+}, m^2_\gamma, m^2_\gamma)(s - 2m^2_{\pi^+})^2 + \\
&D_0(s, m^2_{\pi^+}, u, m^2_{\pi^+}, m^2_{\pi^+}, m^2_{\pi^+}, m^2_\gamma, m^2_\gamma, m^2_{\pi^+}, m^2_{\pi^+})(u - 2m^2_{\pi^+})^2 + \\
&D_0(t, m^2_{\pi^+}, u, m^2_{\pi^+}, m^2_{\pi^+}, m^2_{\pi^+}, m^2_\gamma, m^2_\gamma, m^2_{\pi^+}, m^2_{\pi^+})(u - 2m^2_{\pi^+})^2\Big).
\end{aligned}
\tag{C.7}
$$

Notice that any of the other (4 independent) elastic scattering processes involving π^+, π and/or pi^0 can easily be calculated with the notebook described in appendix B. Therefore the expressions are not given here.

C.2 Non-leptonic kaon decays

The expressions given in this section use the counter-term basis of ref. [EKW93]. They reduce to the off-shell expressions with a static lagrangian given in ref. [KMW91] and in [BPP98], if one translates into the E_i counter-term basis used by these authors. Notice that there is a sign error on E_3 and E_4 in the translation table (2.19) of [BPP98].

C.2.1 $\mathrm{K}_\mathrm{l} \to \pi^0$

Leading order:

$$
\Xi^{(2)} = 4B_0^2((2c_5 - c_2)m^2_\mathrm{K} - c_2 m^2_\pi + c_2 q^2). \tag{C.8}
$$

Logs:

$$
\begin{aligned}
\Xi^{(4)}_{\log} &= \frac{B_0^2}{288 f^2 \pi^2 (m^2_\pi - m^2_\mathrm{K})} \\
&\Big[\log(m^2_\pi/\mu^2)
\end{aligned}
\tag{C.9}
$$

$$9m_\pi^2(3m_\pi^2 - 7m_K^2 + 5q^2)((c_2 - 2c_5)m_K^2 + c_2m_\pi^2 - c_2q^2) +$$

$$\log(m_K^2/\mu^2)$$

$$18m_K^2\left\{(m_\pi^2 - m_K^2)((11c_2 - 10c_5)m_K^2 + 7c_2m_\pi^2) +\right.$$

$$\left.(2(3c_2 + c_5)m_K^2 - 8c_2m_\pi^2)q^2 + c_2q^4\right\} +$$

$$\log(m_\eta^2/\mu^2)$$

$$3m_\eta^2\left\{(10c_5 - 9c_2)m_K^4 + 2(14c_2 - 17c_5)m_K^2m_\pi^2 + 5c_2m_\pi^4\right.$$

$$\left.-2((8c_2 - 9c_5)m_K^2 + 7c_2m_\pi^2)q^2 + 9c_2q^4\right\}\Big].$$

Loop functions (see appendix C.4):

$$\Xi_{JK}^{(4)} = \frac{B_0^2}{18f^2} \tag{C.10}$$

$$\Big[\bar{J}_{m_K m_\eta}(q^2)$$

$$\left\{(11c_2 - 12c_5)m_K^4 + 6(3c_2 - 2c_5)m_K^2m_\pi^2 - 5c_2m_\pi^4 -\right.$$

$$\left.3(3(3c_2 - 2c_5)m_K^2 + c_2m_\pi^2)q^2 + 9c_2q^4\right\} +$$

$$\bar{J}_{m_\pi m_K}(q^2)$$

$$9\left\{-(c_2 + 4c_5)m_K^4 + 2(5c_2 - 2c_5)m_K^2m_\pi^2 - c_2m_\pi^4 +\right.$$

$$\left.((-7c_2 + 10c_5)m_K^2 - 7c_2m_\pi^2)q^2 + 5c_2q^4\right\} +$$

$$(m_\pi^2 - m_K^2)$$

$$6\Big\{-K_{m_K m_\eta}(q^2)((6c_5 - 7c_2+)m_K^2 + c_2m_\pi^2) +$$

$$9K_{m_\pi m_K}(q^2)((c_2-2c_5)m_K^2+c_2m_\pi^2)\Big\}\Big].$$

Strong counter-terms:

$$\Xi^{(4)}_{L_i} = -\frac{64B_0^2}{f^2} \tag{C.11}$$
$$((c_2-2c_5)m_K^2+c_2m_\pi^2-c_2q^2)(m_\pi^2(2L_6+L_8)+m_K^2(4L_6+L_8)).$$

Weak counter-terms contributing also to $K \to \pi$ with $q = 0$:

$$\begin{aligned}\Xi^{(4)}_{N_{5,8,10,11}} = \; & \frac{c_2B_0^2}{f^2 8} \\ & \Big\{-m_\pi^4N_8+q^2(m_\pi^2N_8+2m_K^2(N_5+N_8)) \\ & -2m_K^4(N_5+N_8-2(N_{10}+N_{11})) \\ & +m_K^2m_\pi^2(-2N_5-3N_8+2N_{11}+4N_{12})\Big\}.\end{aligned} \tag{C.12}$$

Weak counter-terms not contributing to $K \to \pi$ with $q = 0$:

$$\begin{aligned}\Xi^{(4)}_{N_{20-23}} = \; & \frac{4c_2B_0^2}{f^2} \\ & \Big\{2q^4N_{20}-(m_\pi^2-m_K^2)^2(2N_{21}+N_{22}+2N_{23}) \\ & +q^2(m_K^2(-2N_{20}-2N_{21}+N_{22}+2N_{23}) \\ & +m_\pi^2(-2N_{20}+2N_{21}+N_{22}+2N_{23}))\Big\}.\end{aligned} \tag{C.13}$$

C.2.2 $K_s \to 2\pi^0$

Leading order:

$$T^{+(2)} = \frac{i}{2f^2}\left\{c_2\,(-m_K^2 + 4m_\pi^2 + q^2 - 3s) + \frac{1}{q^2 - m_K^2}\left(2\,c_5\,(m_K^2 - m_\pi^2)(-m_K^2 + q^2 + s)\right)\right\}. \tag{C.14}$$

Logs:

$$\begin{aligned} T^{+(4)}_{\log,tu} = {} & \frac{i}{\pi^2 f^4 (m_K^2 - m_\pi^2)(q^2 - m_K^2)} \\ & \left[\log(m_\eta^2/\mu^2)\frac{m_\eta^2}{256}\right. \\ & \quad \{((7c_2 - 6c_5)m_K^2 + 6c_5 m_\pi^2)t^2 + \\ & \quad 2((5c_2 + 6c_5)m_K^2 - 6c_5 m_\pi^2)tu + \\ & \quad ((7c_2 - 6c_5)m_K^2 + 6c_5 m_\pi^2)u^2 - \\ & \quad c_2 q^2(7t^2 + 10tu + 7u^2)\} + \\ & \log(m_K^2/\mu^2)\frac{m_K^2}{192} \\ & \quad \{((5c_2 - 18c_5)m_K^2 + 18c_5 m_\pi^2)t^2 + \\ & \quad 2((c_2 - 12c_5)m_K^2 + 12c_5 m_\pi^2)tu + \\ & \quad ((5c_2 - 18c_5)m_K^2 + 18c_5 m_\pi^2)u^2 - \\ & \quad c_2 q^2(5t^2 + 2tu + 5u^2)\} - \\ & \log(m_\pi^2/\mu^2)\frac{m_\pi^2}{768} \end{aligned} \tag{C.15}$$

$$\Big\{-((49c_2+102c_5)m_K^2-102c_5m_\pi^2)t^2-$$
$$2((71c_2+42c_5)m_K^2-42c_5m_\pi^2)tu-$$
$$((49c_2+102c_5)m_K^2-102c_5m_\pi^2)u^2+$$
$$c_2q^2(49t^2+142tu+49u^2)\Big\}\Big].$$

$$T^{+(4)}_{\log,s}=\frac{-i}{6912\,f^4(m_K^2-m_\pi^2)} \tag{C.16}$$
$$\Big[\log(m_\eta^2/\mu^2)\frac{1}{\pi^2(q^2-m_K^2)^2}$$
$$\Big\{8c_5(-m_K^2+m_\pi^2)\Big(2m_\pi^4q^2(-2q^2+15s)-$$
$$m_K^6(-45m_\pi^2-100q^2+108s)-$$
$$m_K^2m_\pi^2(-50q^4+36m_\pi^2s+5q^2(m_\pi^2+12s))$$
$$+m_K^4(9m_\pi^4+5m_\pi^2(-19q^2+18s)+4q^2(-25q^2+21s))\Big)-$$
$$12c_2(-m_K^2+q^2)\Big(-64m_K^8+m_K^2(9m_\pi^6+$$
$$m_\pi^4(22q^2-9s)+3m_\pi^2q^2(8q^2-7s)+$$
$$12q^4(q^2-s))+3m_\pi^2q^4(-q^2+s)-m_\pi^6(9q^2+s)+$$
$$6m_\pi^4q^2(-2q^2+3s)+m_K^6(-97m_\pi^2-8q^2+124s)-$$
$$2m_K^4(5m_\pi^4-30q^4+3m_\pi^2s+q^2(-38m_\pi^2+48s))\Big)\Big\}+$$
$$\log(m_K^2/\mu^2)\frac{18}{\pi^2(m_K^2-q^2)}$$

$$\Big\{-6c_5(-m_K^2+m_\pi^2)\Big(15m_K^6+3m_\pi^2 s(q^2+s)-$$

$$m_K^4(-18m_\pi^2-8q^2+23s)-$$

$$m_K^2(-16m_\pi^4-5q^4+11q^2 s+9m_\pi^2(-2q^2+s))\Big)+$$

$$c_2\Big(-23m_K^8+3m_\pi^2 q^2 s(-q^2+3s)-$$

$$m_K^6(-158m_\pi^2-57q^2+137s)+$$

$$m_K^4(-156m_\pi^4-41q^4+143m_\pi^2 s+q^2(-220m_\pi^2+162s))-$$

$$m_K^2(-7q^6+9m_\pi^2 s^2+q^4(-62m_\pi^2+13s)+$$

$$4q^2(-39m_\pi^4+38m_\pi^2 s))\Big)\Big\}+$$

$$\log(m_\pi^2/\mu^2)\frac{36}{\pi^2(m_K^2-q^2)}$$

$$\Big\{6c_5(-m_K^2+m_\pi^2)\Big(12m_\pi^6+m_\pi^2 q^2(3q^2-7s)+$$

$$2m_\pi^4(4q^2-7s)+2m_K^4(m_\pi^2-s)+$$

$$m_K^2(13m_\pi^4-m_\pi^2(-6q^2+s)+2s(q^2+s))\Big)+$$

$$c_2\Big(3m_\pi^6(25q^2+3s)-m_K^6(17m_\pi^2+6s)-$$

$$4m_\pi^2 q^4(-4q^2+7s)-2m_\pi^4 q^2(-34q^2+19s)-$$

$$m_K^4(46m_\pi^4-64m_\pi^2 s+18s^2-3q^2(-3m_\pi^2+4s))+$$

$$m_K^2(-75m_\pi^6+q^4(10m_\pi^2-6s)+29m_\pi^4 s+$$

$$q^2(-22m_\pi^4-36m_\pi^2 s+18s^2))\Big)\Big\}+$$

$$\frac{288}{q^2 - m_K^2}$$

$$\Big\{k(m_K^2, m_\eta^2)(-m_K^2 + m_\pi^2)^2(-m_\pi^2 + q^2)$$

$$(5c_2 + (6c_5(-m_K^2 + m_\pi^2)))+$$

$$k(m_\pi^2, m_K^2)(-m_K^2 + m_\pi^2)^2(-m_\pi^2 + q^2)$$

$$(c_2 + (6c_5(-m_K^2 + m_\pi^2)))\Big\}\Big]$$

Loop functions (see appendix C.4):

$$T^{+(4)}_{\bar{J}KM^r,c_2} = \frac{i\,c_2}{864\,f^4} \tag{C.17}$$

$$\Big[\bar{J}_{m_\eta^2,m_\eta^2}(s)\ 24m_\pi^2(-13m_K^2 + 4m_\pi^2 - 3q^2 + 9s)+$$

$$\bar{J}_{m_K^2,m_K^2}(s)\ 108s(-3m_K^2 - q^2 + 3s)-$$

$$\bar{J}_{m_\pi^2,m_\pi^2}(s)\ 216(-m_\pi^2 + 2s)(m_K^2 - 4m_\pi^2 - q^2 + 3s)+$$

$$\bar{J}_{m_K^2,m_\eta^2}(t)$$

$$(302m_K^4 - 3q^2(-91m_K^2 + 19m_\pi^2 + 24t)+$$

$$m_K^2(443m_\pi^2 - 480t - 420u)-$$

$$m_\pi^2(97m_\pi^2 + 24t - 60u) + 18t(7t + 5u))+$$

$$\bar{J}_{m_\pi^2,m_K^2}(t)$$

$$9(-42m_K^4 - 13m_\pi^4+$$

$$q^2(-19m_{\mathrm{K}}^2 + 35m_\pi^2 - 16t) -$$

$$4m_\pi^2(16t + u) + 2t(23t + u) +$$

$$m_{\mathrm{K}}^2(103m_\pi^2 - 4(6t + u))) +$$

$$K_{m_{\mathrm{K}}^2, m_\eta^2}(t)$$

$$12(-26m_{\mathrm{K}}^4 + m_{\mathrm{K}}^2(31m_\pi^2 + 13q^2 - 5u) +$$

$$m_\pi^2(17q^2 + 5(-7m_\pi^2 + u))) +$$

$$K_{m_\pi^2, m_{\mathrm{K}}^2}(t)$$

$$36(-10m_{\mathrm{K}}^4 + m_\pi^2(17m_\pi^2 - 11q^2 + u) -$$

$$m_{\mathrm{K}}^2(-23m_\pi^2 + 19q^2 + u)) +$$

$$M^{\mathrm{r}}_{m_{\mathrm{K}}^2, m_\eta^2}(t)\ 540(-m_{\mathrm{K}}^2 + m_\pi^2)(-m_\pi^2 + q^2) +$$

$$M^{\mathrm{r}}_{m_\pi^2, m_{\mathrm{K}}^2}(t)\ 108(-m_{\mathrm{K}}^2 + m_\pi^2)(-m_\pi^2 + q^2) +$$

$$(t \leftrightarrows u)\Big].$$

$$T^{(4)}_{\bar{J}KM^{\mathrm{r}}, c_5} = \frac{i\, c_5 (m_{\mathrm{K}}^2 - m_\pi^2)}{144\, f^4 (q^2 - m_{\mathrm{K}}^2)} \tag{C.18}$$

$$\Big[\bar{J}_{m_\eta^2, m_\eta^2}(s)\ 8m_\pi^2(q^2 + 9(-m_{\mathrm{K}}^2 + s)) +$$

$$\bar{J}_{m_{\mathrm{K}}^2, m_{\mathrm{K}}^2}(s)\ 108s(-m_{\mathrm{K}}^2 + q^2 + s) +$$

$$\bar{J}_{m_\pi^2, m_\pi^2}(s)\ 72(-m_{\mathrm{K}}^2 + q^2 + s)(-m_\pi^2 + 2s) +$$

$$
\begin{aligned}
&\overline{J}_{m_{\mathrm{K}}^2,m_\eta^2}(t) \\
&\qquad (-46m_{\mathrm{K}}^4 + 5m_\pi^4 + 21m_\pi^2 q^2 - 24m_\pi^2 t + \\
&\qquad 18t^2 - 12m_\pi^2 u - 18tu + \\
&\qquad m_{\mathrm{K}}^2(-31m_\pi^2 - 45q^2 + 24t + 84u)) + \\
&\overline{J}_{m_\pi^2,m_{\mathrm{K}}^2}(t) \\
&\qquad 9(-6m_{\mathrm{K}}^4 + q^2(3m_{\mathrm{K}}^2 + 13m_\pi^2 - 8t) - \\
&\qquad m_\pi^2(3m_\pi^2 + 24t - 4u) + \\
&\qquad 2t(9t - u) + m_{\mathrm{K}}^2(25m_\pi^2 - 16t + 4u)) + \\
&K_{m_{\mathrm{K}}^2,m_\eta^2}(t) \\
&\qquad (-12)(2m_{\mathrm{K}}^4 - m_{\mathrm{K}}^2(m_\pi^2 - 5q^2 + u) + \\
&\qquad m_\pi^2(-7m_\pi^2 + q^2 + u)) - \\
&K_{m_\pi^2,m_{\mathrm{K}}^2}(t) \\
&\qquad 36((m_{\mathrm{K}}^2 + m_\pi^2)(2m_{\mathrm{K}}^2 - 3m_\pi^2 + q^2) + \\
&\qquad (-m_{\mathrm{K}}^2 + m_\pi^2)u) - \\
&M^{\mathrm{r}}_{m_{\mathrm{K}}^2,m_\eta^2}(t)\ 108(-m_{\mathrm{K}}^2 + m_\pi^2)(-m_\pi^2 + q^2) - \\
&M^{\mathrm{r}}_{m_\pi^2,m_{\mathrm{K}}^2}(t)\ 108(-m_{\mathrm{K}}^2 + m_\pi^2)(-m_\pi^2 + q^2) + \\
&(t \leftrightarrows u)\Big].
\end{aligned}
$$

(C.19)

Rational contribution from the loops:

$$
\begin{aligned}
T_{\mathrm{pol}}^{+(4)} = {} & \frac{i}{1152 f^4 \pi^2} \\
& \Big[\frac{2c_5(m_{\mathrm{K}}^2 - m_\pi^2)}{(q^2 - m_{\mathrm{K}}^2)}(66q^4 + q^2(147m_{\mathrm{K}}^2 + 283m_\pi^2 - 192s) - \\
& \qquad 3(-27m_{\mathrm{K}}^4 - 90m_\pi^4 + 89m_\pi^2 s + \\
& \qquad m_{\mathrm{K}}^2(-99m_\pi^2 + 37s) + 46tu + 22(t^2 + u^2))) + \\
& c_2(-103m_{\mathrm{K}}^4 - 84q^4 + 5m_{\mathrm{K}}^2(-73m_\pi^2 + 57s) + \\
& \qquad q^2(-187m_{\mathrm{K}}^2 - 311m_\pi^2 + 138s) + \\
& \qquad 3(-90m_\pi^4 + 37m_\pi^2 s + 58tu + 28(t^2 + u^2)))\Big].
\end{aligned}
\tag{C.20}
$$

Strong counter-terms:

$$
\begin{aligned}
T_{L_i}^{+(4)} = {} & \frac{c_5 4i(m_\pi^2 - m_{\mathrm{K}}^2)}{3 f^4 (q^2 - m_{\mathrm{K}}^2)^2} \\
& \Big[q^4\Big\{-2(12L_2 + 3L_3 + 4L_4 + 2L_5 - 8L_6 - 4L_8)m_{\mathrm{K}}^2 - \\
& 2(24L_1 + 12L_2 + 9L_3 - 10L_4 - 4L_6 - 6L_8)m_\pi^2 + \\
& 3(8L_1 + 4L_2 + 3L_3)s\Big\} + \\
& 3m_{\mathrm{K}}^2\Big\{(-((8L_1 + 4L_2 + 3L_3 -
\end{aligned}
\tag{C.21}
$$

$$
\begin{aligned}
&12L_4 - 2L_5 + 8L_6 + 4L_8)m_{\mathrm{K}}^2)- \\
&2(8L_1 + 4L_2 + 3L_3 - 5L_4+ \\
&2(-L_5 + L_6 + L_8))m_\pi^2)s+ \\
&(8L_1 + 4L_2 + 3L_3)s^2+ \\
&2(-((2L_4 + L_5 - 4L_6 - 2L_8)m_{\mathrm{K}}^4)+ \\
&(8L_1 + 4L_2 + 3L_3 - 13L_4- \\
&4L_5 + 18L_6 + 10L_8)m_{\mathrm{K}}^2 m_\pi^2+ \\
&(4L_2 + L_3)m_\pi^4 - (4L_2 + L_3)tu)\Big\}+ \\
&q^2\Big\{6(-2(4L_4 + L_5 - 4L_6 - 2L_8)m_{\mathrm{K}}^2+ \\
&(8L_1 + 4L_2 + 3L_3 - 6L_4 - 2L_5 + 4L_6 + 2L_8)m_\pi^2)s- \\
&3(8L_1 + 4L_2 + 3L_3)s^2+ \\
&2((12L_2 + 3L_3 + 5(2L_4 + L_5 - 4L_6 - 2L_8))m_{\mathrm{K}}^4+ \\
&(29L_4 + 12L_5 - 58L_6 - 36L_8)m_{\mathrm{K}}^2 m_\pi^2- \\
&3(4L_2 + L_3)m_\pi^4 + 3(4L_2 + L_3)tu)\Big\}\Big].
\end{aligned}
\tag{C.22}
$$

Weak counter-terms contributing also to $\mathrm{K} \to \pi$ with $q = 0$:

$$
T^{+(4)}_{N_{5,8,10,11}} = \frac{-ic_2}{3f^4} \tag{C.23}
$$

$$\Big[2(-m_{\rm K}^2+m_\pi^2)(m_\pi^2 N_{11}+2m_{\rm K}^2(N_{10}+N_{11}))$$

$$(m_{\rm K}^2-q^2+3s)/(q^2-m_{\rm K}^2)-$$

$$3\{(-2m_{\rm K}^4(-8(N_{10}+N_{11})+3N_5+3N_8))/3+2m_{\rm K}^2(N_5+N_8)q^2+$$

$$(4m_\pi^4(-6N_{10}-14N_{11}-6N_12+6N_5+12N_7+3N_8))/3+$$

$$m_\pi^2((m_{\rm K}^2(8(N_{10}+5N_{11}+3N_{12})-48N_7+21N_8+18N_9))/3+$$

$$(N_8+2N_9)q^2)-2(m_{\rm K}^2+2m_\pi^2)(N_5-4N_7+3N_8+2N_9)s\}\Big].$$

Weak counter-terms not contributing to $\mathrm{K}\to\pi$ with $q=0$:

$$T^{+(4)}_{N_{20-23}}=\frac{ic_2}{6f^4} \tag{C.24}$$

$$\Big[-3(N_{19}-3N_{20})q^4+q^2(m_\pi^2(-6N_{19}+30N_{20}+16N_{21})+$$

$$m_{\rm K}^2(-12N_{19}+6N_{20}-10N_{21}+3N_{22}+6N_{23})+3(N_{19}-7N_{20})s)+$$

$$3(-6m_\pi^4(N_{19}-N_{20})-m_{\rm K}^4(N_{19}-N_{20}+2N_{21}+N_{22}+2N_{23})+$$

$$2m_{\rm K}^2m_\pi^2(-N_{19}+N_{20}+4N_{21}+2N_{22}+4N_{23})+$$

$$(2m_\pi^2(N_{19}-N_{20}-4N_{21}-2N_{22}-4N_{23})+$$

$$m_{\rm K}^2(N_{19}-N_{20}+2N_{21}+N_{22}+2N_{23}))s)+$$

$$3(N_{19}-N_{20})(t^2+4tu+u^2)\Big].$$

C.3 Decomposition of the kaon decay amplitude

We decompose the amplitude as follows:

$$\begin{aligned} T^+(s,t,u) &= M_0(s) + \frac{1}{3}\Big[N_0(t) + N_0(u)\Big] + \frac{2}{3}\Big[R_0(t) + R_0(u)\Big] \\ &+ \frac{1}{2}\left[\left(s - u - \frac{m_\pi^2\Delta}{t}\right)N_1(t) + \left(s - t - \frac{m_\pi^2\Delta}{u}\right)N_1(u)\right], \end{aligned} \tag{C.25}$$

where $\Delta = m_K^2 - m_\pi^2$. Notice that the terms proportional to N_1 drop out from the physical decay amplitude:

$$\begin{aligned} \mathcal{A}(K \to \pi\pi) &= T^+(m_K^2, m_\pi^2, m_\pi^2) \\ &= M_0(m_K^2) + \frac{2}{3}\Big[N_0(m_\pi^2) + 2R_0(m_\pi^2)\Big]. \end{aligned} \tag{C.26}$$

In the following subsection we give the one loop expressions of the functions M_0, $N_{0,1}$ and R_0. At tree level the amplitude is a polynomial in s, t and u which, by definition, has to be symmetric under $t \leftrightarrows u$ exchange. Since at this chiral order the polynomial is at most linear in the Mandelstam variables, it is only a function of s. At leading order we can choose to have only M_0 different from zero.

At one loop level each of the functions M_0, $N_{0,1}$ and R_0 develops an imaginary part, which is uniquely determined by unitarity. The real part, however, contains polynomial terms which can be shuffled from one term to another – only the amplitude $T^+(s,t,u)$ has a physical significance, not the single variable functions in which it has been decomposed. Indeed one can split the amplitude T^+ into a polynomial part and a rest:

$$\begin{aligned} T^+(s,t,u) &= P(s,t,u) + \overline{T}^+(s,t,u), \\ P(s,t,u) &= x_0 + x_1 s + x_2 s^2 + x_3 (t-u)^2. \end{aligned} \tag{C.27}$$

Only the polynomial coefficients x_i are physical and independent from each other, not the Taylor coefficients of the functions M_0, $N_{0,1}$ and R_0 (see below for a precise definition of the various symbols):

$$\begin{aligned} x_0 &= m_0 + n_1 \frac{m_K^4}{4}\left(1 - 8x_{\pi K}\right) + r_2 \frac{\Sigma_1^2}{6}, \\ x_1 &= m_1 + \Sigma_1\left(n_1 - \frac{1}{3}r_2\right), \\ x_2 &= m_2 + \frac{1}{6}\left(r_2 - \frac{9}{2}n_1\right), \\ x_3 &= \frac{1}{4}\left(n_1 + \frac{2}{3}r_2\right). \end{aligned} \tag{C.28}$$

C.3.1 M_0

We write the chiral expansion of M_0 as

$$M_0(s) = \frac{c_2}{F_0}\left(M_0^{(2)}(s) + M_0^{(4)}(s) + \ldots\right), \tag{C.29}$$

with self-explanatory notation.

$$\begin{aligned} M_0^{(2)}(s) &= \frac{1}{4}\left(3s + m_{\rm K}^2 - 4m_\pi^2\right), \\ M_0^{(4)}(s) &= \frac{1}{F_0^2}\left(m_0 + m_1 s + m_2 s^2 + \bar{\bar{U}}_0(s)\right), \end{aligned} \tag{C.30}$$

$$m_i = m_{\rm K}^{2(2-i)}\left[\frac{m_i^{(0)} + u_i}{N} + m_i^{(1)}L_1^{(5)} + m_i^{(2)}L_2^{(5)} + \sum_k m_{i\,k}\bar{N}_k\right], \tag{C.31}$$

$$\begin{aligned} m_0^{(0)} &= \frac{925}{5184} + \frac{5009}{8640}x_{\pi\rm K} - \frac{15773}{2160}x_{\pi\rm K}^2 + \frac{54823}{6480}x_{\pi\rm K}^3 - \frac{63011}{8640}x_{\pi\rm K}^4 + \frac{9173}{2880}x_{\pi\rm K}^5 \\ &\quad - \frac{9}{16}x_{\pi\rm K}^6 + \frac{1}{15}x_{\pi\rm K}^7 + A_3\left(-\frac{73691}{155520} - \frac{1003}{3888}x_{\pi\rm K} + \frac{3209}{12960}x_{\pi\rm K}^2\right. \\ &\quad \left. - \frac{15041}{77760}x_{\pi\rm K}^3 + \frac{3491}{31104}x_{\pi\rm K}^4 + \frac{5}{1728}x_{\pi\rm K}^5\right) + A_3^2\left(\frac{2687}{31104} - \frac{139}{7776}x_{\pi\rm K}\right. \\ &\quad \left. - \frac{9229}{77760}x_{\pi\rm K}^2 + \frac{133}{7776}x_{\pi\rm K}^3 + \frac{8699}{155520}x_{\pi\rm K}^4 - \frac{919}{38880}x_{\pi\rm K}^5 + \frac{1}{1296}x_{\pi\rm K}^6\right) \\ &+ A_3^3\left(-\frac{713}{46656} + \frac{1523}{58320}x_{\pi\rm K} - \frac{487}{38880}x_{\pi\rm K}^2 + \frac{91}{6480}x_{\pi\rm K}^3 - \frac{4601}{233280}x_{\pi\rm K}^4\right. \\ &\quad \left. + \frac{83}{9720}x_{\pi\rm K}^5 - \frac{17}{14580}x_{\pi\rm K}^6\right) + A_3^4\left(\frac{151}{29160} - \frac{629}{46656}x_{\pi\rm K} + \frac{343}{46656}x_{\pi\rm K}^2\right. \\ &\quad \left. + \frac{329}{46656}x_{\pi\rm K}^3 - \frac{379}{46656}x_{\pi\rm K}^4 + \frac{59}{29160}x_{\pi\rm K}^5\right) \\ &+ A_3^5\left(-\frac{49}{43740} + \frac{23}{6480}x_{\pi\rm K} - \frac{8}{3645}x_{\pi\rm K}^2 - \frac{389}{87480}x_{\pi\rm K}^3 + \frac{29}{3645}x_{\pi\rm K}^4\right. \\ &\quad \left. - \frac{289}{58320}x_{\pi\rm K}^5 + \frac{59}{43740}x_{\pi\rm K}^6 - \frac{1}{7290}x_{\pi\rm K}^7\right), \end{aligned} \tag{C.32}$$

$$\begin{aligned} m_0^{(1)} &= \frac{1}{96}x_{\pi\rm K}\left(13 - 302x_{\pi\rm K} + 1377x_{\pi\rm K}^2 - 2930x_{\pi\rm K}^3\right. \\ &\quad \left. + 3070x_{\pi\rm K}^4 - 1458x_{\pi\rm K}^5 + 262x_{\pi\rm K}^6 - 32x_{\pi\rm K}^7\right), \end{aligned} \tag{C.33}$$

$$
\begin{aligned}
m_0^{(2)} &= -\frac{25}{288}x_{\pi\mathrm{K}} + \frac{25}{96}x_{\pi\mathrm{K}}^3 - \frac{25}{144}x_{\pi\mathrm{K}}^4 + A_3\left(\frac{5}{16}x_{\pi\mathrm{K}} + \frac{5}{144}x_{\pi\mathrm{K}}^2 - \frac{15}{16}x_{\pi\mathrm{K}}^3\right. \\
&\quad \left. + \frac{25}{48}x_{\pi\mathrm{K}}^4 + \frac{5}{72}x_{\pi\mathrm{K}}^5\right) + A_3^2\left(\frac{19}{432} + \frac{203}{1296}x_{\pi\mathrm{K}} - \frac{341}{1296}x_{\pi\mathrm{K}}^2 - \frac{65}{144}x_{\pi\mathrm{K}}^3\right. \\
&\quad \left. + \frac{137}{162}x_{\pi\mathrm{K}}^4 - \frac{215}{648}x_{\pi\mathrm{K}}^5\right) + A_3^3\left(\frac{605}{23328} + \frac{25}{1296}x_{\pi\mathrm{K}} - \frac{583}{2592}x_{\pi\mathrm{K}}^2\right. \\
&\quad \left. + \frac{3151}{11664}x_{\pi\mathrm{K}}^3 - \frac{323}{7776}x_{\pi\mathrm{K}}^4 - \frac{35}{432}x_{\pi\mathrm{K}}^5 + \frac{779}{23328}x_{\pi K}^6 - \frac{5}{3888}x_{\pi\mathrm{K}}^7\right) \\
&+ A_3^4\left(\frac{605}{69984} - \frac{667}{34992}x_{\pi\mathrm{K}} - \frac{439}{23328}x_{\pi\mathrm{K}}^2 + \frac{1661}{17496}x_{\pi\mathrm{K}}^3 - \frac{7901}{69984}x_{\pi\mathrm{K}}^4\right. \\
&\quad \left. + \frac{719}{11664}x_{\pi\mathrm{K}}^5 - \frac{1147}{69984}x_{\pi\mathrm{K}}^6 + \frac{17}{8748}x_{\pi\mathrm{K}}^7\right) + A_3^5\left(\frac{19}{11664} - \frac{13}{1458}x_{\pi\mathrm{K}}\right. \\
&\quad \left. + \frac{245}{11664}x_{\pi\mathrm{K}}^2 - \frac{55}{1944}x_{\pi\mathrm{K}}^3 + \frac{95}{3888}x_{\pi\mathrm{K}}^4 - \frac{41}{2916}x_{\pi\mathrm{K}}^5 + \frac{59}{11664}x_{\pi\mathrm{K}}^6\right. \\
&\quad \left. - \frac{5}{5832}x_{\pi\mathrm{K}}^7\right) + A_3^6\left(-\frac{49}{26244} + \frac{817}{104976}x_{\pi\mathrm{K}} - \frac{335}{34992}x_{\pi\mathrm{K}}^2 - \frac{197}{52488}x_{\pi\mathrm{K}}^3\right. \\
&\quad \left. + \frac{1085}{52488}x_{\pi\mathrm{K}}^4 - \frac{251}{11664}x_{\pi\mathrm{K}}^5 + \frac{1103}{104976}x_{\pi\mathrm{K}}^6 - \frac{65}{26244}x_{\pi\mathrm{K}}^7 + \frac{1}{4374}x_{\pi\mathrm{K}}^8\right),
\end{aligned}
\tag{C.34}
$$

$$
\begin{aligned}
m_1^{(0)} &= -\frac{14633}{25920} - \frac{1109}{405}x_{\pi\mathrm{K}} + \frac{186317}{12960}x_{\pi\mathrm{K}}^2 - \frac{69703}{4320}x_{\pi\mathrm{K}}^3 + \frac{11839}{960}x_{\pi\mathrm{K}}^4 \\
&\quad - \frac{59}{10}x_{\pi\mathrm{K}}^5 + \frac{119}{80}x_{\pi\mathrm{K}}^6 - \frac{3}{20}x_{\pi\mathrm{K}}^7 + A_3\left(\frac{135371}{155520} - \frac{869}{1440}x_{\pi\mathrm{K}} + \frac{4541}{25920}x_{\pi\mathrm{K}}^2\right. \\
&\quad \left. - \frac{511}{7776}x_{\pi\mathrm{K}}^3 - \frac{5}{3456}x_{\pi\mathrm{K}}^4\right) + A_3^2\left(-\frac{527}{3456} + \frac{467}{1944}x_{\pi\mathrm{K}} - \frac{1987}{25920}x_{\pi\mathrm{K}}^2\right. \\
&\quad \left. - \frac{263}{12960}x_{\pi\mathrm{K}}^3 + \frac{1493}{155520}x_{\pi\mathrm{K}}^4 - \frac{1}{2592}x_{\pi\mathrm{K}}^5\right) + A_3^3\left(\frac{7009}{233280} - \frac{9073}{116640}x_{\pi\mathrm{K}}\right. \\
&\quad \left. + \frac{7799}{116640}x_{\pi\mathrm{K}}^2 - \frac{149}{7290}x_{\pi\mathrm{K}}^3 + \frac{281}{233280}x_{\pi\mathrm{K}}^4 + \frac{13}{116640}x_{\pi\mathrm{K}}^5\right) + A_3^4\left(-\frac{95}{11664}\right. \\
&\quad \left. + \frac{691}{23328}x_{\pi\mathrm{K}} - \frac{947}{23328}x_{\pi\mathrm{K}}^2 + \frac{199}{7776}x_{\pi\mathrm{K}}^3 - \frac{169}{23328}x_{\pi\mathrm{K}}^4 + \frac{5}{5832}x_{\pi\mathrm{K}}^5\right. \\
&\quad \left. - \frac{1}{11664}x_{\pi\mathrm{K}}^6\right) + A_3^5\left(\frac{47}{21870} - \frac{869}{87480}x_{\pi K} + \frac{67}{3645}x_{\pi\mathrm{K}}^2 - \frac{188}{10935}x_{\pi\mathrm{K}}^3\right. \\
&\quad \left. + \frac{92}{10935}x_{\pi\mathrm{K}}^4 - \frac{59}{29160}x_{\pi\mathrm{K}}^5 + \frac{1}{4374}x_{\pi\mathrm{K}}^6 - \frac{1}{43740}x_{\pi\mathrm{K}}^7\right),
\end{aligned}
\tag{C.35}
$$

$$\begin{aligned} m_1^{(1)} &= -\frac{1}{2}+\frac{149}{32}x_{\pi\mathrm{K}}-\frac{75}{4}x_{\pi\mathrm{K}}^2+\frac{1361}{32}x_{\pi\mathrm{K}}^3-\frac{241}{4}x_{\pi\mathrm{K}}^4+\frac{427}{8}x_{\pi\mathrm{K}}^5-\frac{441}{16}x_{\pi\mathrm{K}}^6 \\ &\quad +\frac{29}{4}x_{\pi\mathrm{K}}^7-\frac{3}{4}x_{\pi\mathrm{K}}^8, \end{aligned} \tag{C.36}$$

$$\begin{aligned} m_1^{(2)} &= \left(1-x_{\pi\mathrm{K}}\right)^2\left[\frac{25}{288}x_{\pi\mathrm{K}}-A_3\frac{5}{144}x_{\pi\mathrm{K}}\left(9+x_{\pi\mathrm{K}}\right)+A_3^2\left(-\frac{19}{432}-\frac{71}{432}x_{\pi\mathrm{K}}\right.\right. \\ &\quad \left.+\frac{35}{216}x_{\pi\mathrm{K}}^2\right)+\frac{A_3^3}{23328}\left(1-x_{\pi\mathrm{K}}\right)\left(605+365x_{\pi\mathrm{K}}-337x_{\pi\mathrm{K}}^2+15x_{\pi\mathrm{K}}^3\right) \\ &+ -\frac{A_3^4}{69984}\left(1-x_{\pi\mathrm{K}}\right)^2\left(293-58x_{\pi\mathrm{K}}+53x_{\pi\mathrm{K}}^2\right)-A_3^5\frac{5}{34992}\left(1-x_{\pi\mathrm{K}}\right)^4 \\ &+ \left.\frac{A_3^6}{52488}\left(1-x_{\pi\mathrm{K}}\right)^3\left(188-117x_{\pi\mathrm{K}}+12x_{\pi\mathrm{K}}^2-2x_{\pi\mathrm{K}}^3\right)\right], \end{aligned} \tag{C.37}$$

$$\begin{aligned} m_2^{(0)} &= \frac{133}{60}-\frac{21463}{2880}x_{\pi K}+\frac{21437}{2880}x_{\pi\mathrm{K}}^2-\frac{14263}{2880}x_{\pi\mathrm{K}}^3+\frac{593}{320}x_{\pi\mathrm{K}}^4-\frac{71}{240}x_{\pi\mathrm{K}}^5 \\ &+ A_3\frac{5}{144}\left(4-x_{\pi\mathrm{K}}\right)-A_3^2\frac{5}{864}\left(1-x_{\pi\mathrm{K}}\right)\left(4-x_{\pi\mathrm{K}}\right) \\ &+ A_3^3\frac{5}{3888}\left(4-x_{\pi\mathrm{K}}\right)\left(1-x_{\pi\mathrm{K}}\right)^2-A_3^4\frac{5}{15552}\left(4-x_{\pi\mathrm{K}}\right)\left(1-x_{\pi\mathrm{K}}\right)^3 \\ &+ \frac{A_3^5}{11664}\left(4-x_{\pi\mathrm{K}}\right)\left(1-x_{\pi\mathrm{K}}\right)^4, \end{aligned} \tag{C.38}$$

$$m_2^{(1)} = -\frac{1}{48}\left(72-71\,x_{\pi\mathrm{K}}\right)\left(1-x_{\pi\mathrm{K}}\right)^5, \tag{C.39}$$

$$m_2^{(2)} = \frac{5}{34992}A_3^6\left(4-x_{\pi\mathrm{K}}\right)\left(1-x_{\pi\mathrm{K}}\right)^5. \tag{C.40}$$

The only non-zero $m_{i\,k}$ are given in Table C.1.

$$\begin{aligned} U_0(s) &= \bar{J}_{\pi\pi}(s)\frac{1}{4}\left[6s^2+sm_{\mathrm{K}}^2\left(2-11x_{\pi\mathrm{K}}\right)-m_{\mathrm{K}}^4x_{\pi\mathrm{K}}\left(4x_{\pi\mathrm{K}}-1\right)\right] \\ &\quad +\bar{J}_{\eta\eta}(s)\frac{x_{\pi\mathrm{K}}}{36}\left[m_{\mathrm{K}}^4\left(13-4x_{\pi\mathrm{K}}\right)-9sm_{\mathrm{K}}^2\right]. \end{aligned} \tag{C.41}$$

It is useful to know the Taylor expansion of U_0, especially because its coefficient appear in the definition of the m_i coefficients, Eq. (C.31):

$$U_0(s) = \frac{1}{N}\left(u_0+u_1s+u_2s^2\right)+\bar{\bar{U}}_0(s), \tag{C.42}$$

k	$m_{0\,k}$	$m_{1\,k}$	$m_{2\,k}$
5	$2 - 8x_{\pi\mathrm{K}}^2$	$2 + 4x_{\pi\mathrm{K}}$	0
7	$16x_{\pi\mathrm{K}}(1 - x_{\pi\mathrm{K}})$	$8(-1 + x_{\pi\mathrm{K}})$	0
8	$2 - 7x_{\pi\mathrm{K}} - 4x_{\pi\mathrm{K}}^2$	$6 + 3x_{\pi\mathrm{K}}$	0
9	$-6x_{\pi\mathrm{K}}$	$4 + 2x_{\pi\mathrm{K}}$	0
10	$-4(1 + x_{\pi\mathrm{K}} - 2x_{\pi\mathrm{K}}^2)$	$4(1 - x_{\pi\mathrm{K}})$	0
11	$-4 - 14x_{\pi\mathrm{K}} + 18x_{\pi\mathrm{K}}^2$	$2(2 - x_{\pi\mathrm{K}} - x_{\pi\mathrm{K}}^2)$	0
12	$-8x_{\pi\mathrm{K}}(1 + x_{\pi\mathrm{K}})$	0	0
19	$-\frac{1}{2} - 3x_{\pi\mathrm{K}} - x_{\pi\mathrm{K}}^2$	$\frac{3}{2} + 3x_{\pi\mathrm{K}}$	-1
20	$\frac{1}{2} + 3x_{\pi\mathrm{K}} + x_{\pi\mathrm{K}}^2$	$-\frac{3}{2} - 3x_{\pi\mathrm{K}}$	1
21	$1 - 4x_{\pi\mathrm{K}}$	$-1 + 4x_{\pi\mathrm{K}}$	0
22	$\frac{1}{2} - 2x_{\pi\mathrm{K}}$	$-\frac{1}{2} + 2x_{\pi\mathrm{K}}$	0
23	$1 - 4x_{\pi\mathrm{K}}$	$-1 + 4x_{\pi\mathrm{K}}$	0

Table C.1: Values of the coefficients $m_{i\,k}$ which are different from zero.

where

$$\begin{aligned} u_0 &= 0, \\ u_1 &= m_{\rm K}^2\left[-\frac{1}{24}\left(1-4x_{\pi\rm K}\right)+\frac{x_{\pi K}x_{K\eta}}{256}\left(13-4x_{\pi\rm K}\right)\right], \\ u_2 &= -\frac{91}{240}\left(1-\frac{19}{91}\frac{1}{x_{\pi\rm K}}\right)-\frac{1}{24}x_{\pi\rm K}x_{K\eta}\left[1-x_{K\eta}\left(\frac{13}{90}-\frac{2}{45}x_{\pi\rm K}\right)\right]. \end{aligned} \tag{C.43}$$

C.3.2 N_0, R_0 and N_1

The combination $\widetilde{R}_0 := N_0 + 2R_0$ starts at order p^4 and reads:

$$\widetilde{R}_0^{(4)}(s) = \frac{c_2}{F_0^3}\left(r_2 s^2 + V_0^{(2)}(s)\right), \tag{C.44}$$

where

$$r_2 = r_2^{(0)} + r_2^{(1)}L_1^{(5)} + r_2^{(2)}L_2^{(7)} + \sum_k r_{2\,k}\bar{N}_k, \tag{C.45}$$

$$\begin{aligned} r_2^{(0)} &= \frac{1}{2}\left(\bar{N}_{19}-\bar{N}_{20}\right)+\frac{1}{N}\left[\frac{13093}{51840}+\frac{333121}{362880}x_{\pi\rm K}+A_3\left(\frac{77}{720}x_{\pi K}+\frac{53183}{1088640}\right)\right. \\ &+ A_3^2\left(\frac{27791}{1088640}x_{\pi\rm K}+\frac{527}{90720}\right)+A_3^3\left(-\frac{23557}{1224720}x_{\pi\rm K}+\frac{7681}{979776}\right) \\ &+ A_3^4\left(-\frac{559}{979776}x_{\pi\rm K}+\frac{1}{23328}\right)+A_3^5\left(\frac{73}{272160}x_{\pi\rm K}-\frac{2}{76545}\right) \\ &+ \left.A_3^6\left(\frac{7}{34992}x_{\pi\rm K}-\frac{1}{26244}\right)+\left(-\frac{25}{367416}x_{\pi\rm K}+\frac{1}{91854}\right)A_3^7\right], \end{aligned} \tag{C.46}$$

$$r_2^{(1)} = \frac{1}{96}x_{\pi\rm K}, \tag{C.47}$$

$$\begin{aligned} r_2^{(2)} &= \frac{5}{864}x_{\pi\rm K}\left(143A_3-42\right)+A_3^2\left(\frac{1045}{2592}x_{\pi\rm K}+\frac{95}{864}\right) \\ &+ A_3^3\left(-\frac{689}{5832}x_{\pi\rm K}+\frac{947}{11664}\right)+A_3^4\left(\frac{53}{2916}-\frac{775}{11664}x_{\pi\rm K}\right) \\ &+ A_3^5\left(\frac{11}{26244}x_{\pi\rm K}-\frac{7}{209952}\right)+A_3^6\left(\frac{497}{209952}x_{\pi\rm K}-\frac{5}{13122}\right) \\ &+ A_3^8\left(-\frac{29}{157464}x_{\pi\rm K}+\frac{1}{39366}\right). \end{aligned} \tag{C.48}$$

The only non-zero $r_{2\,k}$ are

$$r_{2\,19} = -r_{2\,20} = \frac{1}{2}, \tag{C.49}$$

$$\begin{aligned} V_0(s) &= \bar{J}_{\pi\mathrm{K}}(s)\left[-\frac{15}{32}s^2 + sm_{\mathrm{K}}^2\left(\frac{7}{32}+\frac{5x_{\pi\mathrm{K}}}{8}\right) + m_{\mathrm{K}}^4\left(\frac{15}{32}-\frac{131x_{\pi\mathrm{K}}}{128}\right)\right] \\ &+ \bar{J}_{K\eta}(s)\left[-\frac{3}{32}s^2 + sm_{\mathrm{K}}^2\left(\frac{25}{96}-\frac{x_{\pi\mathrm{K}}}{24}\right) + m_{\mathrm{K}}^4\left(-\frac{23}{216}+\frac{5A_3}{864}(1-2x_{\pi\mathrm{K}})\right.\right. \\ &\qquad \left.\left. -\frac{5x_{\pi\mathrm{K}}}{384A_3}(1+3A_3)\right)\right] \\ &- \frac{m_{\mathrm{K}}^4 x_{\pi\mathrm{K}}}{32}\left[3M^r_{\pi\mathrm{K}}(s) - 5M^r_{K\eta}(s)\frac{1}{A_3}\left(1-4A_3\right)\right] \\ &+ \frac{m_{\mathrm{K}}^4 x_{\pi\mathrm{K}}}{32}K_{\pi\mathrm{K}}(s)(14-29x_{\pi\mathrm{K}}) \\ &+ \frac{m_{\mathrm{K}}^4 x_{\pi\mathrm{K}}}{48}K_{K\eta}(s)\left[19(1-x_{\pi\mathrm{K}}) - \frac{15x_{\pi\mathrm{K}}}{2A_3^2}(9A_3-2)\right]. \end{aligned} \tag{C.50}$$

Also N_1 starts at order p^4:

$$N_1^{(4)}(s) = \frac{c_2}{F_0^3}\left(n_1 s + V_1^{(1)}(s)\right), \tag{C.51}$$

$$n_1 = n_1^{(0)} + n_1^{(1)}L_1^{(3)} + n_1^{(2)}L_2^{(3)}, \tag{C.52}$$

$$\begin{aligned} n_1^{(0)} &= \left(\frac{65}{2592}-\frac{35}{1296}x_{\pi\mathrm{K}}\right)A_3 - \frac{25}{432}+\frac{11}{864}x_{\pi\mathrm{K}}, \\ n_1^{(1)} &= -\frac{x_{\pi\mathrm{K}}}{96}, \\ n_1^{(2)} &= \frac{5}{144}(x_{\pi\mathrm{K}}-1) + \left(\frac{65}{2592}-\frac{5}{96}x_{\pi\mathrm{K}}\right)A_3^2 + \left(\frac{55}{864}-\frac{25}{432}x_{\pi\mathrm{K}}\right)A_3, \end{aligned} \tag{C.53}$$

$$\begin{aligned} V_1(s) &= \bar{J}_{\pi\mathrm{K}}(s)\frac{1}{96}\left[s - 2m_{\mathrm{K}}^2(1+x_{\pi\mathrm{K}})\right] \\ &+ \bar{J}_{K\eta}(s)\frac{5}{288}\left[3s - 2m_{\mathrm{K}}^2(7-x_{\pi\mathrm{K}})\right] \\ &+ \frac{m_{\mathrm{K}}^2}{144}(1-x_{\pi\mathrm{K}})\left[3K_{\pi\mathrm{K}}(s) - 5K_{K\eta}(s)\right]. \end{aligned} \tag{C.54}$$

C.3.3 Notation

$$\begin{aligned} N &= 16\pi^2, \\ x_{\pi\mathrm{K}} &= \frac{m_\pi^2}{m_\mathrm{K}^2}, \\ x_{K\eta} &= \frac{m_\mathrm{K}^2}{m_\eta^2}, \\ A_3 &= 3\frac{m_\eta^2 - m_\mathrm{K}^2}{m_\mathrm{K}^2 - m_\pi^2}, \\ L_1 &= \frac{1}{N}\log(m_\pi^2/m_\mathrm{K}^2), \\ L_2 &= \frac{1}{N}\log(m_\eta^2/m_\mathrm{K}^2). \end{aligned} \tag{C.55}$$

We have also used the following notation for the subtracted functions:

$$V^{(n)}(s) = V(s) - \left[V(0) + V'(0)s + \ldots + \frac{d^n}{ds^n}V(s)_{\big|_{s=0}} s^n\right], \tag{C.56}$$

and for the subtracted logarithms:

$$\begin{aligned} L &:= \frac{1}{N}\log(x), \\ L^{(n)} &:= \frac{1}{(x-1)^{(n+1)}}\left[L + \frac{1}{N}\sum_{i=1}^{n}\frac{(1-x)^i}{i}\right]. \end{aligned} \tag{C.57}$$

C.4 Loop functions

In this appendix we define the loop integrals used in the preceding appendices and in the main text. We consider a loop with two masses, M and m. All two-point functions can be given in terms of the subtracted scalar integral $\bar{J}(t) = J(t) - J(0)$ evaluated in four dimensions,

$$J(t) = -i\int \frac{\mathrm{d}^d p}{(2\pi)^d}\frac{1}{((p+k)^2 - M^2)(p^2 - m^2)}, \tag{C.58}$$

with $t = k^2$. The functions used in the text are then

$$\begin{aligned}
\bar{J}(t) &= -\frac{1}{16\pi^2}\int_0^1 \mathrm{d}x\ \log\frac{M^2 - tx(1-x) - \Delta x}{M^2 - \Delta x} \\
&\quad \frac{1}{32\pi^2}\left\{2 + \frac{\Delta}{t}\log\frac{m^2}{M^2} - \frac{\Sigma}{\Delta}\log\frac{m^2}{M^2} - \frac{\sqrt{\lambda}}{t}\log\frac{(t+\sqrt{\lambda})^2 - \Delta^2}{(t-\sqrt{\lambda})^2 - \Delta^2}\right\}, \\
M^{\mathrm{r}}(t) &= \frac{1}{12t}\{t - 2\Sigma\}\bar{J}(t) + \frac{\Delta^2}{3t^2}\bar{J}(t) + \frac{1}{288\pi^2} - \frac{k}{6} \\
&\quad -\frac{1}{96\pi^2 t}\left\{\Sigma + 2\frac{M^2 m^2}{\Delta}\log\frac{m^2}{M^2}\right\}, \\
K(t) &= \frac{\Delta}{2t}\bar{J}(t), \\
\Delta &= M^2 - m^2, \\
\Sigma &= M^2 + m^2, \\
\lambda &= \lambda(t, M^2, m^2) = (t + \Delta)^2 - 4tM^2.
\end{aligned} \tag{C.59}$$

In the text these are used with subscripts,

$$\bar{J}_{ij}(t) = \bar{J}(t) \quad \text{with} \quad M = m_i, m = m_j, \tag{C.60}$$

and similarly for the other symbols. The subtraction point dependent part is contained in the constant k

$$k = \frac{1}{32\pi^2}\frac{M^2\log\left(\frac{M^2}{\mu^2}\right) - m^2\log\left(\frac{m^2}{\mu^2}\right)}{M^2 - m^2}, \tag{C.61}$$

where μ is the subtraction scale.

The scalar 3-point function C_0 is defined by [tHV79]

$$\begin{aligned}
&C_0(p_1^2, p_2^2, (p_1 + p_2)^2, m_1^2, m_2^2, m_3^2) = \\
&\qquad i\pi^2\int \mathrm{d}^4 q \frac{1}{(q_1^2 - m_1^2)((q_1 - p_1)^2 - m_2^2)((q_1 - p_1 - p_2)^2 - m_3^2)}.
\end{aligned} \tag{C.62}$$

The numerical evaluation of C_0 has been done with *FeynCalc*, which in turn (with the right flags given) uses the infrared expansion,

$$C_0(m_{\pi^+}^2, m_{\pi^+}^2, s, m_{\pi^+}^2, m_\gamma^2, m_{\pi^+}^2) = \tag{C.63}$$

$$\frac{1}{2s\sigma}\Bigg\{-4\mathrm{Li}_2\left(1-\frac{1-\sigma}{1+\sigma}\right)+\frac{4\pi^2}{3}+\log^2\left(\frac{1-\sigma}{1+\sigma}\right)$$
$$+2\left[\log\left(\frac{s}{m_{\pi^+}^2}\right)-\log\left(\frac{m_\gamma^2}{m_{\pi^+}^2}\right)+2\log(\sigma)\right]\left[\log\left(\frac{1-\sigma}{1+\sigma}\right)+i\pi\right]\Bigg\},$$

with

$$\sigma=\sqrt{1-\frac{4m_{\pi^+}^2}{s}}, \tag{C.64}$$

and

$$\mathrm{Li}_2(z)=\int_z^0 \mathrm{d}t\,\frac{\log(1-t)}{t}, \tag{C.65}$$

valid for two equal masses and $m_\gamma \to 0$. The values away from threshold have been checked with *LoopTools* [HPV99] (which uses the algorithms of [vOV90]).

Bibliography

[AB01] B. Ananthanarayan and P. Buttiker. Comparison of pi k scattering in su(3) chiral perturbation theory and dispersion relations. *Eur. Phys. J.*, C19:517–528, 2001. hep-ph/0012023.

[ABT00a] G. Amoros, J. Bijnens, and P. Talavera. K(l4) form-factors and pi pi scattering. *Nucl. Phys.*, B585:293–352, 2000. hep-ph/0003258.

[ABT00b] Gabriel Amoros, Johan Bijnens, and Pere Talavera. Two-point functions at two loops in three flavour chiral perturbation theory. *Nucl. Phys.*, B568:319–363, 2000. hep-ph/9907264.

[ACGL01] B. Ananthanarayan, G. Colangelo, J. Gasser, and H. Leutwyler. Roy equation analysis of pi pi scattering. *Phys. Rept.*, 353:207–279, 2001. hep-ph/0005297.

[AH+99] A. Alavi-Harati et al. Observation of direct cp violation in k(s,l) –> pi pi decays. *Phys. Rev. Lett.*, 83:22, 1999. hep-ex/9905060.

[AL96] A. V. Anisovich and H. Leutwyler. Dispersive analysis of the decay eta -> 3 pi. *Phys. Lett.*, B375:335–342, 1996. hep-ph/9601237.

[AMP87] K. L. Au, D. Morgan, and M. R. Pennington. Meson dynamics beyond the quark model: A study of final state interactions. *Phys. Rev.*, D35:1633, 1987.

[B+88] H. Burkhardt et al. First evidence for direct cp violation. *Phys. Lett.*, B206:169, 1988.

[B+93] G. D. Barr et al. A new measurement of direct cp violation in the neutral kaon system. *Phys. Lett.*, B317:233–242, 1993.

[B+00] S. Bosch et al. Standard model confronting new results for epsilon'/epsilon. *Nucl. Phys.*, B565:3–37, 2000. hep-ph/9904408.

[Bar65] G. Barton. *INTRODUCTION TO DISPERSION TECHNIQUES IN FIELD THEORY*. W. A. Benjamin, New York, 1965.

[BBG86] William A. Bardeen, A. J. Buras, and J. M. Gerard. The delta i = 1/2 rule in the large n limit. *Phys. Lett.*, B180:133, 1986.

[BBG87a] William A. Bardeen, A. J. Buras, and J. M. Gerard. A consistent analysis of the delta i = 1/2 rule for k decays. *Phys. Lett.*, B192:138, 1987.

[BBG87b] William A. Bardeen, A. J. Buras, and J. M. Gerard. The k → pi pi decays in the large n limit: Quark evolution. *Nucl. Phys.*, B293:787, 1987.

[BBJR92] F. C. Barker, B. A. Brown, W. Jaus, and G. Rasche. Determination of v (ud) from fermi decays and the unitarity of the km mixing matrix. *Nucl. Phys.*, A540:501–519, 1992.

[BBL96] Gerhard Buchalla, Andrzej J. Buras, and Markus E. Lautenbacher. Weak decays beyond leading logarithms. *Rev. Mod. Phys.*, 68:1125–1144, 1996. hep-ph/9512380.

[BCE+97] J. Bijnens, G. Colangelo, G. Ecker, J. Gasser, and M. E. Sainio. Pion pion scattering at low energy. *Nucl. Phys.*, B508:263–310, 1997. hep-ph/9707291.

[BCKO01a] M. Buchler, G. Colangelo, J. Kambor, and F. Orellana. Dispersion relations and soft pion theorems for k → pi pi. 2001. hep-ph/0102287.

[BCKO01b] M. Buchler, G. Colangelo, J. Kambor, and F. Orellana. A note on the dispersive treatment of k –> pi pi with the kaon off-shell. *Phys. Lett.*, B521:29–32, 2001. hep-ph/0102289.

[BCMU01] Andrzej J. Buras, Andrzej Czarnecki, Mikolaj Misiak, and Joerg Urban. Two-loop matrix element of the current-current operator in the decay b –> x/s gamma. 2001. hep-ph/0105160.

[BCT98] J. Bijnens, G. Colangelo, and P. Talavera. The vector and scalar form factors of the pion to two loops. *JHEP*, 05:014, 1998. hep-ph/9805389.

[BDG01] Z. Bern, L. Dixon, and A. Ghinculov. Two-loop correction to bhabha scattering. *Phys. Rev.*, D63:053007, 2001. hep-ph/0010075.

[BDS+85] Claude W. Bernard, T. Draper, A. Soni, H. David Politzer, and M. B. Wise. Application of chiral perturbation theory to k → 2 pi decays. *Phys. Rev.*, D32:2343–2347, 1985.

[BEF01] Stefano Bertolini, Jan O. Eeg, and Marco Fabbrichesi. An updated analysis of epsilon'/epsilon in the standard model with hadronic matrix elements from the chiral quark model. *Phys. Rev.*, D63:056009, 2001. hep-ph/0002234.

[BEFL98a] S. Bertolini, J. O. Eeg, M. Fabbrichesi, and E. I. Lashin. The delta(i) = 1/2 rule and b-hat(k) at o(p**4) in the chiral expansion. *Nucl. Phys.*, B514:63–92, 1998. hep-ph/9705244.

[BEFL98b] S. Bertolini, J. O. Eeg, M. Fabbrichesi, and E. I. Lashin. epsilon'/epsilon at o(p**4) in the chiral expansion. *Nucl. Phys.*, B514:93–112, 1998. hep-ph/9706260.

[Ber00] Stefano Bertolini. Final state interactions in epsilon'/epsilon. 2000. hep-ph/0007137.

[Ber02] Stefano Bertolini. Calculation of epsilon'/epsilon. 2002. hep-ph/0201218.

[BGS] S. Bellucci, J. Gasser, and M. E. Sainio. Low-energy photon photon collisions in chiral perturbation theory. In *Maiani, L. (ed.) et al.: The second DAPHNE physics handbook, vol. 2* 559-572.

[BJL93] Andrzej J. Buras, Matthias Jamin, and Markus E. Lautenbacher. The anatomy of epsilon-prime / epsilon beyond leading logarithms with improved hadronic matrix elements. *Nucl. Phys.*, B408:209–285, 1993. hep-ph/9303284.

[BJLW92] Andrzej J. Buras, Matthias Jamin, M. E. Lautenbacher, and Peter H. Weisz. Effective hamiltonians for delta s = 1 and delta b = 1 nonleptonic decays beyond the leading logarithmic approximation. *Nucl. Phys.*, B370:69–104, 1992.

[BJLW93] Andrzej J. Buras, Matthias Jamin, Markus E. Lautenbacher, and Peter H. Weisz. Two loop anomalous dimension matrix for delta s = 1 weak nonleptonic decays. 1. o(alpha-s**2). *Nucl. Phys.*, B400:37–74, 1993. hep-ph/9211304.

[BMR72] R. Barbieri, J. A. Mignaco, and E. Remiddi. Electron form-factors up to fourth order. 1. *Nuovo Cim.*, A11:824–864, 1972.

[BP99] Johan Bijnens and Joaquim Prades. The delta(i) = 1/2 rule in the chiral limit. *JHEP*, 01:023, 1999. hep-ph/9811472.

[BP00] Johan Bijnens and Joaquim Prades. epsilon'(k)/epsilon(k) in the chiral limit. *JHEP*, 06:035, 2000. hep-ph/0005189.

[BPP98] Johan Bijnens, Elisabetta Pallante, and Joaquim Prades. Obtaining k –> pi pi from off-shell k –> pi amplitudes. *Nucl. Phys.*, B521:305–333, 1998. hep-ph/9801326.

[Bur96] U. Burgi. Pion polarizabilities and charged pion pair production to two loops. *Nucl. Phys.*, B479:392–426, 1996. hep-ph/9602429.

[Bur99] Andrzej J. Buras. Theoretical status of epsilon'/epsilon. 1999. hep-ph/9908395.

[Bur00] C. P. Burgess. Goldstone and pseudo-goldstone bosons in nuclear, particle and condensed-matter physics. *Phys. Rept.*, 330:193–261, 2000. hep-th/9808176.

[C+98] Marco Ciuchini et al. Next-to-leading order qcd corrections to delta(f) = 2 effective hamiltonians. *Nucl. Phys.*, B523:501–525, 1998. hep-ph/9711402.

[CCWZ69] Curtis G. Callan, Sidney R. Coleman, J. Wess, and Bruno Zumino. Structure of phenomenological lagrangians. 2. *Phys. Rev.*, 177:2247–2250, 1969.

[CDG00a] Vincenzo Cirigliano, John F. Donoghue, and Eugene Golowich. Electromagnetic corrections to k –> pi pi. i: Chiral perturbation theory. *Phys. Rev.*, D61:093001, 2000. hep-ph/9907341.

[CDG00b] Vincenzo Cirigliano, John F. Donoghue, and Eugene Golowich. Electromagnetic corrections to k –> pi pi. ii: Dispersive matching. *Phys. Rev.*, D61:093002, 2000. hep-ph/9909473.

[CDG00c] Vincenzo Cirigliano, John F. Donoghue, and Eugene Golowich. K –> pi pi phenomenology in the presence of electromagnetism. *Eur. Phys. J.*, C18:83–95, 2000. hep-ph/0008290.

[CFG+99] Marco Ciuchini, E. Franco, L. Giusti, V. Lubicz, and G. Martinelli. epsilon'/epsilon from lattice qcd. 1999. hep-ph/9910237.

[CFMR93] Marco Ciuchini, E. Franco, G. Martinelli, and L. Reina. epsilon-prime / epsilon at the next-to-leading order in qcd and qed. *Phys. Lett.*, B301:263–271, 1993. hep-ph/9212203.

[CFMR94] Marco Ciuchini, E. Franco, G. Martinelli, and L. Reina. The delta s = 1 effective hamiltonian including next-to- leading order qcd and qed corrections. *Nucl. Phys.*, B415:403–462, 1994. hep-ph/9304257.

[CGL00] G. Colangelo, J. Gasser, and H. Leutwyler. The pi pi s-wave scattering lengths. *Phys. Lett.*, B488:261–268, 2000. hep-ph/0007112.

[CGL01a] G. Colangelo, J. Gasser, and H. Leutwyler. pi pi scattering. *Nucl. Phys.*, B603:125–179, 2001. hep-ph/0103088.

[CGL01b] G. Colangelo, J. Gasser, and H. Leutwyler. The quark condensate from k(e4) decays. *Phys. Rev. Lett.*, 86:5008–5010, 2001. hep-ph/0103063.

[CKM96] Andrzej Czarnecki, Bernd Krause, and William J. Marciano. Electroweak corrections to the muon anomalous magnetic moment. *Phys. Rev. Lett.*, 76:3267–3270, 1996. hep-ph/9512369.

[CKS96] K. G. Chetyrkin, J. H. Kuhn, and M. Steinhauser. Heavy quark vacuum polarisation to three loops. *Phys. Lett.*, B371:93–98, 1996. hep-ph/9511430.

[CM60] Geoffrey F. Chew and Stanley Mandelstam. Theory of low-energy pion-pion interactions. *Phys. Rev.*, 119:467–477, 1960.

[CM99] Andrzej Czarnecki and William J. Marciano. Lepton anomalous magnetic moments: A theory update. *Nucl. Phys. Proc. Suppl.*, 76:245–252, 1999. hep-ph/9810512.

[CM01a] Marco Ciuchini and Guido Martinelli. Theoretical status of epsilon'/epsilon. *Nucl. Phys. Proc. Suppl.*, 99B:27–34, 2001. hep-ph/0006056.

[CM01b] Andrzej Czarnecki and William J. Marciano. The muon anomalous magnetic moment: A harbinger for 'new physics'. *Phys. Rev.*, D64:013014, 2001. hep-ph/0102122.

[Con] The World Wide Web Consortium. Extensible markup language (xml). http://www.w3.org/TR/REC-xml.

[CWZ69] Sidney R. Coleman, J. Wess, and Bruno Zumino. Structure of phenomenological lagrangians. 1. *Phys. Rev.*, 177:2239–2247, 1969.

[D$^+$98] C. Dawson et al. New lattice approaches to the delta(i) = 1/2 rule. *Nucl. Phys.*, B514:313–335, 1998. hep-lat/9707009.

[DGL90] John F. Donoghue, J. Gasser, and H. Leutwyler. The decay of a light higgs boson. *Nucl. Phys.*, B343:341–368, 1990.

[DH98] A. Denner and T. Hahn. Radiative corrections to w+ w- –> w+ w- in the electroweak standard model. *Nucl. Phys.*, B525:27–50, 1998. hep-ph/9711302.

[DIR] Cern-ps-212 experiment. http://www.slac.stanford.edu/spires/find/experiments/www2?rawcmd=fin+expt+CERN-PS-212. DIRAC Collaboration.

[DK00] Stephan Durr and Joachim Kambor. Two-point function of strangeness-carrying vector-currents in two-loop chiral perturbation theory. *Phys. Rev.*, D61:114025, 2000. hep-ph/9907539.

[DKR02] A. Demichev, A. Kryukov, and A. Rodionov. Xml-based formulation of field theoretical models. a proposal for a future standard and data base for model storage, exchange and cross-checking of results. 2002. hep-ph/0203102.

[DP01] Ansgar Denner and Stefano Pozzorini. One-loop leading logarithms in electroweak radiative corrections. i: Results. *Eur. Phys. J.*, C18:461–480, 2001. hep-ph/0010201.

[E73] Fnal-e-0731 experiment. http://www.slac.stanford.edu/spires/find/experiments/www2?rawcmd=fin+expt+FNAL-E-0731. Fermilab.

[E83] Fnal-e-0832 experiment. http://www.slac.stanford.edu/spires/find/experiments/www2?rawcmd=fin+expt+FNAL-E-0832. KTEV.

[E86] Bnl-e-0865 experiment. http://www.slac.stanford.edu/spires/find/experiments/www2?rawcmd=fin+expt+BNL-E-0865. Brookhaven.

[Eck98] Gerhard Ecker. Chiral symmetry. 1998. hep-ph/9805500.

[EGPdR89] G. Ecker, J. Gasser, A. Pich, and E. de Rafael. The role of resonances in chiral perturbation theory. *Nucl. Phys.*, B321:311, 1989.

[EKW93] G. Ecker, J. Kambor, and D. Wyler. Resonances in the weak chiral lagrangian. *Nucl. Phys.*, B394:101–138, 1993.

[F$^+$99] V. Fanti et al. A new measurement of direct cp violation in two pion decays of the neutral kaon. *Phys. Lett.*, B465:335–348, 1999. hep-ex/9909022.

[Fer34] E. Fermi. Trends to a theory of beta radiation. (in italian). *Nuovo Cim.*, 11:1–19, 1934.

[FHWW00] A. Freitas, W. Hollik, W. Walter, and G. Weiglein. Complete fermionic two-loop results for the m(w)-m(z) interdependence. *Phys. Lett.*, B495:338–346, 2000. hep-ph/0007091.

[FJTV99] J. Fleischer, F. Jegerlehner, O. V. Tarasov, and O. L. Veretin. Two-loop QCD corrections of the massive fermion propagator. *Nucl. Phys.*, B539:671–690, 1999. hep-ph/9803493.

[FTJR92] J. Fleischer, O. V. Tarasov, F. Jegerlehner, and P. Raczka. Two loop o (alpha-s g (mu) m (t)**2) corrections to the partial decay width of the z0 into b anti-b final states in the large top mass limit. *Phys. Lett.*, B293:437–444, 1992.

[G+93] L. K. Gibbons et al. Measurement of the cp violation parameter re (epsilon-prime / epsilon). *Phys. Rev. Lett.*, 70:1203–1206, 1993.

[G+01] F. Gomez et al. Dirac experiment. *Nucl. Phys. Proc. Suppl.*, 96:259–266, 2001.

[GAA+00] D.E. Groom, M. Aguilar-Benitez, C. Amsler, R.M. Barnett, P.R. Burchat, C.D. Carone, C. Caso, G. Conforto, O. Dahl, M. Doser, S. Eidelman, J.L. Feng, L. Gibbons, M. Goodman, C. Grab, A. Gurtu, K. Hagiwara, K.G. Hayes, J.J. Hernández, K. Hikasa, K. Honscheid, C. Kolda, M.L. Mangano, A.V. Manohar, A. Masoni, K. Mönig, H. Murayama, K. Nakamura, S. Navas, K.A. Olive, L. Pape, A. Piepke, M. Roos, M. Tanabashi, N.A. Törnqvist, T.G. Trippe, P. Vogel, C.G. Wohl, R.L. Workman, W.-M. Yao, B. Armstrong, J.L. Casas Serradilla, B.B. Filimonov, P.S. Gee, S.B. Lugovsky, F. Nicholson, K.S. Babu, D. Besson, O. Biebel, P. Bloch, R.N. Cahn, A. Cattai, R.S. Chivukula, R.D. Cousins, T. Damour, K. Desler, R.J. Donahue, D.A. Edwards, J. Erler, V.V. Ezhela, A. Fassò, W. Fetscher, D. Froidevaux, M. Fukugita, T.K. Gaisser, L. Garren, S. Geer, H.-J. Gerber, F.J. Gilman,. Review of Particle Physics. *The European Physical Journal*, C15:1+, 2000. http://pdg.lbl.gov.

[GHW96] Christoph Greub, Tobias Hurth, and Daniel Wyler. *Phys. Rev.*, D54:3350–3364, 1996. hep-ph/9603404.

[GK95] Eugene Golowich and Joachim Kambor. Two loop analysis of vector current propagators in chiral perturbation theory. *Nucl. Phys.*, B447:373–404, 1995. hep-ph/9501318.

[GK98] Eugene Golowich and Joachim Kambor. Two-loop analysis of axialvector current propagators in chiral perturbation theory. *Phys. Rev.*, D58:036004, 1998. hep-ph/9710214.

[GL82] J. Gasser and H. Leutwyler. Quark masses. *Phys. Rept.*, 87:77–169, 1982.

[GL84] J. Gasser and H. Leutwyler. Chiral perturbation theory to one loop. *Ann. Phys.*, 158:142, 1984.

[GL85] J. Gasser and H. Leutwyler. Chiral perturbation theory: Expansions in the mass of the strange quark. *Nucl. Phys.*, B250:465, 1985.

[Gla61] S. L. Glashow. Partial symmetries of weak interactions. *Nucl. Phys.*, 22:579–588, 1961.

[Glo01] E. W. N. Glover. Overview of nnlo qcd corrections. 2001. hep-ph/0106069.

[GM91a] J. Gasser and Ulf G. Meissner. Chiral expansion of pion form-factors beyond one loop. *Nucl. Phys.*, B357:90–128, 1991.

[GM91b] J. Gasser and Ulf G. Meissner. On the phase of epsilon-prime. *Phys. Lett.*, B258:219–224, 1991.

[Gol61] J. Goldstone. Field theories with 'superconductor' solutions. *Nuovo Cim.*, 19:154–164, 1961.

[Gol00] Maarten Golterman. Chiral perturbation theory, non-leptonic kaon decays, and the lattice. 2000. hep-ph/0011084.

[GR01] T. Gehrmann and E. Remiddi. Progress on two-loop non-propagator integrals. 2001. hep-ph/0101147.

[GTY00] E. W. N. Glover and M. E. Tejeda-Yeomans. Progress towards 2 –> 2 scattering at two-loops. *Nucl. Phys. Proc. Suppl.*, 89:196–202, 2000. hep-ph/0010031.

[GW73a] D. J. Gross and F. Wilczek. Asymptotically free gauge theories. i. *Phys. Rev.*, D8:3633–3652, 1973.

[GW73b] D. J. Gross and F. Wilczek. Ultraviolet behavior of non-abelian gauge theories. *Phys. Rev. Lett.*, 30:1343–1346, 1973.

[GW74] D. J. Gross and F. Wilczek. Asymptotically free gauge theories. 2. *Phys. Rev.*, D9:980–993, 1974.

[Haa58] R. Haag. Quantum field theories with composite particles and asymptotic conditions. *Phys. Rev.*, 112:669–673, 1958.

[Hah01] Thomas Hahn. Generating feynman diagrams and amplitudes with feynarts 3. *Comput. Phys. Commun.*, 140:418–431, 2001. hep-ph/0012260. http://www.feynarts.de/.

[HE36] W. Heisenberg and H. Euler. Consequences of dirac's theory of positrons. *Z. Phys.*, 98:714–732, 1936.

[HHRW01] S. Heinemeyer, W. Hollik, J. Rosiek, and G. Weiglein. Neutral mssm higgs-boson production at e+ e- colliders in the feynman-diagrammatic approach. *Eur. Phys. J.*, C19:535–546, 2001. hep-ph/0102081.

[HKPS00] T. Hambye, G. O. Kohler, E. A. Paschos, and P. H. Soldan. Analysis of epsilon'/epsilon in the 1/n(c) expansion. *Nucl. Phys.*, B564:391–429, 2000. hep-ph/9906434.

[HKS99] T. Hambye, G. O. Kohler, and P. H. Soldan. New analysis of the delta(i) = 1/2 rule in kaon decays and the b-hat(k) parameter. *Eur. Phys. J.*, C10:271–292, 1999. hep-ph/9902334.

[HPV99] T. Hahn and M. Perez-Victoria. Automatized one-loop calculations in four and d dimensions. *Comput. Phys. Commun.*, 118:153–165, 1999. hep-ph/9807565. http://www.feynarts.de/looptools/.

[HS99] R. Harlander and M. Steinhauser. Automatic computation of feynman diagrams. *Prog. Part. Nucl. Phys.*, 43:167–228, 1999. hep-ph/9812357.

[HS01] Thomas Hahn and Christian Schappacher. The implementation of the minimal supersymmetric standard model in feynarts and formcalc. 2001. hep-ph/0105349.

[HW01] S. Heinemeyer and G. Weiglein. Precision observables in the mssm: Leading electroweak two- loop corrections. 2001. hep-ph/0102317.

[Jam99] Matthias Jamin. Theoretical status of epsilon'/epsilon. 1999. hep-ph/9911390.

[JFDH92] Eugene Golowich John F. Donoghue and Barry R. Holstein. *Dynamics of the Standard Model*. Cambridge University Press, 1 edition, 1992.

[JOP00] Matthias Jamin, Jose Antonio Oller, and Antonio Pich. S-wave k pi scattering in chiral perturbation theory with resonances. *Nucl. Phys.*, B587:331–362, 2000. hep-ph/0006045.

[KEM] J. Kublbeck, H. Eck, and R. Mertig. Computeralgebraic generation and calculation of feynman graphs using feynarts and feyncalc. Prepared for 2nd International Workshop on Software Engineering, Artificial Intelligence and Expert Systems for High-energy and Nuclear Physics, La Londe Les Maures, France, 13-18 Jan 1992.

[KEM92] J. Kublbeck, H. Eck, and R. Mertig. Computeralgebraic generation and calculation of feynman graphs using feynarts and feyncalc. *Nucl. Phys. Proc. Suppl.*, 29A:204–208, 1992.

[Kin96] Toichiro Kinoshita. The fine structure constant. *Rept. Prog. Phys.*, 59:1459–1492, 1996.

[KM73] M. Kobayashi and T. Maskawa. Cp violation in the renormalizable theory of weak interaction. *Prog. Theor. Phys.*, 49:652, 1973.

[KMW91] J. Kambor, J. Missimer, and D. Wyler. K $\rightarrow$ 2 pi and k $\rightarrow$ 3 pi decays in next-to-leading order chiral perturbation theory. *Phys. Lett.*, B261:496–503, 1991.

[KN02] M. Knecht and A. Nehme. Electromagnetic corrections to charged pion scattering at low energies. 2002. hep-ph/0201033.

[KS55] G. Kĺallen and A. Sabry. *Dan. Mat. Fys. Medd.*, 29, 1955.

[KU98] Marc Knecht and Res Urech. Virtual photons in low energy pi pi scattering. *Nucl. Phys.*, B519:329–360, 1998. hep-ph/9709348.

[Lan] A. Lanaro. A determination of the s-wave pion pion scattering lengths from the measurement of the lifetime of pionium.

[Lan78] C. B. Lang. The pi k scattering and related processes. *Fortschr. Phys.*, 26:509, 1978.

[Lel01] Laurent Lellouch. Light hadron weak matrix elements. *Nucl. Phys. Proc. Suppl.*, 94:142–158, 2001. hep-lat/0011088.

[LL01] Laurent Lellouch and Martin Luscher. Weak transition matrix elements from finite-volume correlation functions. *Commun. Math. Phys.*, 219:31–44, 2001. hep-lat/0003023.

[LMGPNP] (ed.) L. Maiani, (ed.) G. Pancheri, and (ed.) N. Paver. The second daphne physics handbook. vol. 1, 2. http://www.lnf.infn.it/theory/dafne.html. Frascati, Italy: INFN (1995) 1202 p.

[LR97] S. Laporta and E. Remiddi. The electron (g(e)-2) and the value of alpha: A check of qed at 1 ppb. *Acta Phys. Polon.*, B28:959–977, 1997.

[LSZ55] H. Lehmann, K. Symanzik, and W. Zimmermann. On the formulation of quantized field theories. *Nuovo Cim.*, 1:205–225, 1955.

[MBD91a] R. Mertig, M. Bohm, and A. Denner. Feyncalc: Computer algebraic calculation of feynman amplitudes. *Comput. Phys. Commun.*, 64:345–359, 1991.

[MBD91b] R. Mertig, M. Bohm, and A. Denner. Feyncalc: Computer algebraic calculation of feynman amplitudes. *Comput. Phys. Commun.*, 64:345–359, 1991.

[Mera] R. Mertig. Perturbative qcd with feyncalc. Prepared for 3rd International Workshop on Software Engineering, Artificial Intelligence and Expert systems for High-energy and Nuclear Physics, Oberammergau, Germany, 4-8 Oct 1993.

[Merb] R. Mertig. Perturbative qcd with feyncalc. Prepared for 3rd International Workshop on Software Engineering, Artificial Intelligence and Expert systems for High-energy and Nuclear Physics, Oberammergau, Germany, 4-8 Oct 1993.

[MMS97] Ulf-G. Meissner, G. Muller, and S. Steininger. Virtual photons in su(2) chiral perturbation theory and electromagnetic corrections to pi pi scattering. *Phys. Lett.*, B406:154–160, 1997. hep-ph/9704377.

[MO00] Rolf Mertig and Frederik Orellana. The feyncalc web site: Documentation, download and discussion. 2000. http://www.feyncalc.org/.

[MS98] R. Mertig and R. Scharf. Tarcer: A mathematica program
for the reduction of two-loop propagator integrals. *Comput. Phys. Commun.*, 111:265, 1998. hep-ph/9801383. http://www.feyncalc.org/tarcer/.

[Mus53] N.I. Muskhelishvili. *Singular Integral Equations*. Noordhoof, Groningen, 1953.

[MvN96] R. Mertig and W. L. van Neerven. The calculation of the two-loop spin splitting functions $p_{ij}^{(1)}(x)$. *Z. Phys.*, C70:637–654, 1996.

[MvR00] Kirill Melnikov and Timo van Ritbergen. The three-loop on-shell renormalization of qcd and qed. *Nucl. Phys.*, B591:515–546, 2000. hep-ph/0005131.

[NA3] Cern-na-31 experiment. http://www.slac.stanford.edu/spires/find/experiments/www2?rawcmd=fin+expt+CERN-NA-031.

[NA4] Cern-na-48 experiment. http://www.slac.stanford.edu/spires/find/experiments/www2?rawcmd=fin+expt+CERN-NA-048.

[NR96] H. Neufeld and H. Rupertsberger. The electromagnetic interaction in chiral perturbation theory. *Z. Phys.*, C71:131–138, 1996. hep-ph/9506448.

[Omn58] R. Omnes. On the solution of certain singular integral equations of quantum field theory. *Nuovo Cim.*, 8:316–326, 1958.

[Ore] Frederik Orellana. Phi, a mathematica package for doing loop calculations in chiral perturbation theory. http://www.feyncalc.org/phi/. In preparation.

[Ore02] Frederik Orellana. χpt calculation with feyncalc and feynarts (mathematica notebooks). 2002. http://www.feyncalc.org/phi/examples/.

[P+99] A. Pukhov et al. Comphep: A package for evaluation of feynman diagrams and integration over multi-particle phase space. user's manual for version 33. 1999. hep-ph/9908288.

[P+01] S. Pislak et al. A new measurement of k+(e4) decay and the s-wave pi pi scattering length a(0)(0). *Phys. Rev. Lett.*, 87:221801, 2001. hep-ex/0106071.

[Pan99] G. Pancheri. Meson physics at daphne. *PiN Newslett.*, 15:84–89, 1999.

[Pet57] A. Peterman. *Helv. Phys. Acta*, 30:407, 1957.

[Pol73] H. David Politzer. Reliable perturbative results for strong interactions? *Phys. Rev. Lett.*, 30:1346–1349, 1973.

[PP00] Elisabetta Pallante and Antonio Pich. Strong enhancement of epsilon'/epsilon through final state interactions. *Phys. Rev. Lett.*, 84:2568–2571, 2000. hep-ph/9911233.

[PP01] Elisabetta Pallante and Antonio Pich. Final state interactions in kaon decays. *Nucl. Phys.*, B592:294–320, 2001. hep-ph/0007208.

[PV79] G. Passarino and M. Veltman. One loop corrections for e+ e- annihilation into mu+ mu- in the weinberg model. *Nucl. Phys.*, B160:151, 1979.

[RMD91] M. Böhm R. Mertig and A. Denner. Feyncalc: Computer algebraic calculation of feynman amplitudes. *Comput. Phys. Commun.*, 64:345, 1991.

[Sab62] A. Sabry. *Nucl. Phys.*, 33:401, 1962.

[Sal68] A. Salam. In Almqvist and Wiksell, editors, *Elementary Particle Physics: Relativistic Groups and Analyticity*, 1968.

[Sch49] J. Schwinger. Quantum electrodynamics. iii: The electromagnetic properties of the electron: Radiative corrections to scattering. *Phys. Rev.*, 76:790–817, 1949.

[Sch00] J. Schacher. Experimental status of pionium at cern. 2000. hep-ph/0010085.

[SL94] T. Stelzer and W. F. Long. Automatic generation of tree level helicity amplitudes. *Comput. Phys. Commun.*, 81:357–371, 1994. hep-ph/9401258.

[tHV79] G. 't Hooft and M. Veltman. Scalar one loop integrals. *Nucl. Phys.*, B153:365–401, 1979.

[Tka02] Fyodor V. Tkachov. From novel mathematics to efficient algorithms. do we have proper sd foundation to build future? 2002. hep-ph/0202033. http://www-sc.kek.jp/minami/cpp2001/.

[Tru88] Tran N. Truong. K → pi, k → 2 pi, k → 3 pi amplitudes with unitarity. *Phys. Lett.*, B207:495, 1988.

[Ueh35] E. A. Uehling. Polarization effects in the positron theory. *Phys. Rev.*, 48:55–63, 1935.

[Ure95] Res Urech. Virtual photons in chiral perturbation theory. *Nucl. Phys.*, B433:234–254, 1995. hep-ph/9405341.

[VA73] D. V. Volkov and V. P. Akulov. Is the neutrino a goldstone particle? *Phys. Lett.*, B46:109–110, 1973.

[vOV90] G. J. van Oldenborgh and J. A. M. Vermaseren. New algorithms for one loop integrals. *Z. Phys.*, C46:425–438, 1990.

[vRVL97] T. van Ritbergen, J. A. M. Vermaseren, and S. A. Larin. The four-loop beta function in quantum chromodynamics. *Phys. Lett.*, B400:379–384, 1997. hep-ph/9701390.

[Wei66] Steven Weinberg. *Phys. Rev. Lett.*, 17:336, 1966.

[Wei67a] S. Weinberg. A model of leptons. *Phys. Rev. Lett.*, 19:1264–1266, 1967.

[Wei67b] Steven Weinberg. Dynamical approach to current algebra. *Phys. Rev. Lett.*, 18:188–191, 1967.

[Wei79] Steven Weinberg. Phenomenological lagrangians. *Physica*, A96:327, 1979.

[Wei96] Steven Weinberg. What is quantum field theory, and what did we think it was? 1996. hep-th/9702027.

[WMSBa] G. Weiglein, R. Mertig, R. Scharf, and M. Bohm. Computealgebraic calculation of 2-loop selfenergies in the electroweak standard model. In *La Londe-les-Maures 1992, New computing techniques in physics research II* 617-623.

[WMSBb] G. Weiglein, R. Mertig, R. Scharf, and M. Bohm. Computealgebraic calculation of 2-loop selfenergies in the electroweak standard model. In *La Londe-les-Maures 1992, New computing techniques in physics research II* 617-623.

[Wol00] Steven Wolfram. *The Mathematica Book*. Cambridge University Press, fourth edition, 2000. http://www.mathematica.com/.

[WSB94] G. Weiglein, R. Scharf, and M. Bohm. Reduction of general two loop self-energies to standard scalar integrals. *Nucl. Phys.*, B416:606–644, 1994. hep-ph/9310358.

[WZ74] J. Wess and B. Zumino. Supergauge transformations in four-dimensions. *Nucl. Phys.*, B70:39–50, 1974.

[Y+00] F. Yuasa et al. Automatic computation of cross sections in hep: Status of grace system. *Prog. Theor. Phys. Suppl.*, 138:18–23, 2000. hep-ph/0007053.

Acknowledgements

I thank Daniel Wyler, Günther Rasche and Geoff Oades for making it possible to undertake this work.

I also thank Gilberto Colangelo, Joachim Kambor and Matthias Büchler for much help and interaction and for providing a very nice working environment. Thanks for this last essential point also go to our secretary Esther Meier as well as to all the other PhD students and postdocs of the institute.

Thanks to Rolf Mertig for providing *FeynCalc* and for help with programming issues.

Curriculum Vitae

Persönliche Daten

Name	:	Orellana
Vorname	:	Frederik
Geboren am	:	10. August 1968 in Guatemala
Heimatort	:	Dänemark

Ausbildung

1987	:	Matura, Mulernes Legatskole (Gymnasium), Odense, Dänemark
1988 - 1994	:	Studium der theoretischen Physik an der Universität Aarhus, Dänemark
1994 - 1996	:	Diplomarbeit bei Dr. Geoffrey Oades, ”Hadrons at Low Energies”
1997 - 2002	:	Dissertation am Institut für Theoretische Physik der Universität Zürich bei Prof. Dr. Daniel Wyler, ”Mesonic Final State Interactions”
		Tätigkeit als Assistent und Systemadministrator

Dozentenverzeichnis

K. Hepp
A. Denner
D. Wyler